An investigation of the neural circuitry that mediates inhibitory signalling within the lateral habenula

PhD Thesis

Name: ***Jack Webster***

Supervisor: ***Dr Christian Wozny***

Department: ***Strathclyde Institute of Pharmacy and Biomedical Sciences***

September 2019

Contents

List of figures and tables

Abstract

Background: The lateral habenula (LHb) is a brain structure which is known to be pathologically hyperactive in depression, thus providing enhanced inhibitory input to the brains' reward circuitry. As such, inhibition of the LHb has an antidepressant effect, via disinhibition of the reward circuitry. However, the neural circuity which mediates inhibitory signalling within the LHb remains to be fully described. Hence, the overarching aim of this project was to study inhibitory signalling within the LHb, by studying the circuitry formed by neurons expressing one of three transgenic markers classically considered to be associated with inhibitory neurons: Neuron-derived neurotrophic factor (Ndnf), parvalbumin (PV) and somatostatin (SOM).

Methods: Circuitry was studied *in vitro* using patch-clamp electrophysiology in combination with optogenetic manipulations of neurons expressing the above molecular markers. Additionally, immunohistochemistry and confocal microscopy were used to assess the fraction of neurons expressing these markers which were also GABAergic.

Results: This work identifies three sources of inhibitory input to the LHb, arising from both local PV-positive neurons, and those in the medial dorsal thalamic nucleus; and from SOM-positive neurons in the ventral pallidum. Additionally, we find that within the LHb, these markers are not confined to exclusively inhibitory populations. Rather, we identify physiologically distinct

populations of PV-positive neurons in the medial and lateral LHb; and another SOM-positive population in the superior sub-nucleus of the LHb.

Conclusions: This work sheds new light on inhibitory signalling within the LHb, which should facilitate future study of the circuitry implicated in depression. This hence suggests further inhibitory inputs likely remain to be described, and by continuing to study these we can further enhance our understanding of how the LHb becomes dysregulated in depression, and hence have a greater understanding of how to potentially target this structure in the treatment of this disease.

Acknowledgements

First and foremost, I would like to say a huge thank you to my primary supervisor Dr. Christian Wozny, not only for his input, support and guidance without which the project would not be possible, but also for his guidance in all aspects regarding my development as a scientist and beyond. I would also like to thank my second supervisor Dr. Shuzo Sakata for his help and input, and for providing us with the resources to make the project possible. I would also like to thank Dr. Rozan Vroman for her help with some of the earlier stereotaxic injections, and all other members of the Wozny lab past and present for making it a great and stimulating environment to work in.

Finally, I would like to thank my friends and family for their continued support, and for always believing in me. None more so than Rebecca. Thank you all.

Chapter 1: Introduction

Major depressive disorder (MDD) is the leading cause of disability worldwide, affecting more than 300 million individuals (World Health Organization, 2017). Symptoms vary widely between individuals and can include low mood, inability to experience pleasure, reduced energy and motivation, disturbed sleep and, in severe cases, suicidal ideation (World Health Organization, 2017). Despite this severity however, a 'stigma' exists regarding MDD with an unfortunately common perception that a psychiatric disease may not be perceived as a true illness (Wolpert, 2001), which can result in patients feeling ashamed and failing to seek proper treatment. Complicating matters further, and consistent with the wide variation in symptoms, is the fact that the aetiology of depression varies hugely between patients (Otte *et al.*, 2016) and hence the underlying pathologies are not particularly well understood. Classical views of these pathological factors have focussed on the 'monoamine hypothesis' of depression. This theory is built upon the observation that drugs which increase the levels of monoamine neurotransmitters in the brain are effective as antidepressants, and thus implicates reduced levels of the monoamine neurotransmitters serotonin, dopamine and noradrenaline as causative factors in MDD (Delgado, 2000; Hirschfeld, 2000).

More recently however, the lateral habenula (LHb) has been implicated as a structure critical in the pathogenesis of MDD (Yang *et al.*, 2018b). The LHb is a structure which inhibits the major serotonergic (Wang and Aghajanian, 1977) and dopaminergic (Christoph *et al.*, 1986) centres of the brain. As such,

recent work has shown that hyperactivity of the LHb is a key pathological factor in MDD (Yang *et al.*, 2018b), making it the subject of a huge resurgence in research interest (Geisler and Trimble, 2008). But first, to understand the role that the LHb plays in the pathogenesis of MDD, it helps to understand the greater circuitry that the LHb forms with other brain regions.

Overview of the lateral habenula

The LHb is a nucleus which, together with the medial habenula (MHb), forms the habenular complex (Andres *et al.*, 1999), a structure located in the epithalamus directly dorsal to the thalamus in the forebrain. The macroscale connectivity of the habenular complex with other brain regions is reasonably well described, and has been so for decades (Herkenham and Nauta, 1977, 1979). In an intricate set of tract-tracing experiments, Herkenham and Nauta successfully elucidated the major afferent and efferent connections of the habenular complex. The tract carrying afferent input fibres to the habenular nuclei is known as the stria medullaris (Herkenham and Nauta, 1977), while both nuclei concurrently send their efferent output fibres to downstream targets via the fasciculus retroflexus (Herkenham and Nauta, 1979).

Connectivity of the LHb is diverse, with the most prominent input arriving from the globus pallidus, or the homologous entopeduncular nucleus in rodents, and the lateral hypothalamus with which the LHb is reciprocally connected (Herkenham and Nauta, 1977, 1979). However, perhaps the most

well-defined connections of the LHb are that which it shares with the midbrain reward circuitry; particularly the dopaminergic ventral tegmental area (VTA) and serotonergic dorsal raphe nucleus; both of which are major output targets and with which the LHb is intricately and reciprocally tied (Herkenham and Nauta, 1977; Wang and Aghajanian, 1977; Phillipson and Pycock, 1982; Jhou *et al.*, 2009b; Fakhoury, 2018). Functionally, evidence implies that the LHb acts as an inhibitory modulator of the VTA (Christoph *et al.*, 1986; Ji and Shepard, 2007) and DRN (Wang and Aghajanian, 1977) nuclei. Interestingly however, the majority of LHb neurons are glutamatergic (Brinschwitz *et al.*, 2010) and hence this inhibitory modulation arises via intermediary connections. In the case of the DRN, this intermediary connection has been proposed to arise from specific targeting of local GABAergic neurons in the DRN (Ferraro *et al.*, 1996), but is still not entirely understood (Zhao *et al.*, 2015). In the VTA however, recent studies have identified a sub-structure termed the rostromedial tegmental nucleus (RMTg) comprised largely of GABAergic neurons through which the LHb contacts to exert this negative control (Ji and Shepard, 2007; Jhou *et al.*, 2009b, 2009a). In turn, the dopaminergic projection from the VTA to the ventral striatum known to encode reward and addictive behaviour is inhibited (Fig. 1.1; Ikemoto, 2010).

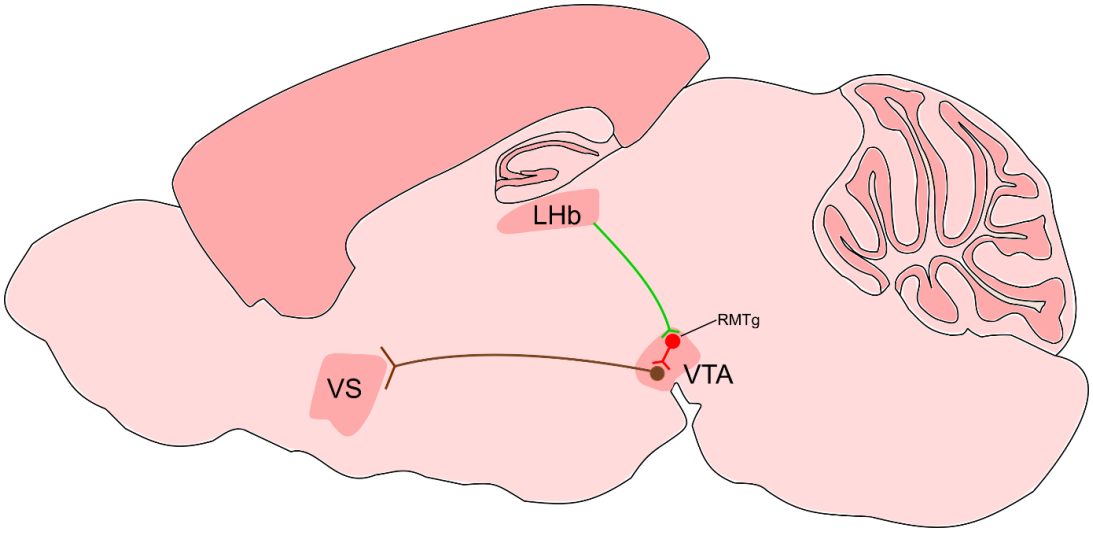

Fig 1.1: Schematic illustration of the circuitry by which the LHb exerts inhibitory influence over the dopaminergic reward pathway. Glutamatergic neurons in the LHb project to and excite GABAergic neurons in the rostromedial tegmental nucleus (RMTg), a sub-structure of the ventral tegmental area (VTA). These neurons then inhibit dopaminergic VTA neurons, which project to the ventral striatum to promote feelings of reward and behavioural reinforcement. Image taken, traced and modified from the Allen Brain Atlas; www.atlas.brain-map.org

Theories of lateral habenula function

Consequently, if the LHb has the net effect of providing inhibitory input to the brains' reward pathways (Christoph *et al.*, 1986; Ji and Shepard, 2007), it would then seem logical that this structure may act to encode the opposite of behaviourally-reinforcing emotions; i.e. aversion. This is indeed the case: in

their seminal work, Matsumoto and Hikosaka (2007) unveiled that the lateral habenula acts as a predictor of 'negative reward' in an intricate set of experiments in Rhesus' monkeys. This conclusion was made following the observation that LHb neurons displayed increased firing, and dopaminergic ventral tegmental area (VTA) neurons displayed reduced firing, in response to Rhesus' monkeys not receiving a juice reward they had been conditioned to expect. The outcome from this work has led to the hypothesis that the LHb acts to encode aversive states by providing net inhibition to dopaminergic neurons in the VTA, hence impeding behavioural reinforcement (Ji and Shepard, 2007; Matsumoto and Hikosaka, 2007; Hikosaka, 2010).

But what could be the functional relevance of a structure which has the overall effect of inhibiting behaviourally-reinforcing emotions and promoting aversive states? From an evolutionary standpoint, the reward system exists to attach a positive motivational valence to behaviours which are critical to an organisms' survival (Wise, 2004), a prime example of which would be feeding. This therefore ensures that the organism will actively seek to perform such behaviours. However, it is not always appropriate to carry these behaviours out (Wagner *et al.*, 2016a). Taking feeding again as an example; if an organism were to be subject to attack from a predator while feeding, then behavioural reinforcement would not be appropriate in this scenario. Were this to be the case and the organism to continue to feed at such a time, then the organism would likely be killed by the predator. Thus, it is necessary to have a system which effectively acts as the 'off-switch' of the reward system, and

ensures that behaviours with negative consequences are not reinforced (Hikosaka, 2010). This is believed to be the primary functional importance of the LHb.

Alternatively, recent work has also suggested a role for the LHb in various cognitive functions. Specifically, LHb-projecting prefrontal cortical neurons have been proposed to have a role in regulating working memory processing (Mathis *et al.*, 2015, 2017; Mathis and Lecourtier, 2017), and also in behavioural flexibility, whereby this pathway is required for adaptively changing a learned behaviour in response to a changing context or environmental conditions (Baker *et al.*, 2015, 2019; Mizumori and Baker, 2017). These works are of particular interest, as they diverge from the classical view of the LHb whereby it specifically acts as an information relay. Instead, they suggest a role for the LHb in gating afferent information, to allow the processing of cortical input signals into behavioural output where the proposed action is evaluated as being efficient in achieving a goal (such as consuming a food reward), or to adaptively switch behaviours in circumstances where it is not (Mizumori and Baker, 2017). This theory is likely not mutually exclusive with the classical theory that the LHb encodes aversive states (Hikosaka, 2010), as both suggest a role for the LHb in encoding negative signals.

The lateral habenula in major depressive disorder

So how then is the LHb implicated in the pathogenesis of MDD? Accounting for the above; we know that under normal conditions the LHb provides inhibitory input to dopaminergic neurons in the VTA (Christoph *et al.*, 1986; Ji and Shepard, 2007), and we know that this results in the encoding of aversive states (Matsumoto and Hikosaka, 2007; Hikosaka, 2010). While the molecular mechanisms by which the LHb is implicated in MDD are still not entirely understood, multiple pathological changes are known to occur. Excitatory input onto midbrain-projecting LHb neurons becomes potentiated (Li *et al.*, 2011), at least in part as a result of a shift in favour of glutamate release from GABA / glutamate co-releasing entopeduncular nucleus neurons which innervate the LHb. Additionally, LHb neurons are known to switch from tonic action potential discharge modality to burst firing (Cui *et al.*, 2018; Yang *et al.*, 2018a), thus resulting in greater synchronicity of neuronal firing. The overall combined effect of these factors is that the LHb becomes hyperactive, thus resulting in enhanced inhibitory input to the reward systems and hence suppression of the associated positive emotions (Hikosaka, 2010; Yang *et al.*, 2018a, 2018b).

These recent breakthroughs linking the LHb to a pathogenic role in MDD have resulted in a huge resurgence of interest in studying this structure (Geisler and Trimble, 2008). While earlier lesioning studies in rats were successful in attributing some aspects of avoidance learning to the habenular complex as a whole (Wilson *et al.*, 1972; Wilcox *et al.*, 1986; Vale-Martinez *et*

al., 1997), these studies could not differentiate between effects mediated by the lateral and medial habenulae due to the crude nature of the lesioning technique. More recently, advances in rodent models of MDD (Henn and Vollmayr, 2005) have provided great insight into the underlying pathology of the disease, and to the role that the LHb plays in its' pathogenesis. Perhaps the most commonly used model of MDD is the learned helplessness model, in which rodents are subjected to an inescapable stressful event such as foot shock, until they display no motivation to escape this treatment when this option is later provided. This model is generally accepted to be comparable to the helplessness and behavioural despair commonly exhibited in human MDD (Henn and Vollmayr, 2005). Studies employing this model have utilized a wide variety of approaches including electrophysiology, optogenetics, pharmacology and behavioural analysis, and are all unified by the finding that the LHb is hyperactive within helpless rodents (Li *et al.*, 2011; Winter *et al.*, 2011; Shabel *et al.*, 2014; Lecca *et al.*, 2016; Cui *et al.*, 2018; Yang *et al.*, 2018a).

These works clearly establish the link between LHb hyperactivity and MDD. This then begs the question of the therapeutic potential of targeting the LHb, and importantly, by what means to do so. A key finding from one of these works (Li *et al.*, 2011) was that it is possible to suppress helpless behaviour by deep brain stimulation (DBS) of LHb afferents. DBS is a novel technique whereby electrical stimulation of neurons nearby an implanted electrode can be used to restore neurotransmission to normal levels. Indeed, this approach

has also been proposed as a potential alternative for treatment-resistant depression in humans (Sartorius and Henn, 2007), in a pioneering study in which implanting a stimulator into the LHb resulted in full remission (Sartorius *et al.*, 2010). While it appears that DBS is to date, one of the most applicable treatment methods in humans (Kiening and Sartorius, 2013), other studies in helpless rodents using invasive pharmacological procedures have also reported success in targeting the LHb with various compounds (Winter *et al.*, 2011; Lecca *et al.*, 2016; Yang *et al.*, 2018a). In a relatively simple investigation, Winter *et al.* (2011) reported alleviation of depressive behaviour following direct injection of the GABAergic agonist muscimol into the LHb, hence providing reasonable evidence that pharmacologically inhibiting the LHb has antidepressant potential. Interestingly, a recent publication reported that inducing helplessness in mice raised activity of protein phosphatase 2 (PP2A), which concurrently reduced $GABA_B$ signalling and this disinhibitory effect resulted in LHb neuron hyperactivity. Consistently, they observed that pharmacological inhibition of PP2A could alleviate helpless behaviour (Lecca *et al.*, 2016). Additionally, while the mechanisms by which ketamine exerts its' antidepressants properties are largely controversial (Zanos and Gould, 2018), work from the group of Hailan Hu revealed that this effect is at least partially as a result of blocking NMDA receptors within the LHb. This was following their observation that direct injection of ketamine into the LHb was sufficient to alleviate depressive symptoms by blocking burst-firing of LHb neurons (Yang *et al.*, 2018a). Finally, in an elaborate set of viral tracing experiments, the Ren group were able to link the antidepressant effects of light therapy to a

disynaptic pathway originating in the retina in which the LHb is ultimately inhibited (Huang *et al.*, 2019).

While these results suggest that there are most likely a variety of mechanisms by which the LHb is implicated in the pathogenesis of MDD, all have reported that targeting this structure has potential as an antidepressant therapy. So again: the question is how best to do so. Of course, we know that the aetiology of MDD varies hugely on a case-by-case basis (Otte *et al.*, 2016). So in order to gain a greater understanding of how to implicate the LHb as a treatment target in MDD, we must first gain a better understanding of the neuronal populations that form the structure itself.

Sub-structural organization of the lateral habenula

To help achieve this, a good starting point would be to attempt to sub-classify the LHb into distinct sub-structures based on the characteristics of the neuronal populations that comprise it. Andres *et al.* (1999) were the first to attempt this. By examining neuronal morphology, they devised a scheme in which the rat habenular complex could be divided into distinct sub-structures, as opposed to the traditional approach of dividing the complex only into the lateral and medial components. Based on neuronal morphology, they proposed that the medial habenula can be further divided into five different sub-regions, while the lateral habenula can be divided into a further ten (Fig 1.2).

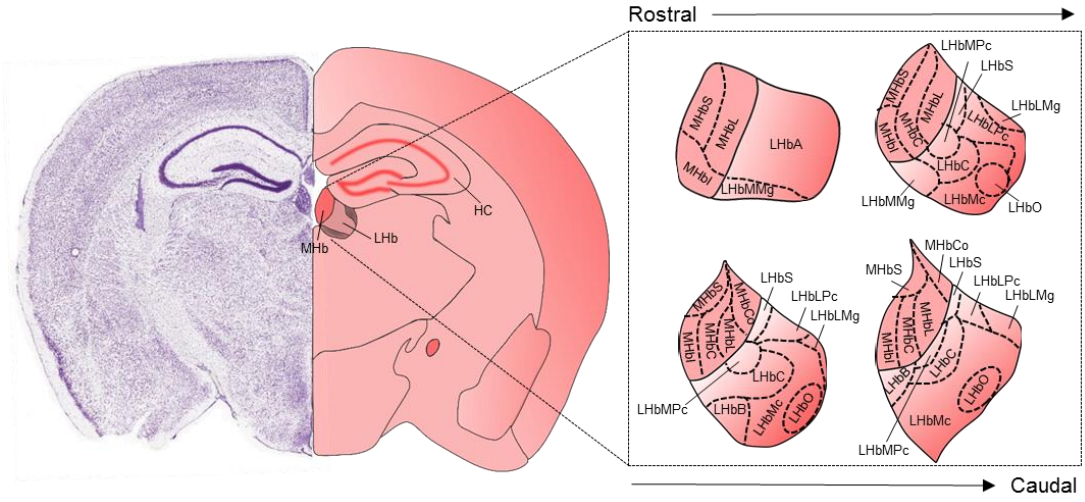

Figure 1.2: Sub-structural organization of the habenular complex as proposed by Andres et al. (1999). Left; Coronal section of Nissl-stained adult mouse brain showing position of medial habenula (MHb), lateral habenula (LHb) in relation to the hippocampal formation (HC). Right; Enlargement of habenular complex with overlay of sub-structural organization as proposed by Andres et al. (1999) through the rostro-caudal axis. Medial habenula is sub-divided into superior (MHbS), inferior (MHbI), central (MHbC), lateral (MHbL) and commissural (MHbCo) areas. Lateral habenula is sub-divided into anterior (LHbA), superior (LHbS), central (LHbC), medial parvocellular (LHbPc), medial marginal (LHbMMg), basal (LHbB), magnocellular (LHbMc), oval (LHbLO), lateral parvocellular (LHbLPc) and lateral marginal parts (LHbLMg) areas. Image taken and traced from the Allen Brain Atlas; www.atlas.brain-map.org

However, more recent advances in molecular biology techniques have made it possible to further sub-classify the habenular structures based on neurochemistry (Aizawa *et al.*, 2012) and on gene expression patterns (Wagner *et al.*, 2016a, 2016b). Based on these approaches, the medial habenula does seem to agree with those boundaries identified by Andres and colleagues: the main transmitters identified in the medial habenula are glutamate, substance P and acetylcholine while interestingly, the superior medial habenula also produced the pro-inflammatory cytokine interleukin-18; all expressed in differing combinations within each sub-nuclei (Aizawa *et al.*, 2012). Gene expression patterns also seem to agree with these boundaries. However, gene expression in the LHb completely disregards the boundaries specified by Andres *et al.* (Wagner *et al.*, 2016b), while neurotransmission is almost uniformly glutamatergic throughout each region (Aizawa *et al.*, 2012). Interestingly, the LHb is more similar to the thalamus than the MHb in terms of gene expression (Wagner *et al.*, 2016a) highlighting the vast difference in functionality between these two adjacent nuclei. The discrepancy in the LHb sub-structural organization proposed by these approaches suggests that the organization of the LHb is most likely more complex and may even be defined on the cellular level rather than the sub-structural level.

Functional aspects of lateral habenular neurons

While the above studies serve as an excellent framework to further study LHb function, there are also still limitations. One such limitation is that these studies do not permit classification based on neuronal physiology, a characteristic defined as one of the key sub-classification criteria in other brain regions (Ascoli *et al.*, 2008).

Investigations into the physiology of the neuronal populations within the LHb are actually somewhat limited (Wilcox *et al.*, 1988; Chang and Kim, 2004; Kim and Chang, 2005; Weiss and Veh, 2011; Cui *et al.*, 2018; Yang *et al.*, 2018a). These studies have found common ground by attempting to sub-classify LHb neurons based on spontaneous action potential discharge patterns. Based on this criteria, LHb neurons can be sub-classified into three broad categories. These are silent neurons, tonically-active and bursting neurons. Silent neurons, as the name implies, do not spontaneously discharge action potentials at rest. Tonically-active neurons do discharge action potentials at rest. These can be further sub-classified into tonic-regular neurons, which discharge action potentials at a continuous frequency, and tonic-irregular neurons, which fire in an irregular stuttering pattern (Weiss and Veh, 2011). The most distinctive physiological phenotype however, is burst-firing neurons. These are defined by a calcium-dependent ‘depolarization wave’, from which a rapid discharge of high frequency action potentials arises (Wilcox *et al.*, 1988; Chang and Kim, 2004; Yang *et al.*, 2018a).

While this classification system offers some insight into the physiological sub-classes of LHb neurons, it is also not without its' drawbacks. Firstly, these sub-classes appear not to share any correlation with the morphological properties of LHb neurons (Weiss and Veh, 2011) nor do they exhibit any form of specific sub-structural localization (Chang and Kim, 2004; Kim and Chang, 2005; Weiss and Veh, 2011). Furthermore, a striking hallmark property of many LHb neurons is that the action potential discharge pattern can be subject to change dependent on the membrane potential; the same neuron can switch from tonic modality when it is relatively depolarized (around -50 mV) to bursting modality when it becomes hyperpolarized (below -65 mV; Wilcox, Gutnick and Christoph, 1988; Chang and Kim, 2004; Yang, Cui, *et al.*, 2018). Therefore, it can be difficult to assign a sub-class to individual LHb neurons based on physiological properties, as the spontaneous action potential discharge pattern changes based on resting membrane potential and this may be altered due to; e.g. potentiated excitatory input onto LHb neurons from other structures in conditions such as MDD (Li *et al.*, 2011; Shabel *et al.*, 2014).

Yet, due to recent work from the Hu group, we know now that this hallmark switching of action potential discharge pattern is critical in the pathogenesis of MDD (Cui *et al.*, 2018; Yang *et al.*, 2018a, 2018b). Bursting behaviour in neurons is believed to be a mechanism by which neurons can achieve synchronicity of firing (Gutnick and Yarom, 1989). Assuming this to be true, then it would also be reasonable to assume that in conditions such as MDD

where the LHb is known to be hyperactive (Li *et al.*, 2011; Winter *et al.*, 2011; Shabel *et al.*, 2014; Lecca *et al.*, 2016; Cui *et al.*, 2018; Yang *et al.*, 2018a), higher synchronicity of LHb neuronal activity could be responsible for a greater output and hence greater silencing of the reward pathways. This is indeed what the Hu group were able to show (Cui *et al.*, 2018; Yang *et al.*, 2018a). They demonstrated a greater proportion of neurons which displayed busting activity at rest in rodent models of depression. Furthermore, they also showed that direct ketamine infusion into the LHb reversed this enhanced bursting resulting in a reversal of depressive symptoms.

The above evidence implies that physiological characteristics alone are most likely not the best criteria by which to attempt to divide LHb neurons into distinct sub-classes. However they do demonstrate that the physiological activity of the neurons are a critical feature in defining the overall activity and output of the LHb to downstream targets. Hence, in order to more fully understand the organization and function of the LHb, we propose that an approach which combines all of the aforementioned criteria; physiology, morphology and molecular expression patterns, to be an important and currently missing link.

Addressing the issue of inhibitory control within the lateral habenula

How best can this problem be approached then? As previously stated, there is now substantial evidence that potentiating inhibitory input to the LHb is

sufficient to reverse depressive symptoms in various rodent models of MDD (Winter *et al.*, 2011; Lecca *et al.*, 2016; Tchenio *et al.*, 2017; Huang *et al.*, 2019). It is also known that the LHb receives a large inhibitory input mediated by both $GABA_A$ and $GABA_B$ receptors (Lecca *et al.*, 2016; Meye *et al.*, 2016; Wagner *et al.*, 2016b; Tchenio *et al.*, 2017) implying that this input arrives from a variety of sources. While some GABAergic projections to the LHb are known (Faget *et al.*, 2018; Huang *et al.*, 2019), this process is still largely a mystery. Furthermore, while it also accepted that the majority of LHb neurons are glutamatergic (Omelchenko *et al.*, 2009; Brinschwitz *et al.*, 2010), to date several studies have identified what are likely locally-targeting inhibitory neurons of at least two distinct sub-classes within the LHb (Weiss and Veh, 2011; Wagner *et al.*, 2016b; Zhang *et al.*, 2018). It would be logical then to speculate that there could be more of these locally-targeting inhibitory neurons within the LHb that have not yet been identified. If this were to be the case, studying these would yield a better understanding into how inhibitory signalling is processed within the LHb, and this could potentially yield a greater insight into how the LHb is implicated in the pathogenesis of MDD.

Inhibitory interneurons within the neocortex and other brain regions

Locally-targeting inhibitory neurons, or inhibitory interneurons, are a well-studied group of neurons in many other brain regions, particularly the neocortex (Tremblay *et al.*, 2016) and hippocampus (Klausberger and

Somogyi, 2008). These represent a broad class of inhibitory neurons which can be further divided into several distinct sub-classes, each with their own defining physiological, morphological and molecular characteristics (Ascoli *et al.*, 2008; Tremblay *et al.*, 2016). In the neocortex, these neurons inhibit principal excitatory neurons to modulate sensory gain (Atallah *et al.*, 2012; Wilson *et al.*, 2012), and their dysfunction is known to be implicated in the pathogenesis of a wide range of psychiatric disorders (Marín, 2012).

Attempts to sub-classify these interneurons have resulted in the proposition and general acceptance of three primary sub-classes, each defined by their own molecular markers (Tremblay *et al.*, 2016). Neurons expressing the protein parvalbumin (PV) form the most homogenous sub-class, unified by their hallmark fast-spiking phenotype, and form synapses with the somata of principal excitatory neurons (Fig. 1.3; Tremblay, Lee and Rudy, 2016), and have been identified and characterised in multiple major brain structures including the neocortex (Celio, 1986; Kawaguchi and Kubota, 1997), the hippocampus (Kawaguchi *et al.*, 1987) and the striatum (Bennett and Bolam, 1994).

Somatostatin-positive neurons (SOM) are a more heterogenous sub-class of inhibitory interneuron which generally form synapses with the dendrites of principal excitatory neurons in the neocortex (Fig. 1.3; Kawaguchi and Kubota, 1997; Tremblay, Lee and Rudy, 2016) and are also known to be present in the hippocampus (Stefanelli *et al.*, 2016).

While the final sub-class of interneurons are not as well-defined, they can generally be further sub-classified as either vasoactive-intestinal peptide-positive (VIP) or non VIP-positive (Tremblay *et al.*, 2016). Of the non VIP-positive interneurons, a further sub-division is the peculiar group of interneurons known as neurogliaform cells (Tamás *et al.*, 2003; Wozny and Williams, 2011; Overstreet-Wadiche and McBain, 2015). These are a group of interneuron commonly found in neocortical layer one (Wozny and Williams, 2011) which mediate slow neurotransmission via $GABA_B$-receptors (Tamás *et al.*, 2003; Price *et al.*, 2008). While the function of these neurons is not as well understood as with other sub-classes of interneuron (Overstreet-Wadiche and McBain, 2015), two studies have claimed to identify these neurons, or at least neurons with identical properties, within the LHb (Weiss and Veh, 2011; Wagner *et al.*, 2016b). This makes them an interesting target to study inhibitory control within this structure. One problem in doing so however, is the lack of suitable molecular markers (Overstreet-Wadiche and McBain, 2015). Neuropeptide Y (NPY) is generally accepted to be expressed by most neurogliaform neurons, however has the limitation that it is also expressed by other neuronal sub-populations (Tricoire *et al.*, 2010; Overstreet-Wadiche and McBain, 2015). More recently, Neuron-derived neurotrophic factor (Ndnf) has been proposed as a more suitable molecular marker, being relatively selective for layer one neocortical neurogliaform cells (Fig. 1.3; Tasic *et al.*, 2016, 2018; Abs *et al.*, 2018).

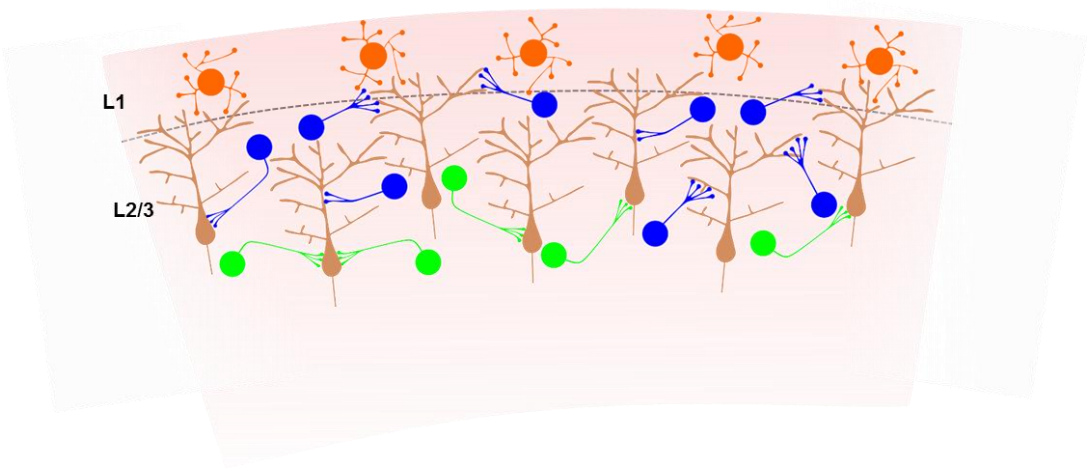

Figure 1.3: Schematic illustration of sub-classes of inhibitory interneurons within the neocortex. Inhibitory interneurons can be sub-classified based on distinct properties such as the molecular markers they express (Ascoli *et al.*, 2008). PV-positive interneurons are a homogenous class of fast-spiking neuron which target the somata of principal excitatory pyramidal neurons. SOM-positive interneurons are a more heterogenous class which tend to target the dendrites of excitatory neurons. Ndnf has recently been proposed as a relatively selective marker layer one (L1) neurogliaform cells (Tasic *et al.*, 2016, 2018; Abs *et al.*, 2018).

Summarizing the above evidence: PV and SOM are two well-accepted markers of sub-classes of inhibitory interneuron in the neocortex (Celio, 1986; Kawaguchi and Kubota, 1997; Tremblay *et al.*, 2016) and in the hippocampus (Kawaguchi *et al.*, 1987; Stefanelli *et al.*, 2016). Ndnf is now thought to be a selective marker for neocortical neurogliaform cells (Tasic *et al.*, 2016, 2018;

Abs *et al.*, 2018), which are also believed to be present in the LHb (Weiss and Veh, 2011; Wagner *et al.*, 2016b). Therefore, referring back to the concept of studying inhibitory control within the LHb; if undiscovered classes of locally-targeting inhibitory neuron were to exist in this structure, these molecular markers should theoretically serve as important tools to study their physiology and the circuitry that they comprise. This was the hypothesis that this body of work was based upon.

Insights from transgenic and optogenetic studies

Some of the great breakthroughs in neuroscience in recent years have been the advent of the optogenetics era (Boyden *et al.*, 2005), and advances in transgenic Cre mouse models permitting genetic targeting of specific neuronal sub-populations (Bouabe and Okkenhaug, 2013). As a result, interrogation of neural circuitry with regards to neuronal sub-populations defined by molecular marker expression has become a mainstay of modern-day neuroscience (Bernstein and Boyden, 2011). Combining these approaches permits specific manipulation of defined populations of neurons (for example PV-positive neurons) with great spatiotemporal precision (Bernstein and Boyden, 2011).

Consequently, many recent works have implemented these techniques to delineate the function of neurons expressing the aforementioned molecular markers not only in the neocortex (Abs *et al.*, 2018; Takesian *et al.*, 2018) but also in many other deeper brain regions (Shang *et al.*, 2015; Knowland *et al.*,

2017; Wallace *et al.*, 2017; Villalobos *et al.*, 2018; Lazaridis *et al.*, 2019). As these markers are traditionally associated with distinct sub-populations of inhibitory neurons in the neocortex (Tremblay *et al.*, 2016), one may expect this to be true in other brain regions (Villalobos *et al.*, 2018). Interestingly this is not always the case: excitatory PV-positive projection neurons have been identified in the superior colliculus (Shang *et al.*, 2015), and two distinct populations of PV-positive excitatory neurons which project to the LHb have been identified in the rodent entopeduncular nucleus (Wallace *et al.*, 2017) and the ventral pallidum (Knowland *et al.*, 2017). Additionally, recent works have also identified a population of LHb-projecting SOM-positive neurons in the entopeduncular nucleus which co-release both GABA and glutamate (Wallace *et al.*, 2017; Lazaridis *et al.*, 2019). While these findings are perhaps not what was originally expected, they serve to highlight that neuronal diversity varies widely between regions, and therefore that one 'rule' regarding an association between a particular marker and neuronal phenotype in a given brain region does not necessarily hold true in other regions. As such, each of these markers should be validated on a region-to-region basis.

Regardless, these studies have certainly provided invaluable data in neural circuitry mapping. Many studies utilizing optogenetic approaches have focussed on the projection from the entopeduncular nucleus to the LHb (Shabel *et al.*, 2014; Meye *et al.*, 2016; Wallace *et al.*, 2017). As previously mentioned, a striking feature of these neurons is that many co-release GABA and glutamate onto LHb neurons (Shabel *et al.*, 2014; Meye *et al.*, 2016;

Wallace *et al.*, 2017; Lazaridis *et al.*, 2019). Earlier work observed that excitatory input from this projection was potentiated in models of depression, thus increasing LHb excitability (Li *et al.*, 2011). More specifically, these recent works have elucidated that the balance of glutamate to GABA release at co-releasing synapses is shifted in favour of glutamate in models of depression, or other aversive states (Shabel *et al.*, 2014; Meye *et al.*, 2016).

Other recent works have focused on further dissecting the reciprocal connection that the LHb shares with the VTA (Stamatakis *et al.*, 2013; Root *et al.*, 2014). Similarly, these works have identified, to date, two distinct sub-populations of projection neurons from the VTA to the LHb. As with the entopeduncular nucleus, one population of LHb-projecting neurons which co-release GABA and glutamate has also been identified within the VTA (Root *et al.*, 2014), leading to the suggestion that the LHb functions as a co-release 'hub' (Shabel *et al.*, 2014) where the balance of excitatory and inhibitory input can be processed into behavioural output on the scale of individual synapses. Rather unusually, the second population of LHb-projecting neurons are believed to be dopaminergic projection neurons which send axon collaterals to the LHb releasing exclusively GABA, and not dopamine (Stamatakis *et al.*, 2013), although this report has since been called into question on the basis that Cre-expression in the tyrosine hydroxylase transgenic mouse model may not have been confined exclusively to dopaminergic neurons (Lammel *et al.*, 2015).

While most evidence implies that the GABA / glutamate co-releasing projection from the entopeduncular nucleus to the LHb is the primary driver in encoding aversive states (Li *et al.*, 2011; Shabel *et al.*, 2014; Meye *et al.*, 2016), other reports have also pointed to a role for the glutamatergic projection from the lateral hypothalamus to LHb (Lecca *et al.*, 2017; Lazaridis *et al.*, 2019; Trusel *et al.*, 2019). Specifically, that potentiation at lateral hypothalamus to LHb excitatory synapses is a critical factor in driving conditioned responses to aversive stimuli (Trusel *et al.*, 2019).

Evidently then, the advent of optogenetics has allowed for dissection with much greater scrutiny of the individual neuronal sub-populations of the primary input pathways to the LHb. In addition to these however, entirely novel circuitry has also been elucidated using similar approaches (Barker *et al.*, 2017; Knowland *et al.*, 2017; Faget *et al.*, 2018; Huang *et al.*, 2019). Indeed it is now known that distinct populations of both excitatory and inhibitory neurons project from the ventral pallidum to the LHb, with the excitatory population also having been shown to promote encoding of aversion (Knowland *et al.*, 2017; Faget *et al.*, 2018). The lateral preoptic area similarly has two populations of LHb-projecting excitatory and inhibitory neurons, which converge on individual LHb neurons, with each driving opposite behavioural outcomes (Barker *et al.*, 2017). Finally, the recently identified projection from the lateral geniculate nucleus of the thalamus to the LHb is primarily GABAergic and hence dampens LHb excitability, counteracting depressive phenotypes (Huang *et al.*, 2019).

But what is the significance of all of this data then? Earlier in this report, a fairly reductionist view of how the LHb encodes aversive states was presented (Fig. 1.1). That is, that glutamatergic LHb neurons project to GABAergic neurons in the rostromedial tegmental nucleus, which then inhibit striatum-projecting dopaminergic neurons in the VTA thus inhibiting behavioural reinforcement. These results clearly show that it is indeed far more complex than that (Fig. 1.4).

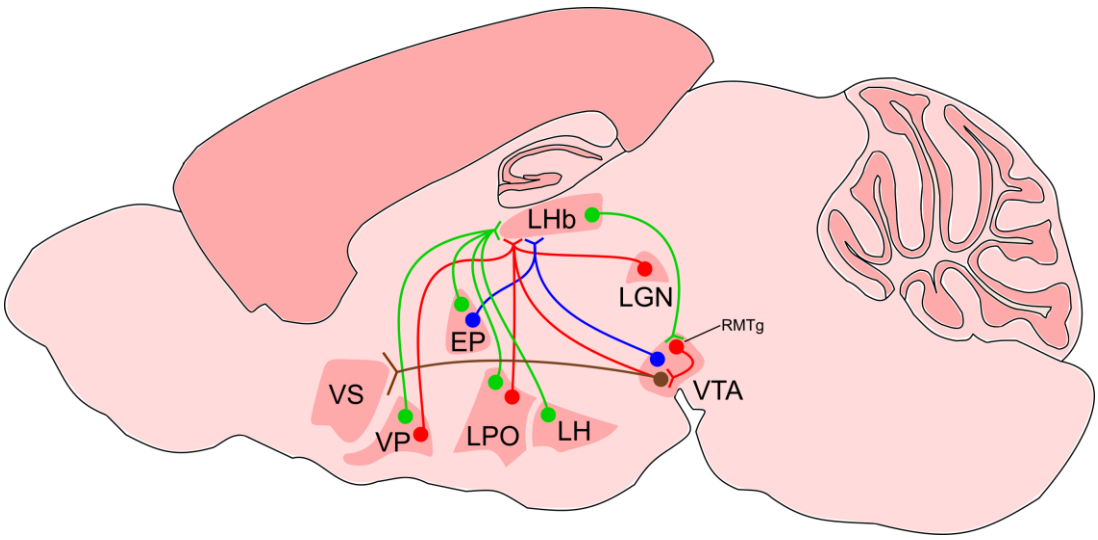

Figure 1.4: An updated illustration of the circuitry by which the LHb encodes aversive states. Findings from recent optogenetic investigations reveal that the LHb receives input from various upstream regions including the entopeduncular nucleus (EP), lateral hypothalamus (LH), ventral pallidum (VP), lateral preoptic area (LPO), lateral geniculate nucleus of the thalamus (LGN) and ventral tegmental area (VTA). Many of these projections consist of distinct sub-populations of neurons which may be excitatory, inhibitory or co-

releasing of GABA and glutamate. The LHb then sends excitatory projections to inhibitory neurons in the rostromedial tegmental nucleus (RMTg) of the VTA, with which it is reciprocally connected, to inhibit dopaminergic projections to the ventral striatum (VS).

Of course, the above illustration is by no means an exhaustive list of the full connectivity of the LHb; for the purpose of this report, the focus has been on the circuitry by which the LHb encodes aversion, and hence the serotonergic raphe nuclei have been omitted as comparatively little data exist regarding the function of this circuitry (Zhao *et al.*, 2015). Furthermore, with so many recent advances relating to the LHb circuitry driving aversive states and depressive phenotypes, it is highly likely that novel projections remain to be defined.

So in summary, classical circuitry tracing methods have been invaluable in providing an overview of the LHb connectivity on a regional scale (Herkenham and Nauta, 1977, 1979). However, optogenetic advances have made it increasingly apparent that this is no longer sufficient to fully describe the LHb connectivity and functionality in encoding aversion. Approaches where afferent projections to the LHb can be dissected into distinct neuronal sub-populations have led to a plethora of novel data (Stamatakis *et al.*, 2013; Root *et al.*, 2014; Shabel *et al.*, 2014; Barker *et al.*, 2017; Wallace *et al.*, 2017; Knowland *et al.*, 2017; Tchenio *et al.*, 2017; Faget *et al.*, 2018; Huang *et al.*,

2019; Lazaridis *et al.*, 2019; Trusel *et al.*, 2019). As such, approaches continuing to take advantage of optogenetics and transgenic mouse models should yield further advances.

Objectives, approach and findings

With this background of information, the overarching aim of this study was to disentangle the circuitry comprised by LHb neurons expressing known markers of inhibitory identity: (i) PV, (ii) SOM, (iii) Ndnf and (iv) NPY (Overstreet-Wadiche and McBain, 2015; Tasic *et al.*, 2016, 2018; Tremblay *et al.*, 2016; Abs *et al.*, 2018). It was therefore proposed that by implementing transgenic Cre mouse models specific for each of these markers in combination with histology, optogenetics and electrophysiology, the circuitry that each of these neurons contributes to within the LHb could be delineated. In the wider context, the original hypothesis was that by studying and characterising novel inhibitory neuronal populations within the LHb, we could gain a better understanding of inhibitory signalling. This should provide avenues for future work to develop novel strategies to potentiate inhibitory signalling within the LHb, which is known to alleviate depressive symptoms (Winter *et al.*, 2011; Lecca *et al.*, 2016; Huang *et al.*, 2019).

To address this, each marker was first histologically tested for co-localisation with GABA. This revealed that only a sub-population of LHb neurons expressing each marker were GABAergic, with the exception of NPY,

where no NPY-positive neuronal somata were observed in the LHb. LHb neurons positive for each marker were next physiologically characterised. Ndnf was not expressed by any particular sub-class of LHb neuron. In striking contrast however, PV-positive neurons formed at least two distinct physiological sub-classes which were clearly confined to either the medial LHb or lateral LHb, while SOM-positive LHb neurons were found to be a unique sub-class which appeared to have hybrid physiological properties of both lateral and medial habenular neurons.

We next tested the input to the LHb mediated by neurons expressing each marker optogenetically, by expressing Channelrhodopsin globally in Ndnf, PV and SOM-positive neurons, and recording postsynaptic events while photostimulating. This revealed that input to the LHb was not exclusively inhibitory in the case of any marker. However, large inhibitory postsynaptic events were observed with relative frequency in LHb neurons while photostimulating either PV-positive or SOM-positive neurons, indicating that a sub-population of neurons expressing each of these markers mediate inhibitory transmission within the LHb.

The final question asked then was whether or not this inhibitory transmission originated from a local source. To answer this question, we utilized stereotaxic injection of both Cre-depedent retrograde vectors (Tervo *et al.*, 2016), and Cre-dependent ChR2-encoding vectors into the LHb in both PV and SOM transgenic Cre lines. In slices from the PV line, inhibitory events were indeed observed, thus confirming the existence of a PV-positive LHb

neuronal sub-class which mediates local inhibitory transmission. Another finding from these experiments was that an inhibitory projection to the LHb arises from PV-positive neurons in the medial dorsal thalamic nucleus adjacent to the LHb. In the case of the SOM experiments, no locally-targeting inhibitory SOM-positive neurons were identified. Instead, this large inhibitory input was found to originate from SOM-positive neurons in the ventral pallidum; likely the same population of GABAergic neurons described by Faget *et al.* (2018).

In summary, the findings from this work are as follows: i) that physiologically distinct sub-populations of PV-positive and SOM-positive neurons exist within the LHb; ii) that the LHb receives inhibitory input from local PV-positive neurons, and extrinsically from PV-positive neurons originating from the medial dorsal thalamus, and from SOM-positive neurons in the ventral pallidum; iii) that while these molecular markers can be implemented to characterise neuronal sub-populations within deeper brain structures such as the LHb, they represent far more diverse neuronal populations here than they are known to in the neocortex (Tremblay *et al.*, 2016). As such, validation and characterisation of neurons expressing these markers should be carried out on a structural basis.

Chapter 2: Materials and methods

In this work, experimental methods were consistent for all transgenic mouse lines used. Therefore, it is most applicable to include a general methods section describing each experimental procedure in its entirety.

Animals

All procedures were approved by the Ethics committee of the University of Strathclyde, Glasgow in accordance with the relevant UK legislation (the Animals (Scientific Procedures) Act, 1986), and carried out under UK Home Office licence P546B085A held by Dr C. Wozny. Male and female mice from each strain were used in this work. All animals were maintained on a C57BL/6 background, and kept on a 12:12 light/dark cycle under standard group housing conditions with unlimited access to water and normal mouse chow. New-born pups were housed with parents until weaning at P21. To generate transgenic reporter-bearing offspring, reporter mouse lines (Ai32 and Ai9) were crossed with transgenic mice of either the PV-IRES-Cre, SOM-IRES-Cre or Ndnf-IRES-Cre driver lines once both parents were at least six weeks old. Information for breeding strains including Cre-expressing strains, reporter strains and C57BL/6 mice can be found in table 2.1:

Strain	Full nomenclature	Jax no.	Reference	Source
C57BL/6	C57 BL/6J	000664	NA (background strain)	Breeding stock maintained in University of Strathclyde
PV-IRES-Cre	B6.129P2-Pvalb$^{tm1(cre)Arbr}$/J	017320	Hippenmeyer *et al.*, (2005)	Jackson Laboratories, Cold Harbor, USA
Ndnf-IRES-Cre	B6.Cg-*Ndnf*$^{tm1.1(folA/cre)Hze}$/J	028536	Tasic *et al.*, (2016)	Jackson Laboratories, Cold Harbor, USA
SOM-IRES-Cre	B6N.Cg-*SSt*-$^{tm2.1(Cre))Zhj}$/J	018973	Taniguchi *et al.*, (2011)	Jackson Laboratories, Cold Harbor, USA
Ai32	B6.Cg-*Gt(ROSA)26Sor*$^{tm32(CAG-COP4*H134R/EYFP)Hze}$/J	025109	Madisen *et al.*, (2012)	Jackson Laboratories, Cold Harbor, USA
Ai9	B6.Cg-*Gt(ROSA)26Sor*$^{tm9(CAG-tdTomato)Hze}$/J	007909	Madisen *et al.*, (2010)	Gift from Dr Hongkui Zeng, Allen Brain Institute, Seattle, USA
NPY-hrGFP	B6.FVB-Tg(Npy-hrGFP)1Lowl/J	006417	van den Pol *et al.*, (2009)	Gift from Prof Csaba Földy, University of Zurich, Switzerland

Table 2.1: Information for breeding mouse strains.

The resulting offspring therefore expressed both ChR2 and enhanced yellow fluorescent protein (eYFP) (the Ai32 reporter line), or the enhanced red fluorescent protein variant TdTomato (the Ai9 reporter line) in a Cre-dependent manner. These offspring strains are hence referred to as: PV-IRES-Cre::Ai32, Ndnf-IRES-Cre::Ai32, SOM-IRES-Cre::Ai32, PV-IRES-Cre::Ai9, SOM-IRES-Cre::Ai9 and Ndnf-IRES-Cre::Ai9.

Stereotaxic viral injections

PV-IRES-Cre mice (P31-48) or SOM-IRES-Cre mice (P34-44) were deeply anaesthetized via inhaled isoflurane (5% for induction; 1-2% for maintenance), transferred to a stereotaxic frame (Narishige, Tokyo, Japan) and were subcutaneously injected with the analgesics carprofen (5 mg/kg) in the nape and lidocaine (4 mg/kg) under the scalp. Intracranial injections were made using a glass micropipette pulled using a PC-100 vertical puller (Narishige, Tokyo, Japan). Under aseptic conditions, the skull was exposed and a small burr hole was drilled above the habenular complex, the ventral pallidum (VP) or the thalamic reticular nucleus (TRN) within the left hemisphere. The injection capillary was then advanced, and AAV vectors were injected into either the LHb, the medial dorsal thalamic nucleus (MDT), the VP or the TRN at a rate of 25 nl / min using a pressure micro-injector (Narishige, Tokyo, Japan). For these experiments, three different vectors were used. For optogenetic experiments, one of two Cre-dependent virions encoding ChR2

and eYFP were injected: ApAAV-EF1α-Switch:NLSmRuby2/ChR2(H134R)-EYFP41 HGHpA (Wozny *et al.*, 2018), an adeno-associated virus containing capsid protein 9 (titre: 2 x 10^{13} infectious particles / mL), or AAV1/2 Ef1α-DIO-hChR2-eYFP (titre: 1.6 x 108 infectious particles / ml), a hybrid of adeno-associated virus particles of serotypes 1 and 2 containing a 1:1 ratio of capsid proteins type 1 and 2 (a gift from Prof. Peer Wulff, Kiel, Germany). For retrograde tracing experiments, rAAV2-retro-FLEX-TdTomato was injected; a Cre-dependent retrograde virion encoding TdTomato (Tervo *et al.*, 2016). All parameters for stereotaxic viral injections can be found in table 2.2. Direction refers to either anterograde AAV injection (i.e. vector encoding ChR2 and eYFP), or retrograde AAV injection (i.e. rAAV2-retro-FLEX-TdTomato). All coordinates are referenced from bregma, in mm. AP = anterior-posterior, ML = medial-lateral. Note for the MDT injections, that the injection parameters were adjusted following data acquisition from the first round of experiments. Following injection, the needle was left for 10 minutes to allow the virus to diffuse before being slowly withdrawn. Animals were allowed to recover from anaesthesia on a heat pad. Following completion of surgery, animals were given at least two weeks to allow expression of the virus for local or short distance connections (LHb or MDT injections), or at least three weeks for long-distance connections (VP or TRN injections). Following this, acute slices were prepared (see below) for animals injected with vectors encoding ChR2 and eYFP, or animals were perfused intracardially (see below) where rAAV2-retro-FLEX-TdTomato had been injected and tissue sections were prepared on a Leica SM2010 R microtome (Leica Biosystems, Newcastle-upon-Tyne, UK).

In both cases, viral spread was assessed by counterstaining slices with DAPI, and imaging on a Leica SP5 or SP8 confocal microscope (Leica Biosystems, Newcastle-upon-Tyne, UK).

Marker	**Injection site**	**Direction**	**No. of mice**	**Age tested (days)**	**Volume of virus**	**AP**	**ML**	**Depth**
PV	LHb	Anterograde	8	46-70	50-100 nl	-1.50	-0.40	3.00
PV	MDT	Anterograde	2	58-63	200 nl	-1.355	-0.75	3.50
PV	MDT	Anterograde	4	62-70	200 nl	-1.155	-0.45	3.70
PV	TRN	Anterograde	2	64-64	100 nl	-1.8	-2.4	3.4
PV	LHb	Retrograde	3	65	100 nl	-1.255	-0.45	3.00
SOM	LHb	Anterograde	4	49-63	50 nl	-1.50	-0.40	3.00
SOM	VP	Anterograde	3	66-68	250 nl	0.145	-1.55	5.65
SOM	TRN	Anterograde	1	77	100 nl	-1.8	-2.4	3.4
SOM	TRN	Anterograde	1	59	100 nl	-1.355	-1.85	4.2
SOM	LHb	Retrograde	3	66	100 nl	-1.255	-0.45	3.00

Table 2.2: Parameters for stereotaxic injections.

Acute brain slice preparation

C57BL/6, PV-IRES-Cre::Ai32, PV-IRES-Cre::Ai9, Ndnf-IRES-Cre::Ai32, Ndnf-IRES-Cre::Ai9, SOM-IRES-Cre::Ai32, SOM-IRES-Cre::Ai9, and surgically injected PV-IRES-Cre or SOM-IRES-Cre mice (table 2.2) were humanely euthanized by cervical dislocation and immediately decapitated, and brains were rapidly removed and transferred to ice-cold oxygenated (0-2 ºC; 95% O_2; 5% CO_2) sucrose-based artificial cerebro-spinal fluid (ACSF) solution containing (in mM): sucrose 50, NaCl 87, $NaHCO_3$ 25, KCl 3, NaH_2PO_4 1.25, $CaCl_2$ 0.5, $MgCl_2$ 3, sodium pyruvate 3 and glucose 10. All data relating to testing strains of mice can be found in table 2.3. Sources and origins of all reagents can be found in table 2.4. Brains sections containing the habenular complex were then cut in the coronal plane at 250-300 µm on a Leica VT1200S vibratome (Leica Biosystems, Newcastle-upon-Tyne, UK). In order to ensure slices contained the habenular complex, the hippocampus was used as a visual guidance due to the easily identifiable structure and immediate proximity to the habenular complex (Paxinos and Franklin, 2012). Following sectioning, slices were incubated in oxygenated sucrose-based ACSF at 35 ºC for 30 minutes, and then incubated for a further 30 minutes at room temperature in ACSF containing (in mM) NaCl 115, $NaHCO_3$ 25, KCl 3, NaH_2PO_4 1.25, $CaCl_2$ 2, $MgCl_2$ 1, sodium pyruvate 3 and glucose 10. Following the incubation period, slices were maintained at room temperature in oxygenated ACSF.

Strain	Age (days)	No. of mice
C57BL/6	21-28	5
PV-IRES-Cre	46-70	19
PV-IRES-Cre::Ai32	23-40	19
PV-IRES-Cre::Ai9	23-33	10
SOM-IRES-Cre	49-77	12
SOM-IRES-Cre::Ai32	19-37	5
SOM-IRES-Cre::Ai9	24-28	3
Ndnf-IRES-Cre::Ai32	21-28	6
Ndnf-IRES-Cre::Ai9	21-36	5

Table 2.3: Data relating to testing animals for electrophysiology. PV-IRES-Cre and SOM-IRES-Cre animals are those animals surgically injected with an AAV encoding ChR2 as described in table 2.2.

Reagent	Source	Origin
Sucrose	Fisher Scientific	Loughborough, UK
NaCl	Sigma-Aldrich	Dorset, UK
$NaHCO_3$	VWR	Leicestershire, UK
KCl	VWR	Leicestershire, UK
NaH_2PO_4	Sigma-Aldrich	Dorset, UK
Sodium pyruvate	Sigma-Aldrich	Dorset, UK
Glucose	Sigma-Aldrich	Dorset, UK
$CaCl_2$ (dihydrate)	Fisher Scientific	Loughborough, UK
$MgCl_2$ (hexahydrate)	Fisher Scientific	Loughborough, UK
K-Gluconate	Dorset, UK	Dorset, UK

Hepes	Dorset, UK	Dorset, UK
EGTA	Dorset, UK	Dorset, UK
NaATP	Dorset, UK	Dorset, UK
NaGTP	Dorset, UK	Dorset, UK
Phosphocreatine Na	Dorset, UK	Dorset, UK
Biocytin	Dorset, UK	Dorset, UK

Table 2.4: Sources and origins of all reagents.

Electrophysiological recordings

Individual acute slices were transferred to a recording chamber and continually perfused with oxygenated ACSF at a flow rate of 2-3 ml / min, and visualized with a Luigs and Neumann LN-Scope System (Luigs and Neumann, Ratingen, Germany). The habenular complex is easily identifiable under differential interference contrast microscopy even at low magnification and hence a 4X objective was used to locate the lateral habenular nucleus. A 60X objective was then used to identify suitable neurons for whole-cell recordings. In the case of transgenic PV-IRES-Cre::Ai9, SOM-IRES-Cre::Ai9 or Ndnf-IRES-Cre::Ai9 slices, TdTomato-expressing neurons could be selectively visualized with an Olympus XM10 fluorescent camera (Olympus, Southend-on-Sea, UK) upon illumination with a blue LED (Cool LED, Andover, UK). Recordings were made with a Multiclamp 700B Amplifier (Molecular Devices, California, USA). Glass micropipettes (3-8 MΩ) were filled with a solution containing (in mM) potassium gluconate 125, HEPES 10, KCl 6, EGTA 0.2, $MgCl_2$ 2, Na-ATP 2,

Na-GTP 0.5, sodium phosphocreatine 5, and with 0.2 % biocytin. pH was adjusted to 7.2 with KOH. For spontaneous current measurement experiments, a reduced chloride intracellular solution was used consisting of (in mM) potassium gluconate 140, potassium chloride 2, EGTA 0.2, Hepes 10, NaATP 2, NaGTP 0.5 and sodium phosphocreatine 5.

Neuronal somata were approached by manoeuvring filled micropipettes with a digital micromanipulator system (Luigs and Neumann, Ratingen, Germany), while constantly applying positive pressure. Due to dense fibre innervation (Herkenham and Nauta, 1977), visibility within the LHb in acute slices is poor and hence these were typically 30-40 µm into the slice, which likely resulted in severed axonal and dendritic processes within recorded neurons.

Micropipette resistance was constantly monitored with a digital oscilloscope as the soma was approached. Increasing resistance and a visible 'dimple' on the cell membrane were taken as indicators that the micropipette was within proximity of the soma to achieve whole-cell patch configuration. Once suitably close to the soma, a 'gigaseal' (1-17 GΩ) was achieved between the micropipette and cell membrane, by a single negative pressure pulse. The cell membrane was then ruptured by applying a series of short negative pressure pulses.

Once in whole-cell configuration, the intrinsic properties of LHb neurons were assessed in current-clamp configuration using an injection of 1 s

increasing current steps (range: -250 to 250 pA; step size: 10 to 50 pA for LHb neurons and -500 to 1000 pA; step size 100 pA for cortical neurons). Action potential firing pattern was assessed in response to depolarizing current injection, while hyperpolarizing current injection allowed the characterisation of rebound action potential firing of neurons. Resting membrane potential (RMP) was assessed by recording the spontaneous activity of each neuron in current-clamp configuration with no current injection for at least 30 seconds, while membrane input resistance was monitored by injecting a small hyperpolarizing pulse (100 ms; -10 to -100 pA) and measuring the voltage change. Spontaneous currents were observed in voltage clamp at a holding potential of -60 mV. Series resistance was monitored throughout. All neuronal voltage and current signals were low pass-filtered at 10 kHz and acquired at 25 kHz using an ITC-18 digitizer interface (HEKA, Pfalz, Germany). The data acquisition software used was Axograph X.

Multi-cell recordings

To assess local connectivity between PV-positive LHb neurons and other LHb neurons, whole-cell patch configuration was achieved in two neurons simultaneously as described above and potential presynaptic neurons were held at -60 mV in current clamp configuration while potential postsynaptic neurons were held in voltage clamp and depolarized to -20 mV. Characterisation of synaptic connections between simultaneously patched

LHb neurons was achieved by repeatedly stimulating one neuron with a 2 ms depolarizing current injection sufficient to reliably generate a single action potential per pulse individually, or as a train of eight 10-20 Hz pulses, and measuring current change where a connection was identified in the postsynaptic neuron.

Optogenetic experiments and pharmacology

For optogenetic experiments, acute brain slices were prepared from transgenic PV-IRES-Cre::Ai32, SOM-IRES-Cre::Ai32 and Ndnf-IRES-Cre::Ai32 mice as above in darkness. Whole-cell patch configuration was achieved and neuronal recordings were obtained as slices were illuminated with a blue LED pulse (a single pulse of 2 to 200 ms, or a train of 2 ms pulses at 10 to 100 Hz) to elicit postsynaptic events. Where postsynaptic events were observed, these were recorded at various holding potentials in both current-clamp and voltage clamp to characterise the reversal potential of the event. Where required, SR-95531 (2 µM; henceforth referred to as GABAzine), NBQX (10 µM) or CGP-52432 (10 µM) (all from Tocris, Bristol, UK) were washed into the perfusion bath via the perfusion pump to test if the observed event was mediated by $GABA_A$-receptors, AMPA-receptors or $GABA_B$-receptors, respectively.

Immunohistochemistry and neuronal recovery

Each antibody used in this study was first validated by staining paraformaldehyde-fixed mouse brain tissue with the antibody at a variety of dilutions as recommended by the provider, and imaging the stained tissue using confocal microscopy to assess which dilution was optimal. Following electrophysiological recordings, slices containing neurons which had been patched and filled with biocytin were fixed overnight in 4% paraformaldehyde (PFA) dissolved in 0.1 M sodium-based phosphate buffered saline (PBS). After fixation, slices were washed 3 x 5 minutes in 0.1 M PBS, and then incubated for 1 hour in a blocking solution consisting of 5% normal goat serum (NGS) and 1% Triton X-100. Slices were then allowed to incubate on a shaker at room temperature overnight in a primary antibody mixture containing 2.5% NGS and 1% Triton in PBS along with the required primary antibodies. Primary antibodies and dilutions used in this study were: mouse anti-PV (1/4000; Swant, Marly, Switzerland) and rabbit anti-GABA (1/200; Sigma-Alrdrich, Dorset, UK). Upon completion of the primary incubation step, slices were washed 2 x 5 minutes in 0.1 M PBS and incubated for 2-3 hours in a secondary antibody cocktail containing the relevant secondary antibodies along with streptavidin as required (conjugated to Alex Fluor 488 or 647; 1/500 dilution; Life Technologies, Paisley, UK), in order to recover neurons which had been patched and filled with biocytin. The secondary antibodies used in this study were: donkey anti-mouse conjugated to Alexa Fluor 488 (1/500 dilution; Life Technologies, Paisley, UK), goat anti-rabbit conjugated to Alexa Fluor 555,

633 or 647 (1/500 dilution; Life Technologies, Paisley, UK) and supplemented with 1% Triton in PBS. Fluorophores excitable at differing wavelengths were implicated depending on whether the slice expressed YFP (Ai32 animals) or TdTomato (Ai9 animals) to minimize crosstalk. Where only neuronal recovery was required, slices were blocked as above and incubated in a solution containing streptavidin supplemented with 1% Triton in PBS. After secondary antibody incubation, slices were washed for 3 x 5 minutes in 0.1 M PBS and mounted on glass slides using Vectashield medium (containing DAPI as a counterstain as required, Vector Labs, Peterborough, UK) and cover-slipped.

Intracardial perfusion and serial sectioning

To prepare tissue for serial sectioning, PV-IRES-Cre::Ai32 (N = 2; P31-35), SOM-IRES-Cre::Ai9 (N = 2; P28); Ndnf-IRES-Cre::Ai32 (N = 2; P25), Ndnf-IRES-Cre::Ai9 (N = 2; P21), NPY-hrGFP (N = 2; P23), C57BL/6 (N = 3; P21-22), or PV-IRES-Cre (N = 3; P65) and SOM-IRES-Cre (N = 3; P66) mice surgically injected with rAAV2-retro-FLEX-TdTomato were terminally anaesthetized by subcutaneous injection with an overdose cocktail of 50% lidocaine and 50% euthatal. Once anaesthetized sufficiently to be non-responsive to noxious tail and toe pinch stimuli, mice were perfused through the left ventricle with 0.1 M PBS followed by perfusion with 4% PFA dissolved in PBS. Brains were then removed and fixed overnight in 4% PFA in PBS, after

which they were cryo-protected in a solution containing 30% (w/v) sucrose in PBS for storage until required for serial sectioning.

For these experiments, brains were embedded in OCT compound (VWR, Leicestershire, UK) and sectioned on a Leica SM2010 R microtome (Leica Biosystems, Newcastle-upon-Tyne, UK) at 60-80 µm. Upon completion of sectioning, slices were washed 3 x 5 min in 0.1 M PBS. Where further staining was required, this was carried out as above (see immunohistochemistry and neuronal recovery), however 0.3 % Triton X-100 was used in place of 1 % and slices were incubated overnight in primary antibody cocktails to minimize tissue damage. Slices were then mounted using Vectashield medium (containing DAPI as necessary, Vector Labs, Peterborough, UK) and cover-slipped.

Confocal Microscopy and neuronal reconstructions

Mounted sections were scanned on either a Leica SP5 or SP8 confocal microscope, imaging z-stacks of each slice at 2-4 µm steps. Confocal laser excitation wavelengths (in nm) were 405, 488, 514, 552 and 603. Objectives used were 10X (dry), 20X (oil immersion), 40X (oil immersion) and 63X (oil immersion) for Leica SP5, or 10X (dry), 20X (dry) and 63X (oil immersion) for SP8. A zoom of up to 2X was applied as required to occasionally visualize soma in enhanced detail. Sections were scanned to ensure that all visible streptavidin-stained cells and their neurites were included in the z-stack. In the

case of slices from animals that had been surgically injected with an AAV encoding either eYFP or TdTomato, viral spread was imaged using the 'navigator' feature of the Leica Application Suite software (Leica Biosystems, Newcastle-upon-Tyne, UK). 3D reconstructions of neurons were carried out using NeuTube 3D reconstruction software (Feng *et al.*, 2015).

Data analysis

Analysis of electrophysiological recordings was carried out using Axograph X. Passive intrinsic properties were calculated as described above, while active intrinsic properties (action potential initial frequency, amplitude, rise-time and half-width) were calculated by subtracting the baseline and then using the event detection feature to analyse the first action potential elicited in response to a 50 pA depolarizing pulse. Neuronal spontaneous activity was classified as either bursting (a clearly distinctive behaviour; Weiss and Veh, 2011), tonic or silent (where spontaneous action potential frequency was < 1 Hz). For optogenetically evoked events, peak size was measured at various holding potentials. For spontaneous current measurements, representative example traces of postsynaptic currents were first generated and currents were detected and measured using the event detection feature.

Image analysis was carried out using ImageJ. Confocal z-stacks were compressed into a single image and brightness and contrast were adjusted to enhance cellular visualization. Total numbers of immunoreactive neurons

were counted using the cell-counter plugin. For these experiments, serial sections from the habenular complex were imaged and analysed from one animal for each strain, and for remaining animals every second or third section was imaged and analysed to allow quantification of markers with fair representation of the habenular sub-nuclei. Images were then transferred to PowerPoint 2013 where cells of interest were marked.

Graphs were generated and statistical analysis was performed using GraphPad Prism 5 (California, USA). Statistical tests used were: two-tailed unpaired t-test for single comparisons of passive physiological properties; one-way ANOVA with Tukey's multiple comparison test for comparison of physiological properties between multiple groups; two-way ANOVA with Bonferroni's multiple comparison for assessing relationship between input current and action potential discharge (fI analysis), or Fishers' exact test. Once graphs were generated, they were transferred to PowerPoint 2013 for formatting and assembly into figures. Statistical significance thresholds for all tests were: * $p < 0.05$; ** $p < 0.01$; and *** $p < 0.001$.

Chapter 3: Ndnf and NPY do not act as selective markers for sub-populations of inhibitory neurons within the lateral habenula

Inhibitory signalling in the lateral habenula is comparable to that in the somatosensory cortex

The key theme of this project was to define and study populations of inhibitory neurons within the LHb, by implementing molecular markers known to represent sub-populations of inhibitory neurons within the neocortex (Tasic *et al.*, 2016; Tremblay *et al.*, 2016). While inhibitory signalling within the LHb is well-accepted (Lecca *et al.*, 2016; Meye *et al.*, 2016), the subject of locally-targeting inhibitory neurons within the LHb is still one of much debate (Brinschwitz *et al.*, 2010; Weiss and Veh, 2011; Wagner *et al.*, 2016a; Zhang *et al.*, 2018). If locally-targeting inhibitory neuronal populations similar to those in the neocortex were present here, then inhibitory signalling comparable to that in neocortex should also be observable.

To test this, spontaneous currents were recorded in both LHb neurons (n = 10; N = 5 mice) and L2/3 pyramidal neurons (n = 9; N = 4 mice) in the somatosensory cortex, in acute slices from C57BL/6 mice. Using a reduced-chloride intracellular solution (methods), it was possible to observe both excitatory and inhibitory currents simultaneously (Fig. 3.1a). The ratio of

excitatory to inhibitory events was first compared between regions. This was far greater in the LHb than in cortical neurons (Fig. 3.1b; 22.9 vs 2.3, respectively), suggesting that the balance of excitation to inhibition was far more shifted towards excitatory input in the LHb. However, inhibitory currents within the LHb could also clearly be observed (Fig. 3.1a). Furthermore, these were comparable to those recorded in cortical neurons in frequency (Fig. 3.1c; 0.1 ± 0.0 Hz vs 0.5 ± 0.3 Hz, respectively; $p = 0.23$; $F = 88.0$; $df = 17$; two-tailed unpaired t-test), amplitude (Fig. 3.1c; 13.8 ± 1.3 pA vs 12.6 ± 1.1 pA, respectively; $p = 0.49$; $F = 1.0$; $df = 12$ two-tailed unpaired t-test) and kinetics (Fig. 3.1d; rise time 1.3 ± 0.2 ms vs 1.0 ± 0.1 ms, respectively; $p = 0.11$; $F = 1.7$; $df = 12$; half-width 2.1 ± 0.3 ms vs 1.7 ± 0.4 ms, respectively; $p = 0.45$; $F = 2.1$; $df = 11$; decay 16.1 ± 3.4 ms vs 13.4 ± 4.1 ms, respectively; $p = 0.64$; $F = 2.0$; $df = 12$ two-tailed unpaired t-test). Taking this data into account, we asked whether these inhibitory events were therefore mediated by similar inhibitory neurons as those in the neocortex, by implementing the use of molecular markers specific for sub-populations of neocortical inhibitory neurons.

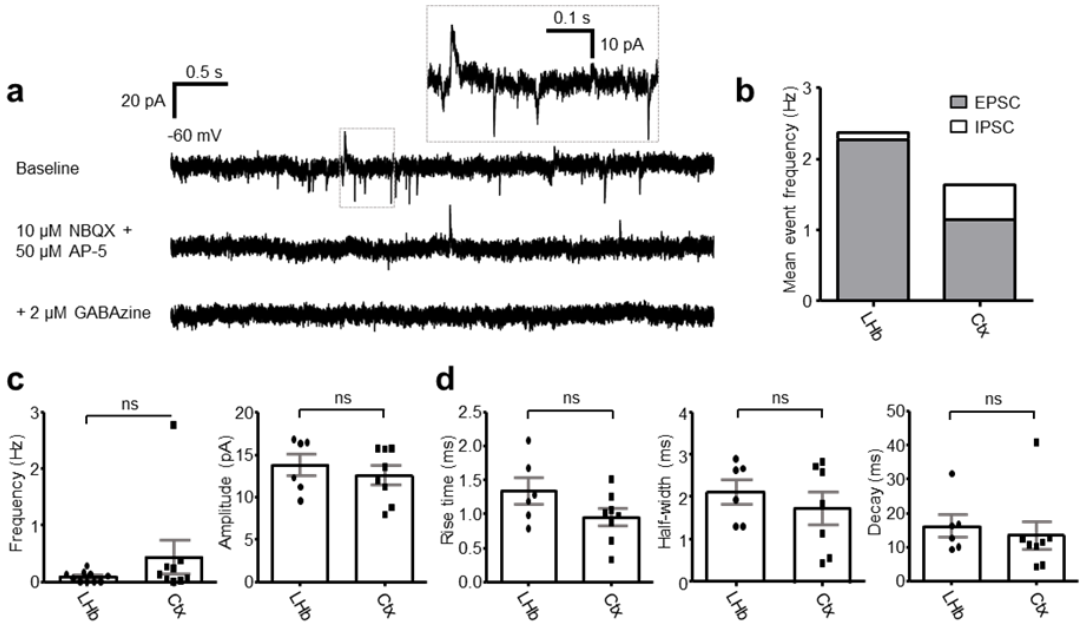

Figure 3.1: Spontaneous inhibitory currents within the lateral habenula and somatosensory cortex. (a) Example traces of spontaneous currents in an LHb neuron recorded in voltage clamp configuration. AMPA and NMDA-mediated excitatory currents and $GABA_A$-mediated inward currents could be observed simultaneously using a low-chloride intracellular solution. **(b)** Relative frequency of excitatory vs inhibitory currents in both LHb neurons (n = 10 neurons from 5 mice) and somatosensory cortex L2/3 pyramidal neurons (n = 9 neurons from 4 mice). **(c)** Comparison of frequency (left) and amplitude (right) between inhibitory currents in LHb neurons and L2/3 pyramidal neurons. Data are mean ± SEM. **(d)** Comparison of kinetics (rise time, half-width and decay) between inhibitory currents in LHb neurons and L2/3 pyramidal neurons. Note for 4 LHb neurons, and 1 cortical neuron, no inhibitory currents were observed. For these neurons, frequency value was 0 Hz. However, as

there were no measurable currents, these neurons have been excluded from analyses of current amplitude and kinetics.

Neurogliaform cells: a rare form of locally-targeting inhibitory neuron

The first class of neuron that we sought to investigate were neurogliaform cells. Neurogliaform cells are a rare class of inhibitory neuron known to be present in the neocortex (Tamás *et al.*, 2003; Olah *et al.*, 2007; Wozny and Williams, 2011), hippocampus (Vida *et al.*, 1998; Price *et al.*, 2005, 2008; Armstrong *et al.*, 2011), striatum (Ibanez-Sandoval *et al.*, 2011) and also thought to exist within the LHb (Weiss and Veh, 2011; Wagner *et al.*, 2016a). While their function is not entirely understood, they are known to mediate slow GABAergic signalling via volume transmission (Oláh *et al.*, 2009), whereby GABA spill-over from neurogliaform cell axon terminals can act on receptors outside of the synapse (Szabadics *et al.*, 2007; Karayannis *et al.*, 2010). This permits for prolonged GABAergic signalling lasting tens of milliseconds, and hence continuous tonic inhibition of large populations of excitatory neurons within the axonal 'cloud' of a single neurogliaform cell (Szabadics *et al.*, 2007; Oláh *et al.*, 2009). Additionally however, neurogliaform cells in the CA1 region of the hippocampus (Price *et al.*, 2008) and dentate gyrus (Armstrong *et al.*, 2011) are also known to mediate feed-forward inhibition of local excitatory neurons.

If a similar mechanism were to exist in the LHb, then one could speculate that potentiating excitatory input onto these neurons would have an antidepressant effect, via increased inhibition of local LHb neurons. Neurogliaform cells are well-known to mediate inhibitory signalling via $GABA_B$-receptors (Tamás *et al.*, 2003; Price *et al.*, 2008). Indeed $GABA_B$-signalling is present in the LHb, and dysfunction of this signalling is known to be implicated in driving depressive behaviour, while restoring $GABA_B$-signalling alleviates the depressive phenotype (Lecca *et al.*, 2016). However, whether this $GABA_B$-signalling arises from neurogliaform cells is still unknown. If this were to be the case, then evidently the dysfunction of these neurons would also be a driving factor in the pathogenesis of MDD. While these ideas are as-of-yet largely speculation, they certainly make studying the functionality of these neurons within the LHb an interesting prospect.

Absence of NPY-positive neurons within the lateral habenula

However, the problem in studying these neurons in other brain regions has been the lack of selective molecular markers (Overstreet-Wadiche and McBain, 2015). As previously mentioned (introductory chapter), Neuropeptide Y (NPY) has classically been used as one such marker in cortical circuits (Tricoire *et al.*, 2010; Overstreet-Wadiche and McBain, 2015), in that it is expressed by almost all neurogliaform cells, but also has the limitation that it is expressed by other neuronal populations.

The first question asked was therefore if similarly, NPY acted as a selective marker for a particular population of inhibitory neurons within the LHb. To test this, we first made use of NPY-hrGFP mice, which express green fluorescent protein (GFP) in NPY positive neurons throughout the brain (van den Pol *et al.*, 2009). Brains from these mice (N = 2) were sectioned in the coronal plane at 60 µm thickness and imaged on a confocal microscope. To first confirm that GFP expression was indeed confined to NPY-positive neurons, the neocortex and dentate gyrus were imaged (Fig. 3.2a), where NPY expression is well-documented (Karagiannis *et al.*, 2009; Tricoire *et al.*, 2010). Consistent with these reports, GFP-positive somata were observed throughout these structures, including neocortical layer 1 where neurogliaform cells are known to be localized (Tamás *et al.*, 2003; Wozny and Williams, 2011), thus validating that GFP-expression was indeed confined to NPY-positive neurons, including neurogliaform cells, in the NPY-hrGFP transgenic line.

We next imaged the LHb in serial coronal sections (N = 2 mice), thus allowing imaging of GFP-expression throughout the whole LHb in the rostro-caudal axis (Fig. 3.2b). In contrast to both the neocortex and the dentate gyrus, no GFP-positive neuronal somata were observed within this structure. Some sparse fibres were observed however (Fig. 3.2b), indicating that while the LHb likely receives long-distance input from NPY-positive neurons in upstream regions, no locally-targeting NPY-positive neurons exist within the LHb. Thus we conclude that NPY does not act as a selective marker for inhibitory neurons within the LHb.

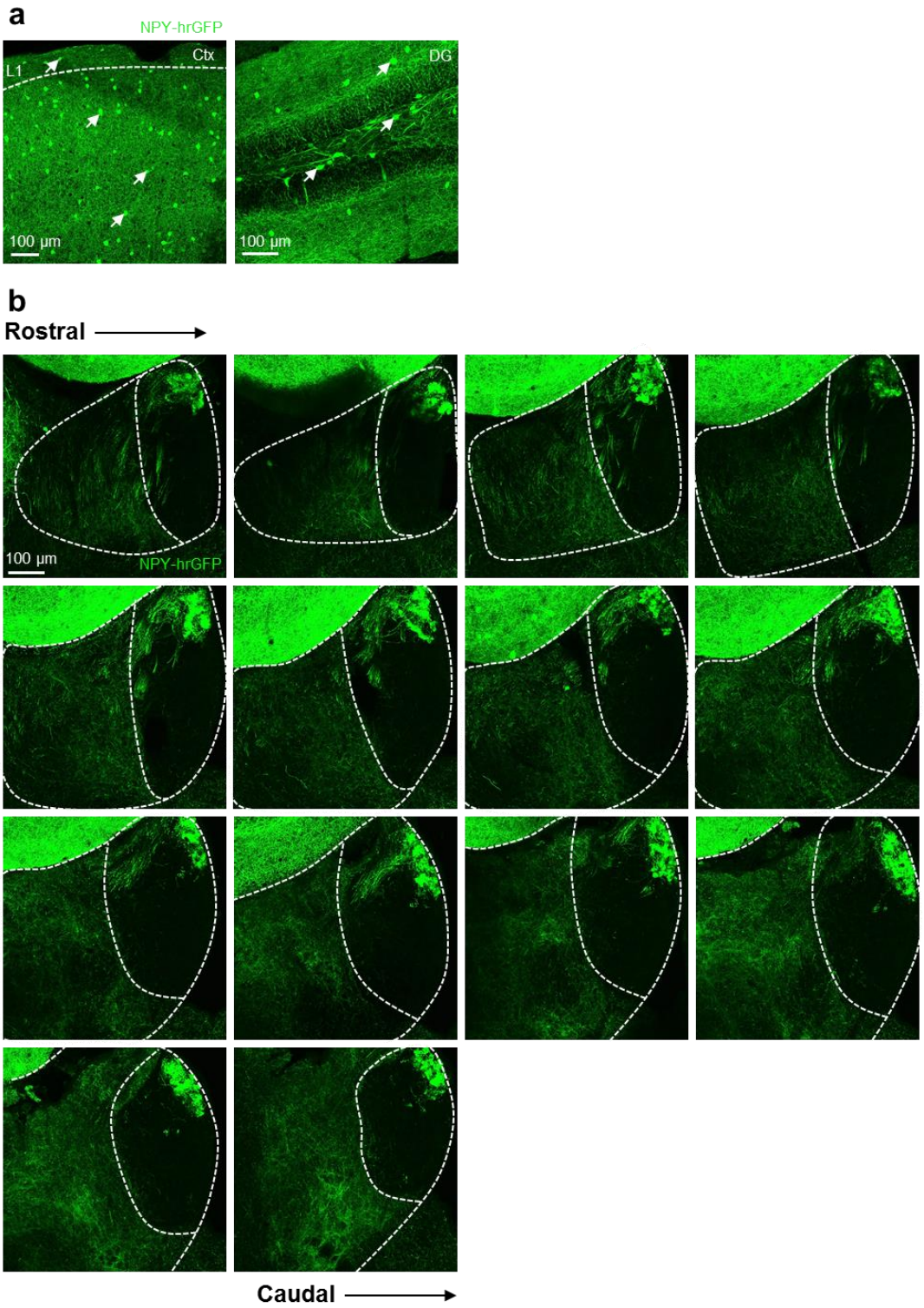
a
NPY-hrGFP
Ctx
L1
100 μm
DG
100 μm
b
Rostral
100 μm
NPY-hrGFP
Caudal

Figure 3.2: Absence of NPY-positive neuronal somata within in the LHb. **(a)** Confocal micrographs of the neocortex (Ctx) and dentate gyrus (DG) depicting GFP-expression throughout these structures. Arrows indicate GFP-positive neuronal somata. **(b)** Confocal micrographs of habenular sections from NPY-hrGFP mice (N = 2) depicting GFP-expression throughout the LHb in the rostral-caudal plane. Images are maximum intensity projections of 50 µm tissue. Note that no GFP-positive somata are located within the LHb.

Ndnf: a novel marker for neocortical neurogliaform cells?

More recently however, Neuron-derived neurotrophic factor (Ndnf) has been proposed as a selective marker for L1 neurogliaform cells in the neocortex (Tasic *et al.*, 2016); however further studies have since argued that this protein is also not entirely confined the these neurons (Abs *et al.*, 2018; Tasic *et al.*, 2018). Although this project was primarily concerned with the LHb, we first sought to test the validity of this protein as a marker for L1 neurogliaform cells in the somatosensory cortex, as this is still a subject of debate.

Ndnf-IRES-Cre mice were crossed with Ai9 reporter mice, to generate offspring which expressed TdTomato in Ndnf-positive neurons (Fig. 3.3a). Brains from these offspring (N = 2) were sectioned at 60 µm, and co-stained with an antibody against GABA to quantify the proportion of TdTomato-positive neurons which were GABAergic (Fig. 3.3b and c). Confocal imaging revealed that while TdTomato-expression was largely confined to neocortical L1, some

TdTomato-positive neurons were also observed in deeper layers (Fig. 3.3b). Consistently, most (75.8 % of 33) but not all TdTomato-positive neocortical neurons co-stained with GABA, indicating that not all were inhibitory.

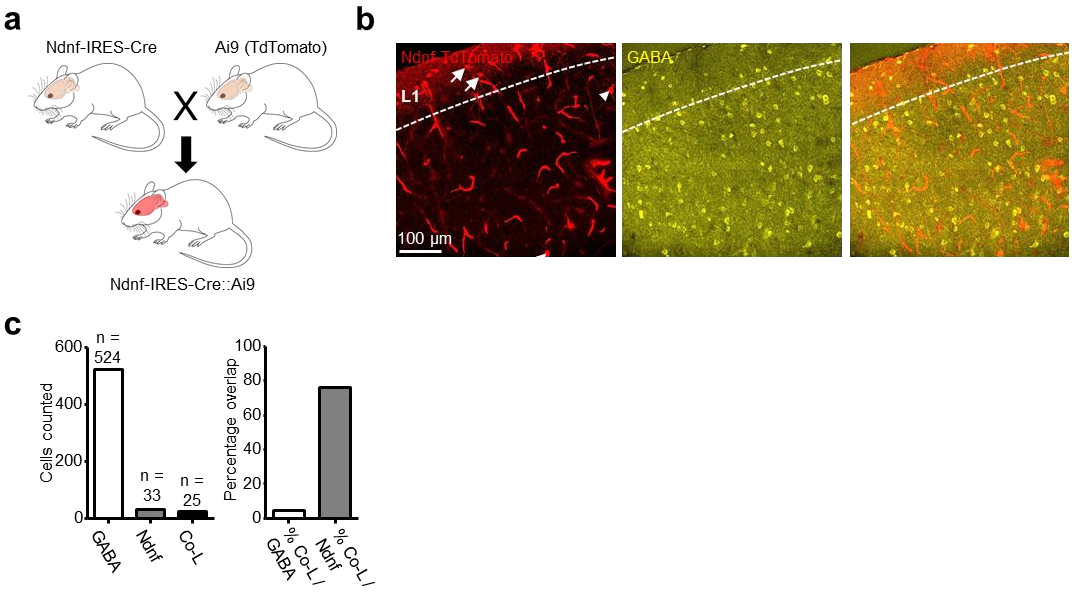

Figure 3.3: Ndnf is expressed selectively but not exclusively by GABAergic L1 neurons in the somatosensory cortex. (a) Schematic illustrating breeding scheme for generating Ndnf-IRES-Cre::Ai9 mice. **(b)** Confocal micrograph from Ndnf-IRES-Cre::Ai9 slices depicting TdTomato-positive neurons in L1 of the somatosensory cortex (arrows), but also a TdTomato-positive neuron in the deeper somatosensory cortex which was not immunoreactive for GABA (arrowhead). **(c)** Left: bar chart quantifying total number of GABA-immunoreactive, and TdTomato-positive neurons counted and the number which co-expressed both (N = 2 mice). Right: fraction of

neurons expressing both markers as a percentage of GABA-immunoreactive neurons, and as a percentage of TdTomato-positive neurons.

Assuming that Ndnf-positive neocortical neurons are mostly L1 neurogliaform cells, then Ndnf-positive neurons in the neocortex should provide inhibitory input to local excitatory neurons (Wozny and Williams, 2011). To test this, ChR2 was expressed in Ndnf-positive neurons by crossing Ndnf-IRES-Cre mice with Ai32 reporter mice (Fig. 3.4a). We made acute slices from these mice (N = 6), and recorded postsynaptic potentials in L2/3 pyramidal neurons (n = 7) elicited upon photostimulation (Fig. 3.4b). Large inhibitory postsynaptic potentials (IPSP) were observed in all pyramidal neurons recorded. However in two neurons application of $GABA_A$ and $GABA_B$ antagonists unmasked a small excitatory postsynaptic potential (EPSP; Fig. 3.4c and d), implying that Ndnf is also expressed by some excitatory neurons either within or projecting to the neocortex.

As inhibitory signalling mediated by neurogliaform cells is known to have slower kinetics than inhibitory signalling mediated by other interneuron sub-classes (Tamás *et al.*, 2003; Price *et al.*, 2005, 2008; Wozny and Williams, 2011), we also expressed ChR2 in PV-positive neurons (termed PV-IRES-Cre::Ai32 mice) and compared L2/3 pyramidal neuron postsynaptic potentials in Ndnf-IRES-Cre::Ai32 slices to those in PV-IRES-Cre::Ai32 slices (Fig. 3.4e; n = 7; N = 6 mice) upon photostimulation. Consistently, we observed large

IPSPs with comparable amplitude in both lines, but with slower kinetics in the Ndnf-IRES-Cre::Ai32 slices (Fig. 3.4e) indicative of a larger $GABA_B$-component. Finally, post-hoc confocal imaging of these slices also revealed that, consistent with the Ndnf-IRES-Cre::Ai9 line (Fig. 3.3), eYFP-positive neurons were mostly, but not exclusively, confined to neocortical L1 (Fig. 3.4f).

Altogether, these results are consistent with the recent literature (Tasic *et al.*, 2016, 2018; Abs *et al.*, 2018) in that we find Ndnf to be a relatively selective marker for L1 neurogliaform cells in the neocortex, but it is also expressed by some non-inhibitory neurons outside of L1.

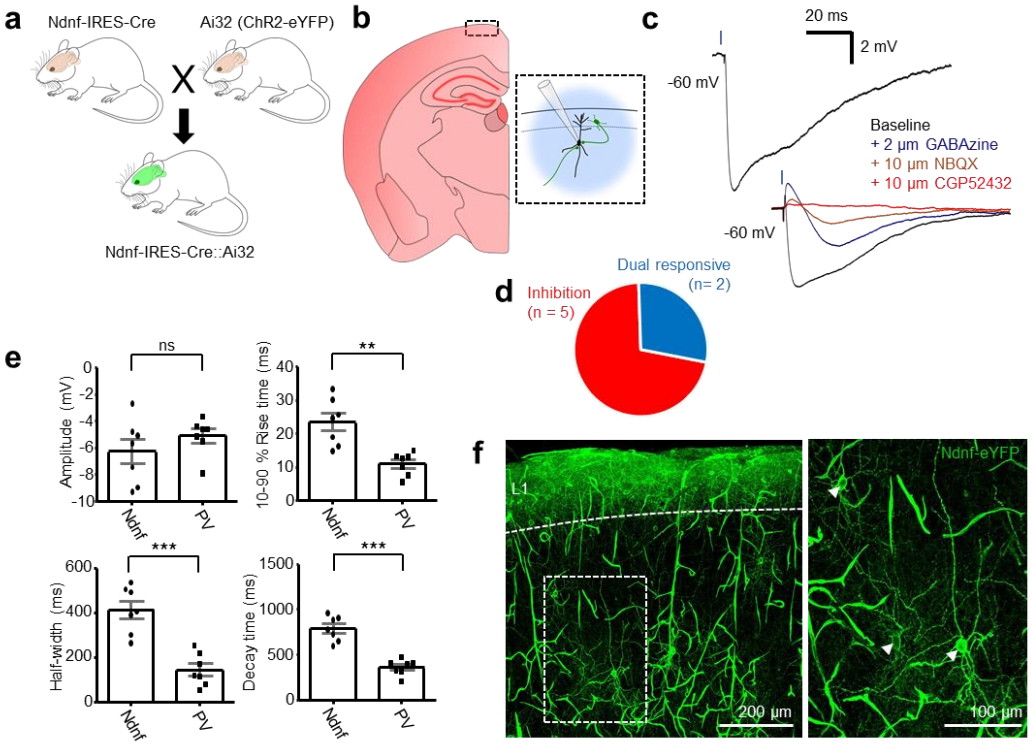

Figure 3.4: Ndnf-positive neurons provide primarily inhibitory input to local pyramidal neurons. (a) Schematic illustrating breeding scheme for generating Ndnf-IRES-Cre::Ai32 mice. **(b)** Schematic of recording scheme. L2/3 pyramidal neurons were patched and blue light was used to stimulate both local and long-distance Ndnf-positive neurons. **(c)** Example traces from a neuron displaying an IPSP in response to photostimulation (top) and from one neuron in which an NBQX-sensitive EPSP was unmasked upon application of GABAzine (bottom). **(d)** Pie chart quantifying nature of postsynaptic potentials elicited in response to photostimulation. n = 7 neurons. **(e)** Scatter plots comparing amplitude (-6.3 ± 0.9 mV vs -5.1 ± 0.5 mV; p = 0.29; F = 3.1; df = 12; two-tailed unpaired t-test) and kinetics (rise time 23.5 ± 2.7 ms vs 11.1 ± 1.3 ms; p = 0.001; F = 4.2; df = 12; half-width 414.6 ± 39.1 ms vs 146.0 ± 27.6 ms; p = 0.0001; F = 2.0; df = 12; decay 787.4 ± 51.9 ms vs 361.3 ± 32.8 ms; $p < 0.0001$; F = 2.5; df = 12; two-tailed unpaired t-test) of photostimulation-induced IPSPs in Ndnf-IRES-Cre::Ai32 slices vs PV-IRES-Cre::Ai32 slices. **(f)** Left: confocal micrograph depicting localization of eYFP-positive neurons in the somatosensory cortex. Right: zoom-in of the same image on left showing Ndnf-positive neurons not located within neocortical L1 (arrowheads).

Ndnf is not selectively expressed by inhibitory neurons within the lateral habenula

With this data in mind, we next asked whether we could implicate our Ndnf transgenic line to study neurogliaform cells, or other specific populations of inhibitory neurons, within the LHb with a similar degree of reliability. As with the neocortex, Ndnf-IRES-Cre::Ai9 mice were generated (Fig. 3.5a) and brains from these mice (N = 2) were sectioned coronally, co-stained with GABA, and the LHb was imaged in the rostro-caudal axis. TdTomato-positive neuronal somata could be clearly observed within the LHb (Fig. 3.5b). However, only a fraction of these (14.3 % of 126) co-stained with GABA (Fig. 3.5ci), indicating that the majority of TdTomato-positive LHb neurons are not inhibitory. In a subset of slices (n = 5), the fraction of TdTomato-positive and GABA-immunoreactive neurons as a percentage of total LHb cells was also quantified (Fig. 3.6cii). TdTomato-positive neurons represented 0.9 % of total LHb cells, and 0.1 % of total LHb cells were GABAergic TdTomato-positive neurons (Fig. 3.5cii).

To gain a better insight into the characteristics of Ndnf-positive LHb neurons, we also characterised their physiological properties in acute slices from Ndnf-IRES-Cre::Ai9 mice (n = 29; N = 5 mice), by patching and recording from TdTomato-positive neurons throughout the LHb (Fig. 3.5d). In two of these cells, action potential discharge could not be elicited upon current injection and hence these were assumed to be glial cells and excluded from further analysis. Physiological properties were assessed in the remainder (n =

27) and no difference was observed in resting membrane potential in comparison to recordings from the general population of neurons in wild-type C57/BL6 mice (Fig. 3.5e; n = 28 from 5 C57BL/6 mice; -54.6 ± 1.3 vs 55.2 ± 1.4; p = 0.78; F = 1.2; df = 53 for TdTomato-positive vs general population neurons; two-tailed unpaired t-test). We did, however, observe a significant difference in input resistance (Fig. 3.5e; 775.9 ± 76.5 vs 544.0 ± 53.3 for TdTomato vs general population; p = 0.03; F = 2.2; df = 50; two-tailed unpaired t-test), and we also observed an overall difference in the relationship between input current and action potential discharge frequency (Fig. 3.5f; p = 0.0008; F = 11.5; df = 1; two-way ANOVA; n = 23 neurons tested) in comparison to the general population (n = 28 neurons tested). This was likely due to the fact that many recorded TdTomato-positive neurons were located on the boundary with the medial habenula (Fig. 3.5d; n = 9), where neurons are known to have very high input resistances (Choi *et al.*, 2016) and different firing patterns (Kim and Chang, 2005). This finding also supports the notion of the recently identified intermediary region between the lateral and medial habenula consisting of intermingled neurons from both regions (Wagner *et al.*, 2016b). Otherwise, physiological properties of TdTomato-positive LHb neurons were largely consistent with previously described LHb neuronal physiologies (Chang and Kim, 2004; Kim and Chang, 2005; Weiss and Veh, 2011) in that almost all (n = 22 from 24 neurons tested) displayed rebound action potential discharge upon hyperpolarizing current injection, and a combination of tonic and bursting action potential discharge upon depolarizing current injection (Fig. 3.5gi). We also reconstructed a small subset of these neurons (n = 5) and observed that

all neurons reconstructed exhibited 4-6 primary dendrites, and a long unbranching axon (Fig. 3.5gii), therefore lacking the characteristic axonal arbour that is a hallmark of neocortical neurogliaform cells (Overstreet-Wadiche and McBain, 2015). Hence, we conclude that Ndnf-expression in the LHb is not exclusively confined to neurogliaform cells, or other inhibitory neurons, but rather appears to be expressed mostly by stereotypical LHb neurons.

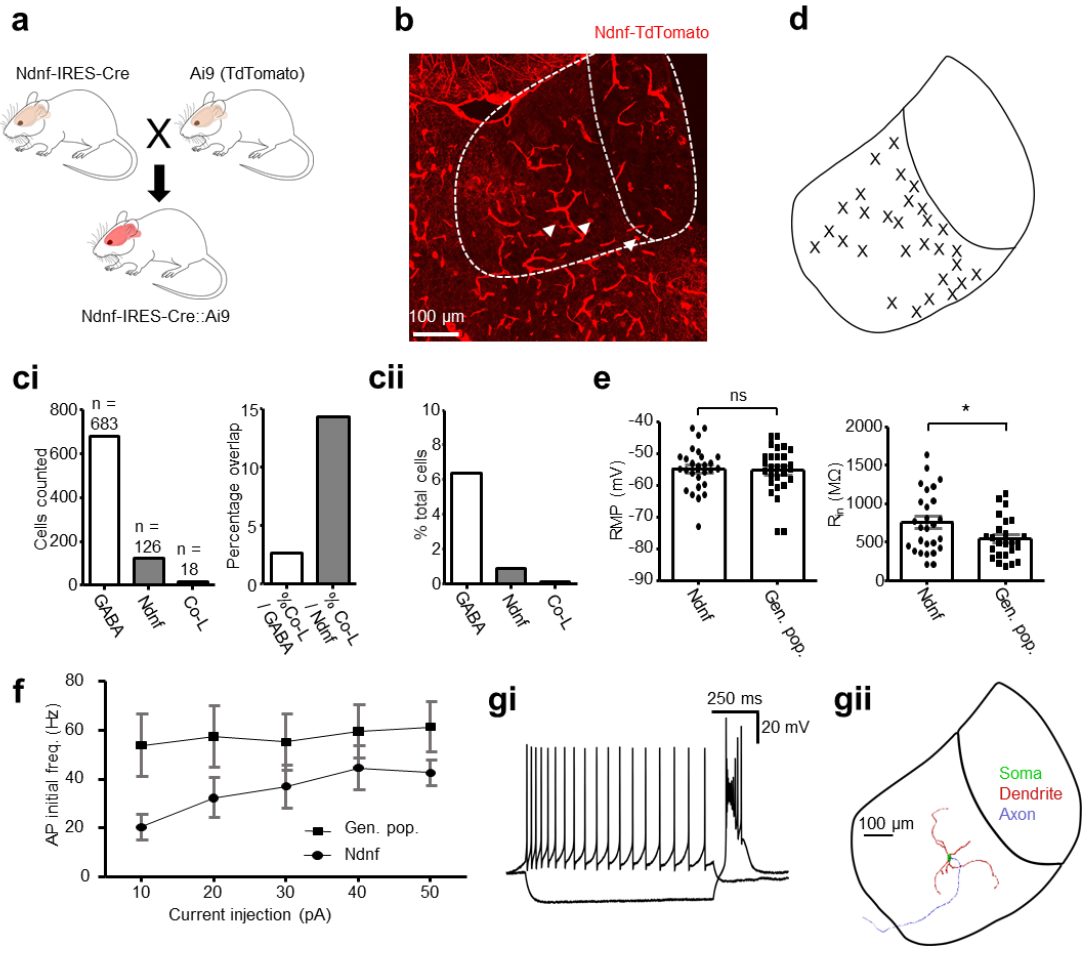

Figure 3.5: Ndnf-positive neurons are primarily non-inhibitory within the LHb. (a) Schematic illustrating breeding scheme for generating Ndnf-IRES-Cre::Ai9 mice. **(b)** Confocal micrograph from an Ndnf-IRES-Cre::Ai9 mouse depicting TdTomato-positive neurons within the LHb (arrowheads). **(ci)** Left: bar chart quantifying total number of GABA-immunoreactive, and TdTomato-positive neurons counted and the number which co-expressed both (N = 2 mice). Right: fraction of neurons expressing both markers as a percentage of GABA-immunoreactive neurons, and as a percentage of TdTomato-positive neurons. **(cii)** Fraction of neurons expressing either GABA, TdTomato or both markers as a fraction of total cells (using DAPI as a proxy for cell count). **(d)** Schematic illustrating location of patched neurons throughout the habenular complex. In this case, all neurons recorded have been compressed onto one schematic to allow clear visualization of neurons recorded near the border with the medial habenula vs throughout the rest of the LHb. **(e)** Comparison of passive properties of TdTomato-positive LHb neurons (n = 27; N = 5 mice) and from the general population of LHb neurons recorded in C57 mice (n = 28; N = 5 mice). Data are mean ± SEM. **(f)** Comparison of firing frequency of the first induced action potential versus current injection for both TdTomato-positive LHb neurons (n = 18; N = 8 mice) and the general population of LHb neurons (n = 28; N = 5 mice) recorded in C57 mice. Data are mean ± SEM. An overall difference was observed in the response to current injection between TdTomato-positive neurons and the general population (p = 0.0008; F = 11.5; df = 1; two-way ANOVA), however no difference was observed for any individual current injection value (p > 0.05; Bonferroni's multiple

comparison test) **(gi)** Example traces from a TdTomato-positive neuron in response to current injection. Current steps: -50 pA and 50 pA; 1 s duration. (**gii**) Example morphological reconstruction from an Ndnf-positive neuron. All reconstructed neurons (n = 5) displayed 4-6 primary dendrites and a single unbranching axon.

However, the majority of LHb neurons are known to be projection neurons (Brinschwitz *et al.*, 2010) and thus, if these non-GABAergic Ndnf-positive neurons fell into this category, then it would be unlikely that they would make local contacts. Indeed, the majority of Ndnf-positive LHb neurons displayed physiology and morphology similar to what is known for the general population of LHb neurons (Fig. 3.5e and f), and therefore one would predict that these are projection neurons. Theoretically then, even if only a fraction of Ndnf-positive LHb neurons were inhibitory as the data suggests (Fig. 3.5ci), one could expect that these would be more likely to synapse with other local neurons. To first verify the presence of local Ndnf-positive fibres within the LHb, we expressed eYFP in Ndnf-positive neurons (termed Ndnf-IRES-Cre::Ai32 mice), and imaged the LHb in the rostro-caudal axis (N = 2 mice) to observe both eYFP-positive somata and fibres. Both somata and fibres could clearly be observed throughout the whole of the LHb (Fig. 3.6). Thus we asked if these mediated inhibitory transmission.

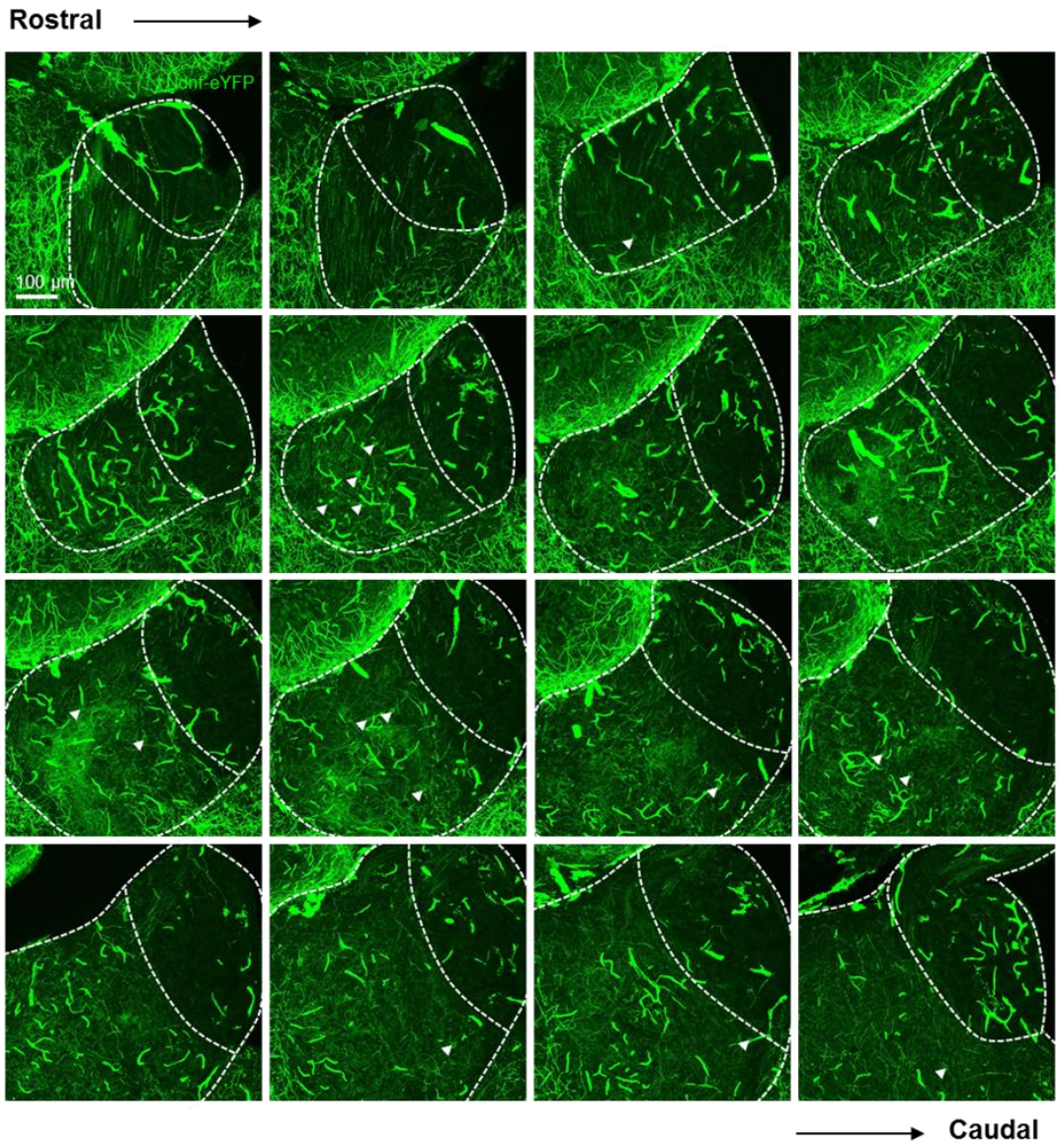

Figure 3.6: **Localization of Ndnf-positive neuronal somata and processes throughout the LHb.** Confocal micrographs of habenular sections from Ndnf-IRES-Cre::Ai32 mice (N = 2) depicting eYFP-expression throughout the LHb in the rostral-caudal plane. Images are maximum intensity projections of the most superficial 30 µm of tissue from 60 µm slices. Arrowheads indicate eYFP-positive neurons.

Using the same mouse line, ChR2 was also expressed in Ndnf-positive neurons (Fig. 3.7a). We created acute slices from these mice (N = 6) and recorded postsynaptic potentials in LHb neurons (Fig. 3.7b; n = 21) in response to photostimulation. In the LHb, most responsive neurons (n = 5 of 6) displayed a solely excitatory postsynaptic potential, while one neuron displayed a postsynaptic potential with both an NBQX-sensitive excitatory component and a GABAzine-sensitive inhibitory component (Fig. 3.7c and d). Consistent with the imaging data (Fig. 3.6), these responses were spread fairly evenly throughout the LHb (Fig. 3.7e). Therefore, while Ndnf-positive fibres are located within the LHb, these appear not to arise from local inhibitory neurons and are presumably excitatory projection fibres from upstream regions. Hence, the overall finding from this body of work is that Ndnf cannot be used as a selective marker to study inhibitory neurons within the LHb, but rather is broadly expressed by excitatory neurons which are most likely projection neurons.

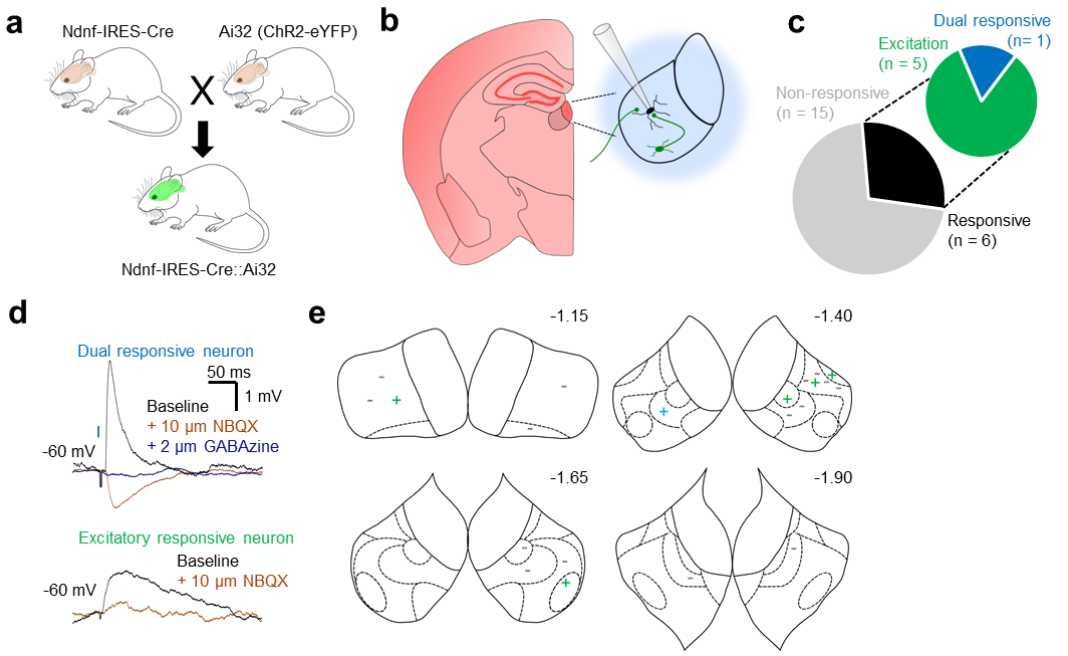

Figure 3.7: Ndnf-positive neurons mediate primarily excitatory transmission within the LHb. (a) Schematic illustrating breeding scheme for generating Ndnf-IRES-Cre::Ai32 mice. **(b)** Schematic of recording scheme. LHb neurons were patched and blue light was used to stimulate both local and long-distance Ndnf-positive neurons. **(c)** Pie chart quantifying fraction of neurons responsive to photostimulation, and the nature of those responses. **(d)** Example traces from two separate neurons in which photostimulation elicited a response with both an NBQX-sensitive excitatory component, and a GABAzine-sensitive inhibitory component (top) and from a neuron in which photostimulation elicited an excitatory response (bottom). **(e)** Schematic illustrating locations of patched neurons within the habenular complex, projected rostrally (top left) through caudally (bottom right). Non-responsive neurons are indicated by – while responsive neurons are indicated by: + EPSP only; + dual response. Sub-nuclear boundaries as defined by Andres et al.,

(1999) are indicated by dashed lines. Approximate rostral-caudal distances from Bregma (in mm) are indicated.

Discussion

In this chapter, we sought to first test the validity of Ndnf as a selective marker for inhibitory neocortical neurogliaform cells, and then asked if Ndnf or NPY could act as such a marker in the LHb. Consistent with recent reports (Tasic *et al.*, 2016, 2018; Abs *et al.*, 2018), we find that Ndnf is expressed mostly, but not exclusively, by inhibitory L1 neurons within the neocortex. However, within the LHb we report that neither of these proteins acts as a selective marker for any sub-population of inhibitory neuron within the LHb, and instead report that the majority of input to LHb neurons from Ndnf-positive neurons is excitatory.

Evidence for the existence of neurogliaform cells within the lateral habenula

Evidence in favour of the existing of locally-targeting neurogliaform cells within the LHb is currently very sparse (Weiss and Veh, 2011; Wagner *et al.*, 2016b), and from this work we can provide no further evidence in favour of this. A possible explanation for the discrepancy between these results and the published literature could simply be a species difference, as previous work was carried out in rats (Weiss and Veh, 2011; Wagner *et al.*, 2016b), while this

work was carried out in mice. Nonetheless, we did observe GABA-immunoreactive Ndnf-positive LHb neurons. However, these only represent a small fraction of Ndnf-positive neurons (14.3 %; Fig. 3.5c), and indeed background staining with our anti-GABA antibody is very high; hence this may even be an over-estimation. We did attempt to manipulate these neurons in preliminary experiments by injection of a Cre-dependent ChR2-encoding AAV into the LHb of Ndnf-IRES-Cre mice, and observed no viral transduction (data not shown). Hence, while it is therefore possible that neurogliaform cells are present within the mouse LHb, we conclude that neither Ndnf nor NPY can be used as a marker to study them.

A need for more selective markers to study neurogliaform cells in the lateral habenula

This lack of neurogliaform cell specificity of these two markers is in contrast to the neocortex (Tricoire *et al.*, 2010; Overstreet-Wadiche and McBain, 2015; Tasic *et al.*, 2016, 2018; Abs *et al.*, 2018). This then raises an interesting point of discussion regarding whether a neuron can truly be sub-classified into a distinct sub-population based on gene expression. Indeed, molecular marker expression has classically been thought of as one of the key criteria for defining populations of interneurons (Ascoli *et al.*, 2008). However, the presence of these neurons within the LHb has previously been proposed based on a similar morphological and physiological profile to those in the

neocortex (Weiss and Veh, 2011; Wagner *et al.*, 2016a). Therefore, if the genetic profile of such a neuron were to be entirely different to its' neocortical counterpart, one could argue that it may be an entirely different sub-population of neuron. This can be complicated further by the matter that there is still debate as to the criteria by which neurogliaform cells can be differentiated from other L1 neurons within the neocortex (Schuman *et al.*, 2019). Therefore, a clearer definition of these neurons is still required, as are more selective markers. Meeting these conditions will permit studying the circuitry and function of these neurons in far greater detail both within the neocortex and the LHb, and perhaps future work may reveal that these proposed LHb neurogliaform cells are in fact an entirely novel sub-class of inhibitory neuron altogether.

Chapter 4: Inhibitory input to the lateral habenula arises from two distinct sources of PV-positive neurons

The role of PV-positive neurons in mediating the balance of excitation to inhbition

Parvalbumin-positive (PV) neurons are a very well-established class of inhibitory interneuron in several major brain regions including the neocortex (Tremblay *et al.*, 2016), the hippocampus (Klausberger and Somogyi, 2008) and the striatum (Tepper *et al.*, 2011). These neurons generally exhibit a fast-spiking phenotype and are known to powerfully inhibit local excitatory neurons within the neocortex (Atallah *et al.*, 2012) and the hippocampus (Ognjanovski *et al.*, 2017). These neurons are therefore central in controlling the ratio of excitatory to inhibitory signalling (Ferguson and Gao, 2018) and as such dysfunctions in these neurons results in an unbalancing of this ratio and a shift in favour of excitatory signalling. This is known to become manifest as serious psychiatric diseases such as autism and schizophrenia (Marín, 2012; Ferguson and Gao, 2018).

Whether similar neurons mediate inhibitory signalling within the LHb remains unknown. It is now well-established that in depression, the balance of excitatory to inhibitory input to the LHb is largely shifted in favour of excitatory input (Li *et al.*, 2011; Shabel *et al.*, 2014; Lecca *et al.*, 2016; Tchenio *et al.*,

2017). Thus, if a similar class of neuron were to exist here and serve a similar function in controlling the ratio of excitation to inhibition, then one would expect that these neurons would indeed be dysregulated in depression.

PV-positive lateral habenular neurons form multiple physiologically distinct sub-classes

Considering the previous data that the kinetics and frequency of inhibitory events within the LHb are comparable to those within the neocortex (Fig. 3.1), we therefore sought to clarify if similar inhibitory PV-positive neurons were present within the LHb, and if so, if they mediated local inhibitory signalling.

We first sectioned the brains of C57BL/6 mice (N = 3) and co-stained with an antibody against GABA, and one against PV, and imaged the LHb in serial sections in the rostro-caudal axis, and the somatosensory cortex for comparison. Almost all (98.13 %) of PV-immunoreactive neocortical neurons were found to be GABAergic (Fig. 4.1a and b), thus validating the specificity of both antibodies. Within the LHb, the majority of PV-immunoreactive neurons were non-GABAergic (Fig. 4.1c and e) and appeared to be mostly localized within two distinct clusters; one within the medial LHb and one within the lateral LHb along the rostral-caudal axis (Fig. 4.1d). However, a sub-population of these neurons (8.8 %) displayed very bright GABA co-labelling and were to be confined to the lateral portion of the LHb (Fig. 4.1c and d). Therefore, while these results indicate that the majority of PV-positive LHb

neurons are not GABAergic, they do suggest that a sub-population of these neurons are indeed inhibitory.

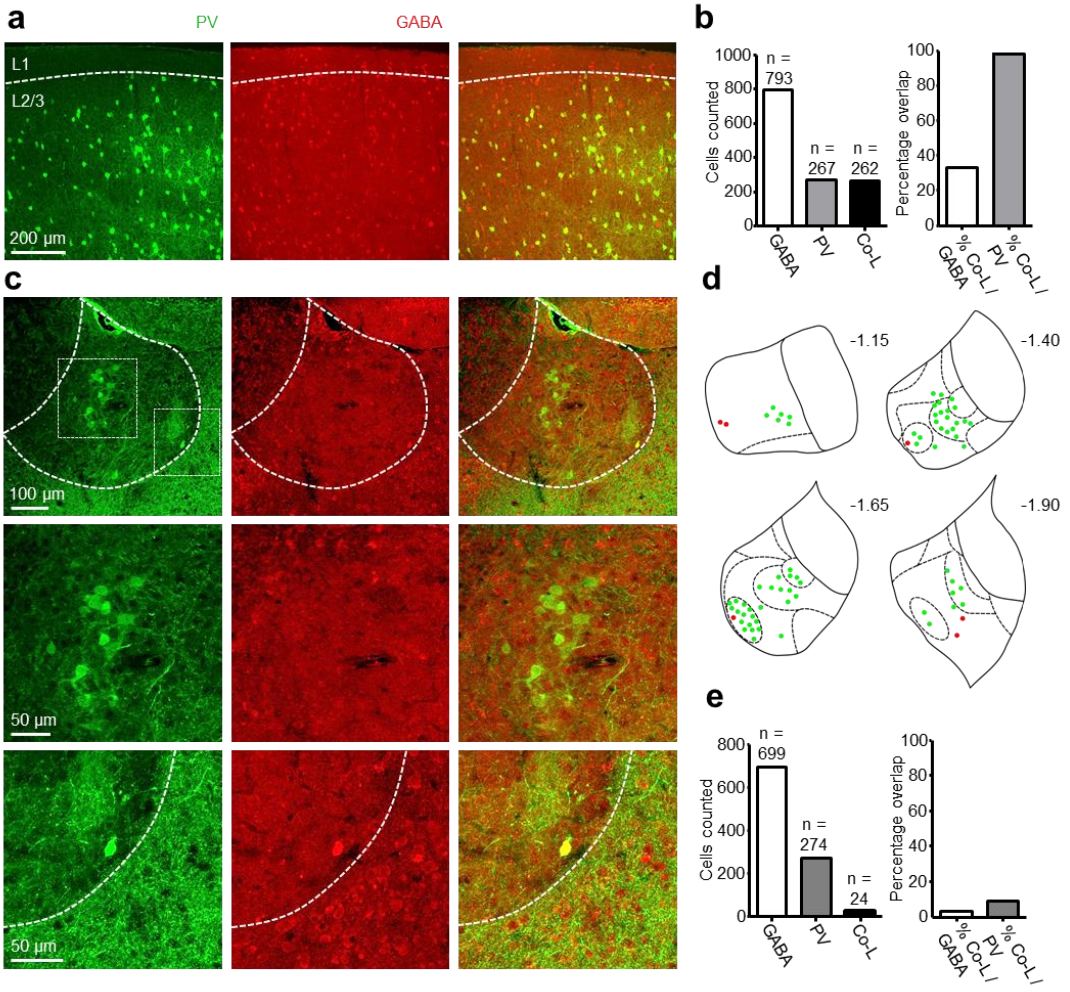

Figure 4.1: PV-immunoreactive neurons within the lateral habenula are primarily non-GABAergic. (a) 20x representative confocal micrographs displaying PV-immunoreactivity (left), GABA-immunoreactivity (middle) and merge of both (right) within the somatosensory cortex. **(b)** Bar graphs showing total number of GABA-immunoreactive, PV-immunoreactive and GABA / PV

co-localising (Co-L) neocortical neurons (left) and fractions of co-localising neurons as a percentage of total PV-immunoreactive and of GABA-immunoreactive neurons (right; N = 3 mice). **(c)** Top: 20x representative confocal micrographs displaying PV-immunoreactivity (left), GABA-immunoreactivity (middle) and merge of both (right) within the LHb. Middle: Zoom of boxed region in top row depicting PV-immunoreactive neurons which did not co-localise with GABA. Bottom: Zoom of boxed region in top row depicting a PV-immunoreactive neuron which did co-localise with GABA. **(d)** Schematic illustrating location of PV-immunoreactive only, or PV / GABA co-labelled neurons throughout the LHb in the rostral-caudal plane from one mouse, in which every second 60 µm section was analysed. Sub-nuclear boundaries as defined by Andres et al., (1999) are indicated by dashed lines. Approximate rostral-caudal distances from Bregma (in mm) are indicated. **(e)** Bar graphs showing total number of GABA-immunoreactive, PV-immunoreactive and GABA / PV co-localising (Co-L) LHb neurons (left) and fractions of co-localising neurons as a percentage of total PV-immunoreactive and of GABA-immunoreactive neurons (right; N = 3 mice).

We sought to further characterise these neurons by assessing their physiological properties. We crossed PV-IRES-Cre mice with a Cre-dependent TdTomato reporter line (Ai9; Madisen *et al.*, 2010) to generate PV-IRES-Cre::Ai9 transgenic offspring which express TdTomato under the control of the PV promoter (Fig. 4.2a), and used fluorescence-assisted patch-clamp

recordings to record from TdTomato-positive LHb neurons in acute slices (n = 19; N = 8 mice). Consistent with our histological data, most TdTomato-positive neurons were clustered in either the medial or lateral LHb (Fig. 4.2b and c). When we compared the whole population of TdTomato-positive neurons to the general population of LHb neurons recorded in wild-type C57/BL6 mice (n = 28 from 5 mice), there was a clear difference in the firing frequency of the first induced action potential in response to depolarising current injection (Fig. 4.2d and f; $p < 0.0001$; F = 23.4; df = 1; two-way ANOVA). This was as a result of the fact that only a minority (4 of 19) of TdTomato-positive neurons exhibited any kind of high-frequency bursting behaviour (Fig. 4.2f), and this was only observed upon larger current injections (Fig. 4.2d). This was a striking observation as high-frequency bursting has long been considered a hallmark physiological phenotype of most LHb neurons (Wilcox *et al.*, 1988; Chang and Kim, 2004; Weiss and Veh, 2011; Yang *et al.*, 2018a). TdTomato-positive neurons were more comparable to the general population when passive physiological properties were compared, with only a slightly lower mean input resistance (366.2 ± 39.1 vs 544.0 ± 53.3 MΩ; $p = 0.015$; F = 2.4; df = 42; two-tailed unpaired t-test) and similar resting membrane potential (-59.4 ± 2.6 vs -55.2 ± 1.4 mV; $p = 0.13$; F = 2.3; df = 45; two-tailed unpaired t-test; Fig. 4.2e). However, the TdTomato-positive neurons in the medial and lateral LHb could clearly be further differentiated based on their physiological profiles (Fig. 4.2f and g). TdTomato-positive neurons in the medial LHb frequently exhibited sub-threshold voltage oscillations (6 of 8 medial LHb neurons) while their counterparts in the lateral LHb did so very rarely (1 of 11 lateral LHb neurons,

p = 0.006; Fishers exact test; Fig. 4f). Furthermore, a second distinctive population of TdTomato-positive neurons appeared in the lateral LHb, identifiable by their hyperpolarized resting membrane potential (5 of 11 lateral LHb neurons; -77.0 ± 1.3 mV vs -59.4 ± 2.6 mV for all 19 TdTomato-positive neurons; *p* = 0.001; F = 12.9; df = 23; two-tailed unpaired t-test) and lack of rebound action potential discharge (Fig. 4.2f and g).

We also performed morphological reconstruction of these neurons (Fig. 4.2h). Ten neurons were sufficiently reconstructed to visualize a prolonged section of the axon. In nine of these, this was an unbranching axon, possibly indicative of a projection neuron (Fig. 4.2h). However, as the focus of this study was on local inhibitory control within the LHb, we did not further test possible downstream projection targets of these neurons. In the one remaining neuron, we did observe the axon to branch locally and extensively, suggesting this to be a locally-targeting neuron. To study the local connectivity of PV-positive LHb neurons, we also performed dual electrophysiological recordings of TdTomato-positive neurons and other non TdTomato-expressing neurons within the LHb (n = 7 connections tested) and only observed one postsynaptic IPSC from these recordings, upon electrical stimulation of the same locally branching neuron with a 2 ms depolarizing current injection (Fig. 4.2i).

Taken together, these results indicate that PV-positive LHb neurons can be further divided into multiple distinct sub-populations. While we do find that a

small proportion of these are GABAergic, the majority are non-GABAergic neurons which we assume to be projection neurons. Furthermore, these non-GABAergic neurons can be classified into distinct sub-populations based on physiological profile and location within the LHb.

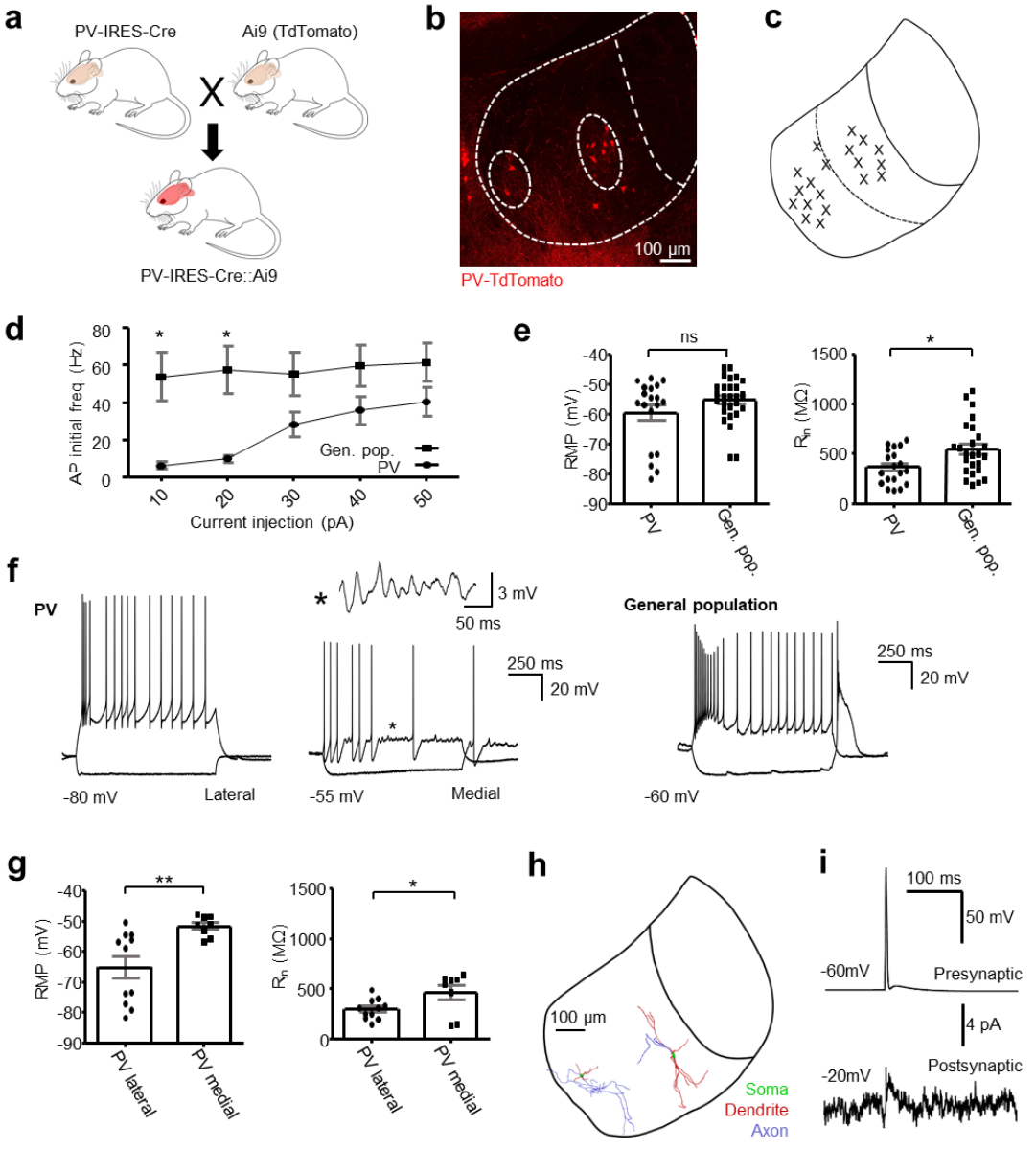

Figure 4.2: PV-positive LHb neurons comprise multiple physiologically diverse populations. (a) Schematic illustrating breeding scheme for generating PV-IRES-Cre::Ai9 mice. **(b)** Confocal micrograph depicting localization of TdTomato-positive neurons within the LHb. The central and oval sub-nucleus approximate boundaries are indicated by dashed white lines. **(c)** Schematic illustrating location of patched neurons throughout the habenular complex. In this case, all neurons recorded have been compressed onto one schematic to allow clear visualization of neurons recorded in the lateral vs medial LHb. **(d)** Comparison of firing frequency of the first induced action potential versus current injection for both TdTomato-positive LHb neurons (n = 18; N = 8 mice) and the general population of LHb neurons (n = 28; N = 5 mice) recorded in C57 mice. An overall difference was observed in the response to current injection between TdTomato-positive neurons and the general population ($p < 0.0001$; $F = 23.4$; df = 1; two-way ANOVA), while an individual difference was also observed for 10 and 20 pA current injections ($p < 0.05$; Bonferroni's multiple comparison test). Data are mean ± SEM. **(e)** Comparison of passive properties of PV-positive LHb neurons (n = 19; N = 8 mice) and from the general population of LHb neurons recorded in C57 mice (n = 28; N = 5 mice). Data are mean ± SEM. **(f)** Example traces from TdTomato-positive neurons in response to current injection. For PV, left: traces from a neuron in the lateral LHb; right: traces from a neuron in the medial LHb Asterisk indicates a section from the recording displaying characteristic sub-threshold voltage oscillations. Current steps: -50 pA and 50 pA; 1 s duration. Right panel: example traces from an LHb neuron recorded in

a C57BL/6J mouse which exhibits a generic LHb physiological profile. Note the rebound burst following hyperpolarising current injection. Current steps: -40 pA and 50pA. **(g)** Comparison of passive properties between TdTomato positive neurons in the lateral LHb (n = 11) and medial LHb (n = 8). Data are mean ± SEM. **(h)** Example reconstructions from two TdTomato-positive neurons. Left: a neuron with an extensively-branching axon (observed in 1 of 10 reconstructions). Right: a representative reconstruction of neuron which displays an unbranching axon (observed in 9 of 10 reconstructions). **(i)** Example traces from a presynaptic TdTomato-positive neuron electrically stimulated to fire an action potential (top; note this is the same neuron as is reconstructed in E; right), and the corresponding IPSC in the simultaneously recorded postsynaptic neuron.

Input to the lateral habenula from PV-positive neurons is both excitatory and inhibitory

Thus far, we have identified that PV-positive LHb neurons comprise multiple distinct sub-classes which are both GABAergic and non-GABAergic (Figs. 4.1 and 4.2); therefore indicating that these are not a homogenous sub-class of inhibitory neurons as they are known to be in other major brain regions (Klausberger and Somogyi, 2008; Tepper *et al.*, 2011; Tremblay *et al.*, 2016). Additionally, other works have identified that PV-positive glutamatergic projection neurons in the entopeduncular nucleus (Wallace *et al.*, 2017) and

ventral pallidum (Knowland *et al.*, 2017) project to and excite the LHb. Taking this information into account, we next asked if PV-positive neurons provide primarily inhibitory or excitatory input to the LHb.

To address this, we generated PV-IRES-Cre::Ai32 mice, where both eYFP and ChR2 are expressed under the control of the PV promoter (Madisen *et al.*, 2012). We first sectioned and imaged the LHb in brains from these mice (N = 2; Figs. 4.3 and 4.4). In this mouse line, eYFP is uniformly expressed throughout the whole neuron. Thus, this line provides the additional advantage that clear visualization of neuronal somata and processes is permitted.

We first sought to validate that eYFP expression was indeed confined to PV-positive neurons in this line, by staining a sub-section of slices (n = 5 for somatosensory cortex; n = 14 for LHb; N = 2 mice) with an antibody against PV (Fig. 4.2). As expected, co-localisation of eYFP and PV-immunoreactivity was very high in the somatosensory cortex (96.4 % of eYFP-positive neurons; 95.5 % of PV-immunoreactive neurons; Fig. 4.3ai and aii). However, this was not the case within the LHb (Fig. 4.3b). Surprisingly, 64.4 % of eYFP-positive neurons were PV-immunoreactive, while only 44.6 % of PV-immunoreactive neurons were eYFP-positive (Fig. 4.3bii). It is indeed known that off-target expression of Cre recombinase is a common feature of many Cre driver lines, and Cre expression can change on a tissue-to-tissue basis within individual animals (Heffner *et al.*, 2012), therefore providing a likely explanation for this result. Additionally, mice used for these experiments were rather young (P31-35), and as such expression of PV at this point may be low (Lecea *et al.*, 1995),

which may also effect expression of Cre. However, as eYFP expression was clearly confined to PV-immunoreactive neocortical neurons (Fig. 4.3a), and the majority of eYFP-positive LHb neurons were also PV-immunoreactive (Fig. 4.3b) we assumed that our PV-IRES-Cre::Ai32 line permitted visualisation and optogenetic activation of the majority of PV-positive LHb neurons and imaged eYFP expression in the rostro-caudal axis (Fig. 4.4).

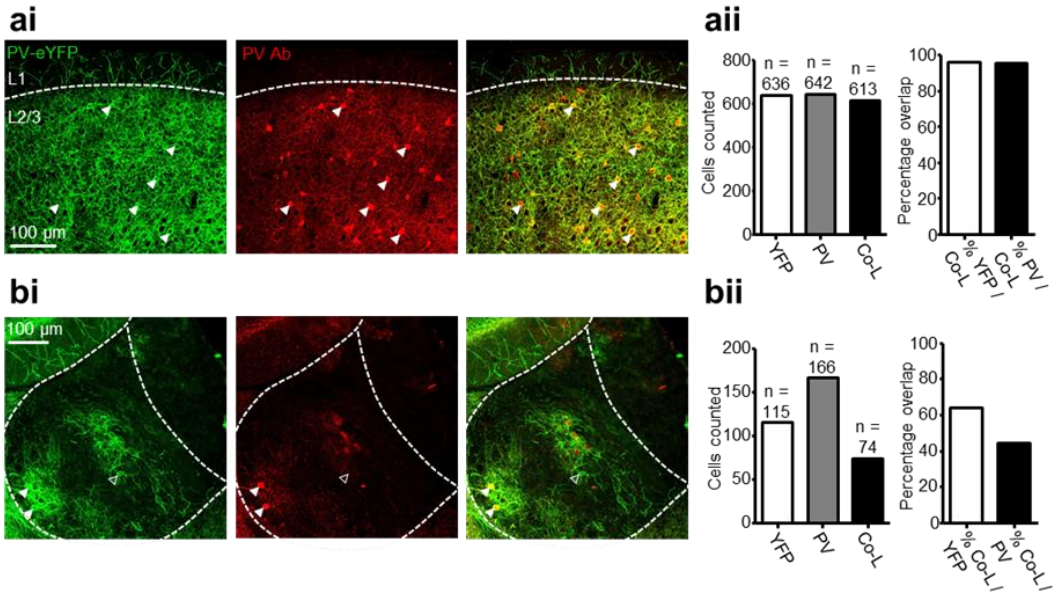

Figure 4.3: Histological validation of PV-IRES-Cre::Ai32 transgenic line. **(ai)** 20X representative confocal micrographs depicting eYFP expression (left), PV-immunoreactivity (middle) and merge of both (right) within the somatosensory cortex. Arrowheads indicate neurons which were both eYFP-positive and PV-immunoreactive. **(aii)** Bar graphs showing total number of eYFP-positive, PV-immunoreactive and eYFP / PV co-localising (Co-L) neocortical neurons (left) and fractions of co-localising neurons as a

percentage of total eYFP-positive and of PV-immunoreactive neurons (right; N = 2 mice). **(bi)** As for (ai), within the LHb. Filled arrowheads indicate two neurons which were both eYFP-positive and PV-immunoreactive. Open arrowhead indicates an eYFP-positive neuron which was not PV-immunoreactive. **(bii)** As for (aii), within the LHb.

As with the histological data (Fig. 4.1) neuronal somata appeared to be largely confined to two distinct sub-regions (Fig. 4.4), which appeared to correlate to the previously described central sub-nucleus of the medial LHb, and the oval sub-nucleus of the lateral LHb (Andres *et al.*, 1999). The oval sub-nucleus in particular appeared densely enriched with fibres from eYFP-positive neurons (Fig. 4.4), and our histological data also suggests that the GABAergic PV-positive neurons are confined to the lateral LHb (Fig. 4.1). We therefore speculated that this dense enrichment of fibres may arise from local GABAergic PV-positive neurons. Interestingly however, excitatory PV-positive projection neurons are known to selectively target the oval sub-nucleus of the LHb (Wallace *et al.*, 2017). Considering this, we tested whether PV-positive neurons provided primarily excitatory or inhibitory input to the LHb.

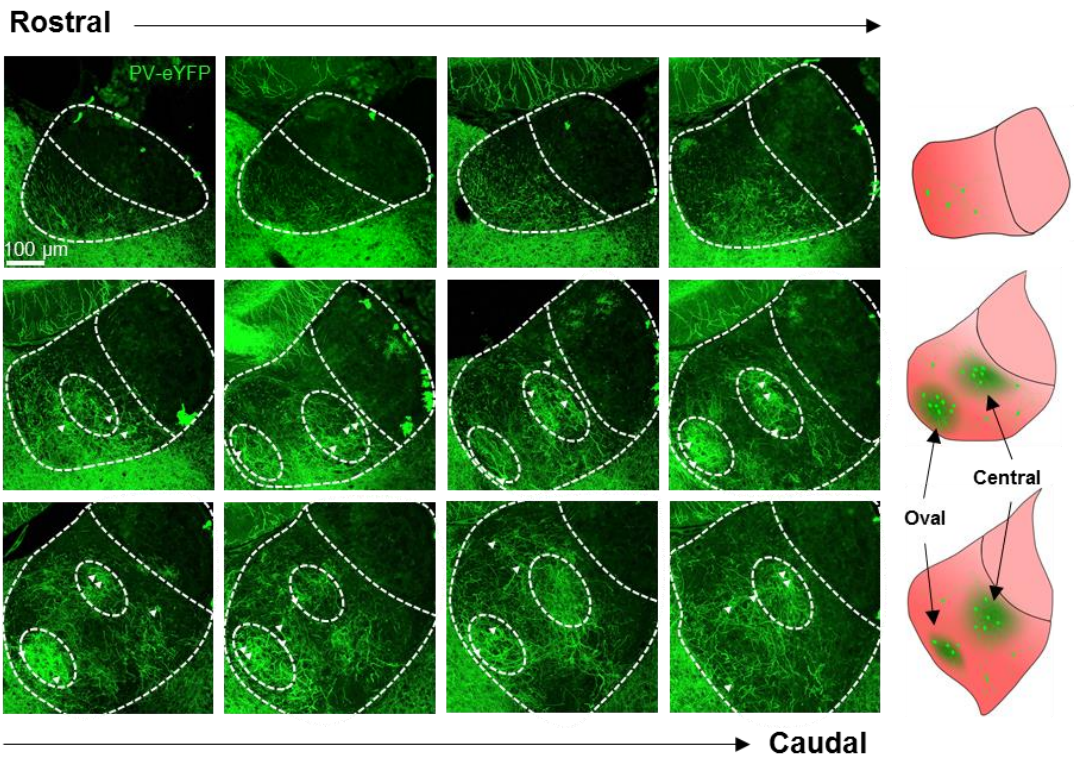

Figure 4.4: Localization of PV-positive neuronal somata and processes throughout the LHb. Left: Confocal micrographs of 30 µm thick maximum intensity projections of habenular sections from PV-IRES-Cre::Ai32 mice (N = 2) depicting localization of eYFP-positive neuronal somata and neuronal processes throughout the LHb in the rostral-caudal plane. 60 µm thick spacing between images. Arrowheads indicate eYFP-positive neurons. Right: graphical illustrations of habenular sections indicating the oval and central lateral habenular sub-regions, where eYFP-expression was most prominent. Images each represent one third of the habenula in the rostral-caudal plane.

To test this, we made acute slices from PV-IRES-Cre::Ai32 offspring (N = 19 animals; Fig. 4.5a), and optogenetically stimulated ChR2-positive neurons while recording from the general population of LHb neurons in whole-cell configuration (Fig. 4.5b), thus allowing us to test whether PV-positive neurons provided excitatory or inhibitory input to LHb neurons. Photostimulation-induced postsynaptic potentials were observed in 29 of 76 (38.2 %) neurons recorded (Fig. 4.5c-f). The majority of these (18 of 29; 62.1 %) displayed a solely excitatory response (Fig. 4.5c, e and f). However, solely inhibitory responses were also observed with relative frequency (6 of 29 responsive cells; 20.7%) while on two occasions, we recorded postsynaptic potentials consisting of both an excitatory and inhibitory component (Fig. 4.5c-f). While we did observe that neurons recorded in the oval sub-nucleus exhibited a higher proportion of responses (7 of 11; 63.6 %) than neurons recorded throughout the entirety of the LHb (29 of 76; 38.2 %), this was not statistically significant (p = 0.18; Fisher's exact test), and was comprised of a mix of excitatory and inhibitory responses (Fig. 4.5d), indicating that the observed fibre enrichment (Fig. 4.4) was likely as a result of both local inhibitory neurons and upstream projection neurons. Furthermore, from all recorded neurons, inhibitory postsynaptic potentials (IPSPs) were comparably larger than excitatory postsynaptic potentials (EPSPs) (mean 5.6 ± 1.3 mV vs 2.3 ± 0.6 mV, respectively; p = 0.013; F = 2.6; df = 22; unpaired t-test; Fig. 4.5f). Consistently, in some of these neurons (n = 3), the induced IPSP was sufficiently large to momentarily silence spontaneous action potential discharge of the recorded neuron (Fig. 4.5g) in a manner which could be

blocked by application of GABAzine; therefore indicating that this is likely a physiologically important source of inhibition to the LHb. Thus, we report that while PV-positive neurons mediate primarily excitatory input to the LHb which most likely arises from upstream sources (Knowland *et al.*, 2017; Wallace *et al.*, 2017), inhibitory PV-positive neurons also provide powerful input to LHb neurons capable of silencing spontaneous firing.

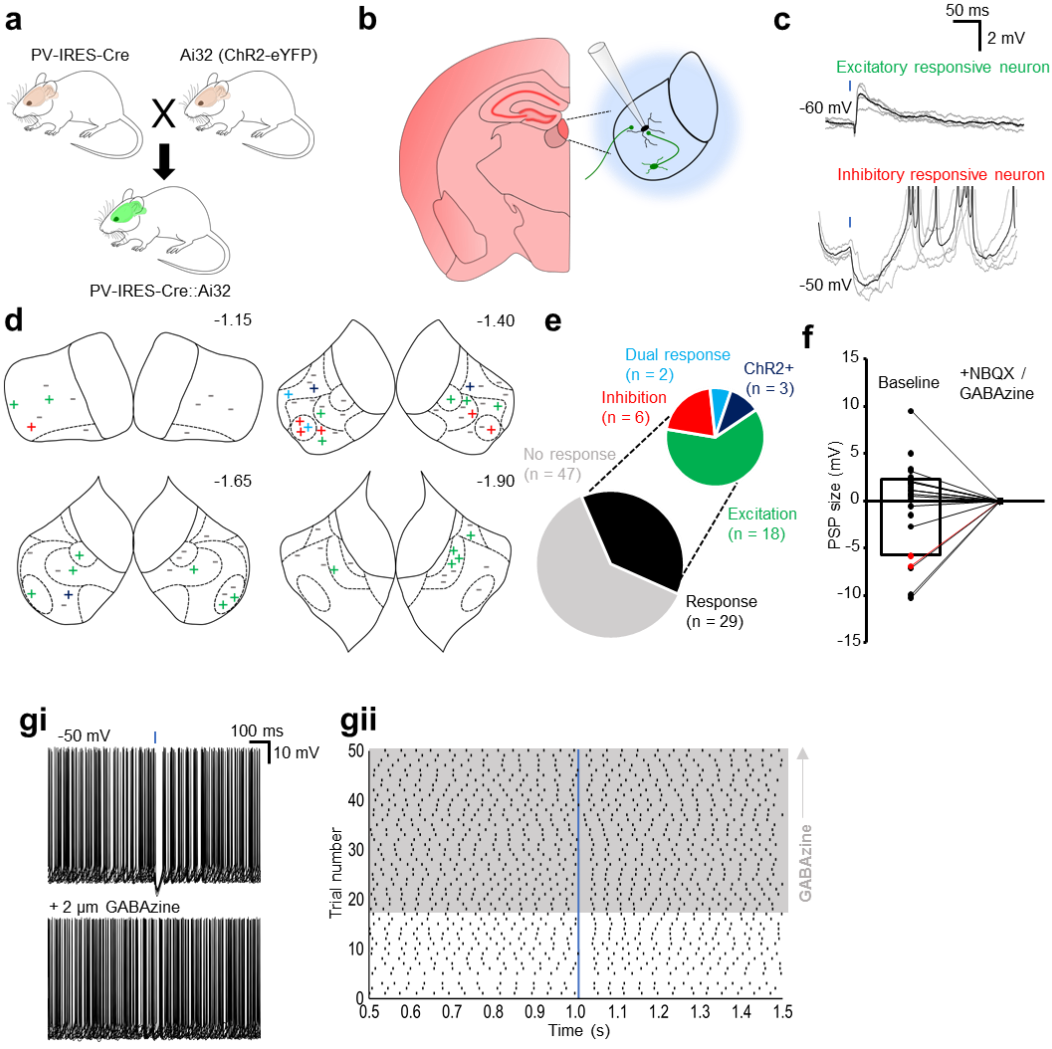

Figure 4.5: PV-positive neurons mediate both excitatory and inhibitory neurotransmission within the lateral habenula. (a) Schematic illustrating breeding scheme for generating PV-IRES-Cre::Ai32 mice. **(b)** Schematic of recording scheme. LHb neurons were patched and blue light was used to stimulate both local and long-distance ChR2-positive neurons. **(c)** Example traces from two separate neurons in which photostimulation elicited an EPSP (top) and one in which it elicited an IPSP (bottom). Traces are averages of multiple traces superimposed over the traces from which the average was derived. Blue square denotes 2 ms light pulse. **(d)** Schematic illustrating location of patched neurons within the habenular complex, projected rostrally (top left) through caudally (bottom right). Non-responsive neurons are indicated by – while responsive neurons are indicated by: + EPSP only; + IPSP only; + dual response consisting of both an excitatory and inhibitory component and; + ChR2-expressing neuron in which an action potential not sensitive to NBQX was triggered upon photostimulation. Sub-nuclear boundaries as defined by Andres et al., (1999) are indicated by dashed lines. Approximate rostral-caudal distances from Bregma (in mm) are indicated. **(e)** Pie-chart summarizing (c). Pie-of-pie sub-categorizes neurons based on response to light-stimulation. **(f)** Before-after plot showing PSP size for neurons responsive to light which exhibited EPSPs (n = 16; note 2 neurons did not display a measurable EPSP at -50 mV) and IPSPs (n = 6) at -50 mV and with application of either GABAzine (2 μM) or NBQX (10 μM) to abolish the PSP. Two neurons which displayed both excitatory and inhibitory components are highlighted in red. One of these neurons was tested

pharmacologically, where both GABAzine and NBQX were applied to fully abolish the PSP (red line). **(gi)** Example traces overlaid from a neuron in which light-stimulation was sufficient to inhibit spontaneous action potential firing (top), and which was completely blocked in the presence of GABAzine (bottom). n = 3 neurons. **(gii)** Raster plot of (Gi). Grey area denotes presence of GABAzine. Blue bar denotes light 2 ms photostimulation.

PV-positive neurons mediate local inhibitory signalling within the lateral habenula

The excitatory input from PV-positive neurons to the LHb that we observed is consistent with previous excitatory projections reported in the rodent entopeduncular nucleus (Wallace *et al.*, 2017) and the ventral pallidum (Knowland *et al.*, 2017). However, the inhibitory responses remain unaccounted for. Referring to our histological data (Fig. 4.1) and dual recordings in PV-IRES-Cre::Ai9 slices (Fig. 4.2i), we show that these GABA-immunoreactive PV neurons are likely mediating local inhibition. To further test this, we intracranially injected PV-IRES-Cre mice (N = 8) with Cre-dependent AAVs (Fig. 4.6a and methods) driving expression of ChR2 and eYFP in Cre-expressing neurons into the LHb, so as to express ChR2 selectively in PV-positive LHb neurons.

Two or more weeks following surgery, we observed robust eYFP expression within the LHb (Fig. 4.6b). Recording from LHb neurons (n = 54)

we occasionally observed inhibitory responses upon photostimulation (Fig. 4.6 c and d; n = 5) which were confined to the lateral portion of the LHb (Fig. 4.6e). Interestingly, we also observed one NBQX-sensitive excitatory response, and one consisting of both an excitatory and inhibitory component (Fig. 4.6c), possibly indicative that the non-GABAergic PV-positive LHb neurons (Fig. 4.1) also form some local connections. Together with our histological (Fig. 4.1) and electrophysiological (Fig. 4.2i) data, these results indicate the existence of a small sub-population of locally-targeting inhibitory PV-positive neuron within the LHb.

However, while our vector clearly drove transgene expression in the LHb, we found that the viral spread could occasionally not be exclusively confined to this structure. Therefore, we observed some infection in nearby thalamic neurons. In particular we noted that the medial-dorsal thalamic nucleus (MDT) directly ventral to the habenular complex appeared to exhibit a high number of infected neurons (data not shown); thus we speculated upon a novel PV-positive connection between the MDT and LHb.

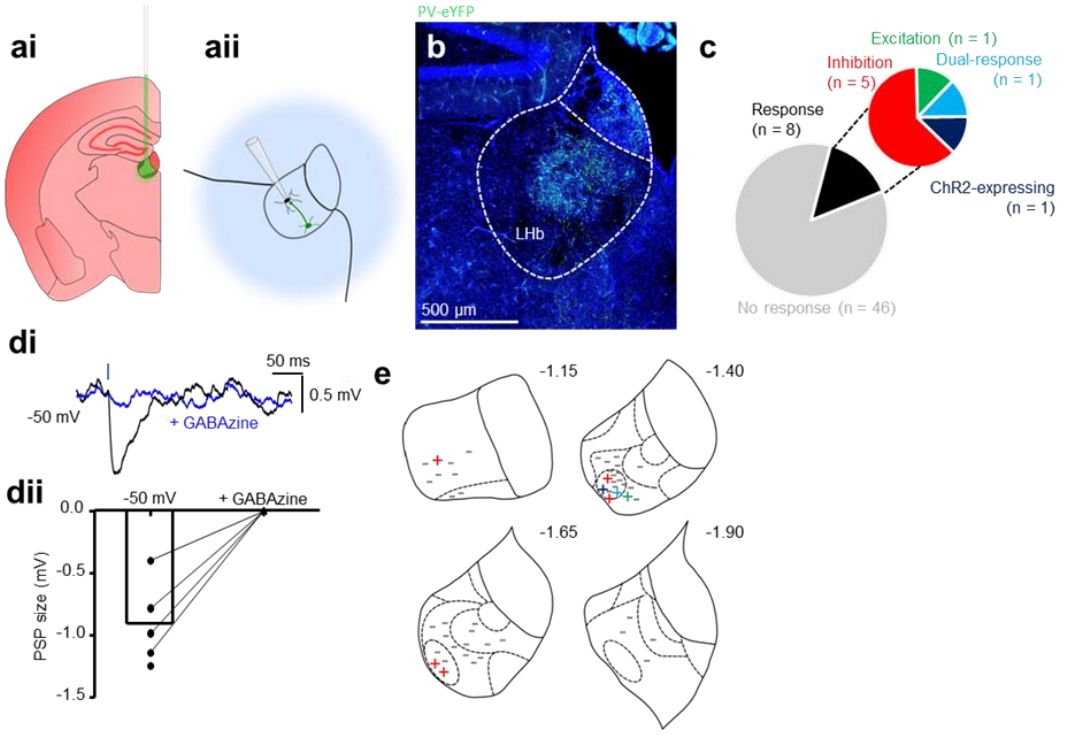

Figure 4.6: PV-positive neurons mediate local inhibitory signalling within the LHb (ai) Schematic illustrating stereotaxic injection protocol into the LHb. **(aii)** Schematic illustrating electrophysiology recording protocol for LHb neurons following stereotaxic viral injection. Transduced ChR2-positive neurons are photostimulated while recording from nearby LHb neurons. **(b)** Confocal micrograph depicting neurons transduced to express eYFP following viral injection. **(c)** Pie chart quantifying fraction of neurons responsive to photostimulation. **(di)** Example traces from one neuron in which an IPSP could be elicited following photostimulation. Blue bar denotes 2 ms photostimulation. **(dii)** Before-after plot of the IPSP amplitude from 5 different neurons before and after application of GABAzine (4 neurons). **(e)** Schematic illustrating location of patched neurons throughout the habenular complex. Sub-nuclear

boundaries as defined by Andres et al., (1999) are indicated by dashed lines. Approximate rostral-caudal distances from Bregma (in mm) are indicated.

Retrograde labelling of PV-positive inputs to the lateral habenula

To address this question, we implemented a Cre-dependent retrograde AAV encoding TdTomato in the presence of Cre recombinase (Tervo *et al.*, 2016). Hence, by injecting this virus into the LHb of PV-IRES-Cre mice (N = 3), we could selectively label inputs to the LHb from PV-positive neurons (Fig. 4.7).

Mice were perfused 28 days post-injection and brains were sectioned and imaged in the coronal plane (N = 2; Fig. 4.7a-e) or sagittal plane (N = 1; Fig. 4.7f-i). As predicted, labelled neurons were clearly observed in the MDT in all cases (Fig. 4.7b,c,g and i), thus providing evidence that PV-positive neurons in the MDT project to the LHb. Surprisingly, in all cases, neuronal labelling could be observed in anterior cortical regions. While this was rather sparse in two brains (data not shown), this was by far most prominent in the one brain sectioned in the sagittal plane (Fig. 4.7f-h). In this animal, dense neuronal labelling was observed specifically in L5 of the motor cortex (Fig. 4.7g and h), thus suggesting the presence of cortical PV-positive projection neurons. Due to the inconsistency between the three brains, this was assumed to be as a result of viral leakage into the nearby thalamus, and was not pursued further. Nonetheless, while striatum-projecting PV-positive neocortical neurons have previously been described (Jinno and Kosaka, 2004), such thalamus-

projecting neocortical PV-positive projection neurons are a novel concept which will warrant future investigation. Additionally, some sparse labelling was also observed in the entopeduncular nucleus (Fig. 4.7e), consistent with reports of LHb-projecting PV-positive neurons here (Wallace *et al.*, 2017). Finally, labelled neurons were also observed in the thalamic reticular nucleus (TRN) in all cases (Fig. 4.7d,e and g). Recent work has identified that PV-positive TRN neurons project to thalamic regions adjacent to the LHb (Clemente-Perez *et al.*, 2017), but no direct connection with the LHb is known. This therefore may have been a result of viral spillage into these regions.

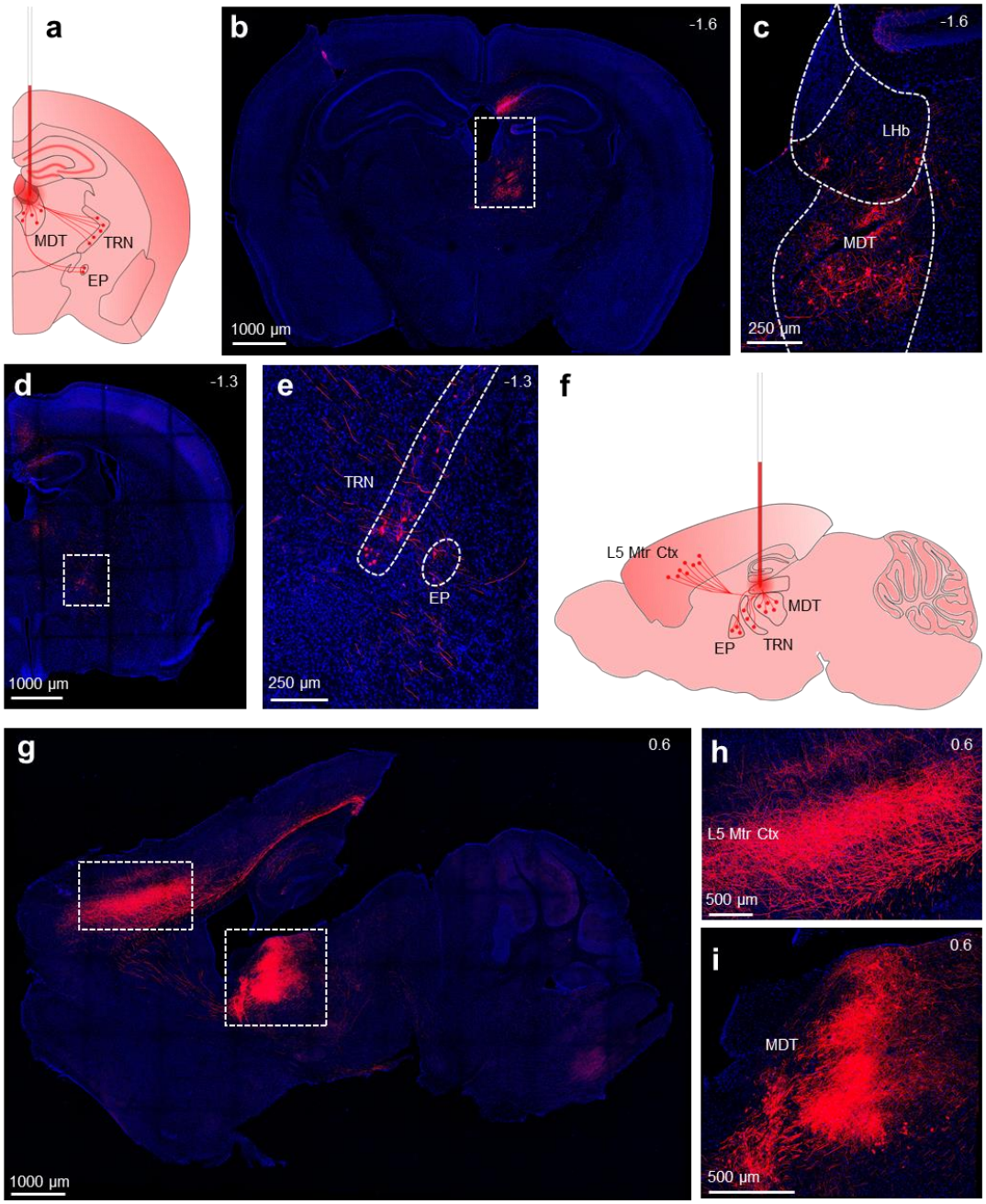

Figure 4.7: Retrograde labelling of PV-positive inputs to the LHb. (a) Schematic illustrating stereotaxic injection protocol into the LHb. Virus was injected, and brains were sectioned and imaged in the coronal plane (N = 2), allowing labelling of PV-positive neurons which project to the LHb. MDT = mediodorsal thalamus. EP = entopeduncular nucleus. TRN = thalamic reticular

nucleus. **(b)** Confocal micrograph of a whole coronal slice depicting labelled neurons in the LHb and adjacent MDT. **(c)** Zoom of boxed area in (b). **(d)** Confocal micrograph depicting labelled neurons in the TRN and EP. **(e)** Zoom of boxed area in (d). **(f)** Schematic illustrating stereotaxic injection protocol into the LHb. Virus was injected, and brains were sectioned and imaged in the sagittal plane (N = 1), allowing labelling of PV-positive neurons which project to the LHb. MDT = mediodorsal thalamus. EP = entopeduncular nucleus. TRN = thalamic reticular nucleus. L5 Mtr Ctx = Layer 5 of the motor cortex. **(g)** Confocal micrograph of a whole sagittal slice depicting labelled neurons in the MDT, TRN and L5 Mtr Ctx. **(h)** Zoom of left boxed region in (g). **(i)** Zoom of right boxed region in (g). Numerical values in top right of images indicate approximate distance from Bregma (in mm) in the rostro-caudal axis (coronal images) or the medio-lateral axis (sagittal images).

Nonetheless, to clarify this, we injected PV-IRES-Cre mice (N = 2) with a Cre-dependent AAV encoding ChR2 and eYFP into the TRN and recorded photostimulation-induced postsynaptic potentials in both the LHb and the adjacent thalamus (Fig. 4.8a and d). When recording from thalamic neurons, we observed IPSPs in 2 of 5 neurons (Fig. 4.8b). However, in the LHb we observed no axon terminals from infected TRN neurons (Fig. 4.8cii) and consistently observed no postsynaptic potentials while recording from LHb neurons (Fig. 4.8e). Thus, the PV-positive TRN neurons project to thalamic nuclei adjacent to the LHb, but not the LHb itself, and hence the observed

retrograde labelling was as a result of viral leakage into this regions (Fig. 4.7). Hence the MDT remained as the most probable candidate as the source of the observed inhibitory input to the LHb (Fig. 4.5).

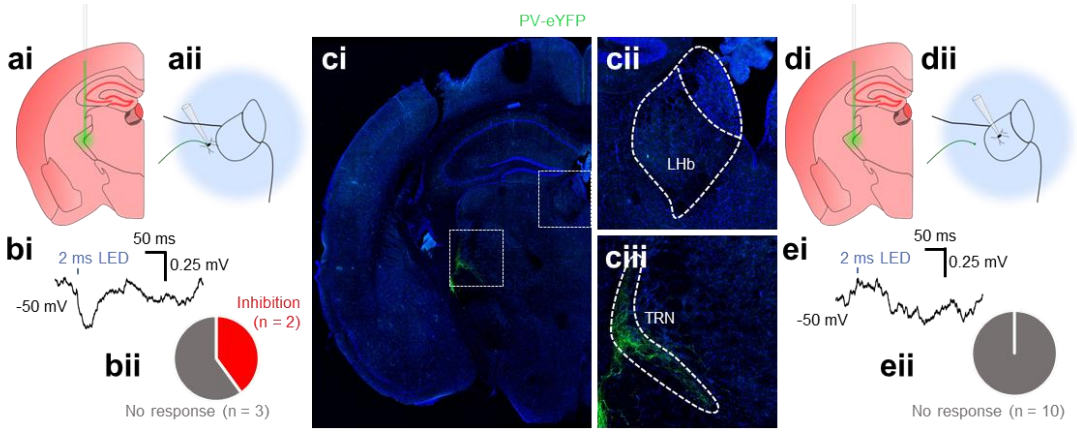

Figure 4.8: PV-positive TRN neurons provide inhibitory input to thalamic nuclei adjacent to the LHb. (ai) Schematic illustrating stereotaxic injection protocol into the TRN. **(aii)** Schematic illustrating electrophysiology recording protocol for thalamic neurons following stereotaxic viral injection. Transduced ChR2-positive neurons are photostimulated while recording from postsynaptic thalamic neurons. **(bi)** Example traces from a thalamic neuron in which an IPSP was elicited upon photostimulation. Trace is an average of multiple sweeps. **(bii)** Pie chart quantifying fraction of thalamic neurons responsive to photostimulation. **(ci)** Confocal micrograph depicting the infected TRN. **(cii)** Zoom of top boxed region in (ci) depicting the LHb. **(ciii)** Zoom of bottom boxed region in (ci) depicting the infected TRN. **(di)** and **(dii)** As for (ai) and (aii), recording from LHb. **(ei)** Example traces from an LHb neuron in which no

response was elicited upon photostimulation. Trace is an average of multiple sweeps. **(eii)** Pie chart quantifying fraction of LHb neurons responsive to photostimulation.

PV-positive medial dorsal thalamic neurons provide inhibitory input to the lateral habenula

However, this retrograde labelling approach still presents the problem of viral leakage; if the virus had leaked into the MDT upon injection, then locally-targeting PV-positive neurons would also be infected. To address this problem, and to identify whether this proposed MDT-LHb pathway was indeed inhibitory, we again implemented a Cre-dependent AAV encoding ChR2 and eYFP (Wozny *et al.*, 2018). By specifically targeting injections to the ventral MDT, we could confine injections to this region without also infecting the LHb (N = 6 mice, Fig. 4.9a and d). Upon confocal imaging, we could visualize fibres which appeared to be projecting dorsally from neuronal somata located in the MDT to the LHb (Fig. 4.9dii). Consistently, we recorded from LHb neurons (n = 47) while photostimulating MDT ChR2-positive neurons and observed inhibitory events in seven neurons (Fig. 4.9b and c; note in three these were only visible when the neuron was strongly depolarized). Strikingly, and consistent with our observation of fibre enrichment (Fig. 4.4), these fibres appeared to be exclusively targeting the lateral LHb; particularly the oval sub-nucleus where all responsive neurons were recorded (Fig. 4.9e). We also filled TdTomato-

positive MDT neurons (n = 8) with biocytin in slices from PV-IRES-Cre::Ai9 mice (N = 2), and upon reconstruction could observe fibres penetrating the LHb in 5 of 8 neurons (Fig. 4.9f). Hence, these results provide evidence for a novel projection arising from PV-positive neurons in the MDT which exerts inhibitory influence over the LHb.

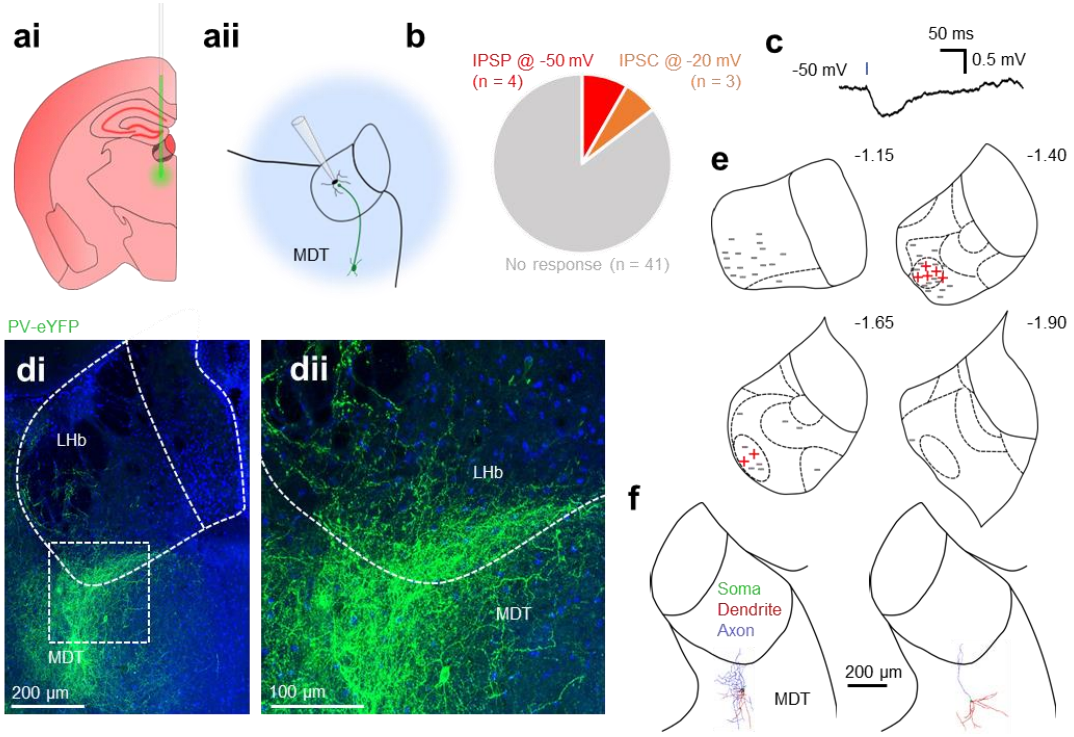

Figure 4.9: PV-positive mediodorsal thalamic neurons provide inhibitory input to the LHb (ai) Schematic illustrating stereotaxic injection protocol into the MDT. **(aii)** Schematic illustrating electrophysiology recording protocol for LHb neurons following stereotaxic viral injection. Transduced ChR2-positive neurons are photostimulated while recording from nearby LHb neurons. **(b)** Pie chart quantifying fraction of neurons responsive to photostimulation. **(c)**

Example traces from one neuron in which an IPSP could be elicited following photostimulation in voltage clamp (top) and current clamp (bottom). Blue bar denotes 2 ms photostimulation. **(di)** Confocal micrograph depicting eYFP expression within the MDT following stereotaxic viral injection. **(dii)** Zoom of the outlined region in (di). Note the presence of fibres originating from neurons in the MDT which penetrate the LHb. **(e)** Schematic illustrating location of patched neurons throughout the habenular complex. All neurons responsive to photostimulation were located in the oval sub-nucleus of the lateral habenula. Sub-nuclear boundaries as defined by Andres et al., (1999) are indicated by dashed lines. Approximate rostral-caudal distances from Bregma (in mm) are indicated. **(f)** Example reconstructions from 2 TdTomato-positive MDT neurons which had axonal fibres projecting to the LHb.

Discussion

The key findings from this body of work are that we have defined and characterized two novel source of inhibitory input to the LHb; one arising from locally-targeting PV-positive neurons within the LHb, and one from PV-positive neurons in the MDT. Additionally, we also provide evidence that PV-positive neurons within the LHb can be sub-divided into multiple physiologically distinct sub-classes, which we assume are most likely projection neurons.

PV neurons provide input to the lateral habenula from a variety of sources

The subject of locally-targeting inhibitory neurons within the LHb has classically been a topic of debate (Brinschwitz *et al.*, 2010; Weiss and Veh, 2011). In this work we show that at least two distinct populations of PV-positive neurons provide inhibitory input to the LHb. Strikingly, these neurons appear to selectively target neurons located within the lateral LHb; particularly the oval sub-nucleus (Figs. 4.5d and 4.9e). While the efferent targets of the LHb have long been known (Herkenham and Nauta, 1979), dissecting the output pathways with respect to distinct habenular sub-regions is a relatively novel idea (Quina *et al.*, 2015). Indeed it is now known that topographical organisation of LHb outputs exist and it is believed that neurons in the lateral LHb specifically project to the rostromedial tegmental nucleus (RMTg) (Quina *et al.*, 2015), the primary inhibitory modulator of the VTA (Jhou *et al.*, 2009a, 2009b). Thus it is interesting to speculate whether these two distinct sources of inhibition converge specifically on RMTg-projecting neurons in the lateral LHb. If this were to be the case, theoretically these neurons would be well poised to reduce excitatory output to the RMTg and reduce the 'reward aversion' signalling from the LHb, which one would expect to have an antidepressant effect (Matsumoto and Hikosaka, 2007; Li *et al.*, 2011; Winter *et al.*, 2011). Building on this concept, we did observe that the amplitude of induced IPSPs in the PV-IRES-Cre::Ai32 line was rather large (mean 5.6 ± 1.3 mV), to the extent that they were frequently capable of silencing spontaneous

neuronal firing (Fig. 4.5g). In contrast, we observed far smaller IPSPs when photostimulating only a single population of neurons (Figs. 4.6 and 4.9). Hence, it may be that there is yet another source of inhibition mediated by PV-positive neurons, or perhaps these multiple sources are working synergistically to produce a greater inhibitory influence on the LHb. Regardless, we clearly demonstrate that PV-positive neurons provide powerful inhibitory input to the LHb (Fig. 4.5). Hence, further circuit mapping experiments can serve to delineate the target specificity of these inhibitory sources at the single cellular level, and further studies utilizing *in vivo* optogenetic and chemogenetic manipulations should serve to elucidate how these inhibitory neurons act to influence behavioural state.

In addition to these two populations of PV-positive inhibitory neurons, our results also imply the existence of several physiologically diverse sub-populations of PV-positive neurons within the LHb (Fig. 4.2), which we assume to be projection neurons. These neurons possess clearly distinct physiological properties from the generic LHb neuron physiology (Chang and Kim, 2004; Kim and Chang, 2005; Weiss and Veh, 2011), and also appear to be roughly obey sub-nuclear boundaries (Andres *et al.*, 1999). Thus we also speculate that these neurons may have differing projection targets and consequently differing functions. Further studies employing the use of Cre-dependent viral tracers are necessary to delineate the circuitry that these probable projection neurons comprise.

Methodological considerations

Within this body of work, we have implemented an approach of stereotaxic injection of AAVs to map the circuitry of PV-positive neurons within and projecting to the LHb. While this is a very powerful technique, one major limitation lies in the propensity of the virus; particularly AAV vectors of serotype 9; to spread to nearby tissue and transduce neurons off-target (Aschauer *et al.*, 2013). As such, in some experiments; particularly those where we have aimed to specifically infect the LHb, co-infection of nearby neurons has presented a problem in that photostimulation may also activate these neurons. Ideally, monitoring of viral spread using 'switch vectors' which encode a second fluorescent reporter protein in the absence of Cre (Wozny *et al.*, 2018) can be used to fully assess and control the viral infection region. However, these vectors still remain to be fully optimized. Nonetheless, we have also demonstrated local connectivity via dual electrophysiological recordings of presynaptic inhibitory PV-positive inhibitory LHb neurons and postsynaptic partners (Fig. 4.2i) and hence we can therefore confirm that photostimulation induced IPSPs are as a result of local inhibition.

Another consideration is the apparent lack of overlap found between YFP-positive cells in PV-IRES-Cre::Ai32 slices and PV-immunostaining (Fig. 4.3). This could perhaps be explained by Cre 'mosaicism', where Cre is not expressed uniformly throughout neural tissue and may also exhibit some off-target expression, and additionally Cre presence is believed to induce some neuronal toxicity (Heffner *et al.*, 2012) perhaps contributing to this discrepancy.

Interestingly, we also observe PV-immunoreactive cells of differing fluorescence intensities within the LHb, in contrast to the neocortex where all PV-immunoreactive cells are clearly and strongly labelled (Figs. 4.1 and 4.3). This could then lead to the question as to whether PV is expressed uniformly throughout the LHb, and perhaps other brain regions. Indeed, we are already aware that PV marks a more heterogenous neuronal population within the LHb (Figs. 4.1 and 4.2), so perhaps then these differing populations of neurons may express PV at differing levels, some of which may not be sufficient to drive Cre expression. As of yet, there is no clear answer to this problem (Heffner *et al.*, 2012). However, this certainly serves as a reminder of some of the limitations of using Cre transgenic lines.

Finally, the specificity of our antibodies must be considered; primarily the anti-GABA antibody for which background staining is very high and thus the quantification of the fraction of PV-positive neurons that are GABAergic may be an overestimation (Fig. 4.1). An alternative approach could be to use in situ hybridisation to specifically label neurons that contain mRNA for GABAergic markers, such as VGAT. We have performed these experiments (Webster *et al.*, 2019), and consistently find populations of VGAT / PV-positive neurons in the lateral LHb, and VGlut2 / PV-positive neurons in the medial LHb. One notable discrepancy in comparison to the immunohistochemistry (Fig. 4.1) is that we do not observe non-GABAergic PV-positive neurons in the lateral LHb. While this may imply some non-specific labelling of the PV-antibody, it also could be explained by a developmental difference in that the

immunohistochemistry and in situ hybridisations were carried out at different time points.

Chapter 5: SOM-positive neurons form a physiologically distinct sub-class within the lateral habenula, and provide long-range inhibitory input arising from the ventral pallidum

Another molecular marker known to be representative of locally-targeting inhibitory neurons in many brain structures is the neuropeptide somatostatin (SOM) (Tepper *et al.*, 2011; Stefanelli *et al.*, 2016; Tremblay *et al.*, 2016). SOM-positive neocortical neurons are thought to be a more heterogeneous population of neurons than PV-positive neurons (Yavorska and Wehr, 2016) that are known to largely target the dendrites of local excitatory neurons (Wang *et al.*, 2004), but have a similar role in modulating excitatory gain (Li *et al.*, 2015). Such locally-targeting inhibitory neurons also have a similar role in the hippocampus, which is known to be critical for encoding memory (Stefanelli *et al.*, 2016).

Interestingly however, some SOM-positive neurons in the hippocampus are known to have long-range projections to the subiculum, cortex and septum (Jinno *et al.*, 2007), and within the entopeduncular nucleus (EP), SOM-positive neurons project to the LHb and co-release GABA and glutamate onto LHb neurons (Wallace *et al.*, 2017; Lazaridis *et al.*, 2019). Taking this information into account, we therefore asked if i) SOM-positive LHb neurons were locally-targeting inhibitory neurons, or another distinct population, and ii) if other populations of SOM-positive neurons than those previously identified projected to and modulated the LHb.

SOM-positive lateral habenular neurons form a physiologically distinct sub-class largely confined to the superior sub-nucleus of the lateral habenula

To address this first question, we crossed SOM-IRES-Cre mice with Ai9 reporter mice to generate SOM-IRES-Cre::Ai9 mice, which express TdTomato in SOM-positive neurons (Fig. 5.1a). Sectioning brains from these offspring (N = 2) and staining with an antibody against GABA revealed that very few TdTomato-positive neurons within the LHb were GABAergic (3.6 % of total SOM-positive neurons; Fig. 5.1b and c). Strikingly however, we observed that TdTomato-positive LHb neurons were localized within one cluster in particular, which appeared to correlate with the previously described superior sub-nucleus of the LHb (Andres, Von Düring and Veh, 1999; Fig. 5.1b). Interestingly, more recent work has proposed to term this region 'HbX' (Wagner *et al.*, 2016b), as analysis of neuronal transcriptomes from this region implies that it may act as an area of overlap between the lateral and medial (MHb) habenula, consisting of intermingled neurons between the two. We therefore speculated that while not GABAergic, these may be an undescribed population distinct to the well-characterised general population of LHb neurons (Wilcox *et al.*, 1988; Chang and Kim, 2004; Kim and Chang, 2005; Weiss and Veh, 2011), that may feature some characteristics of both LHb and MHb neurons.

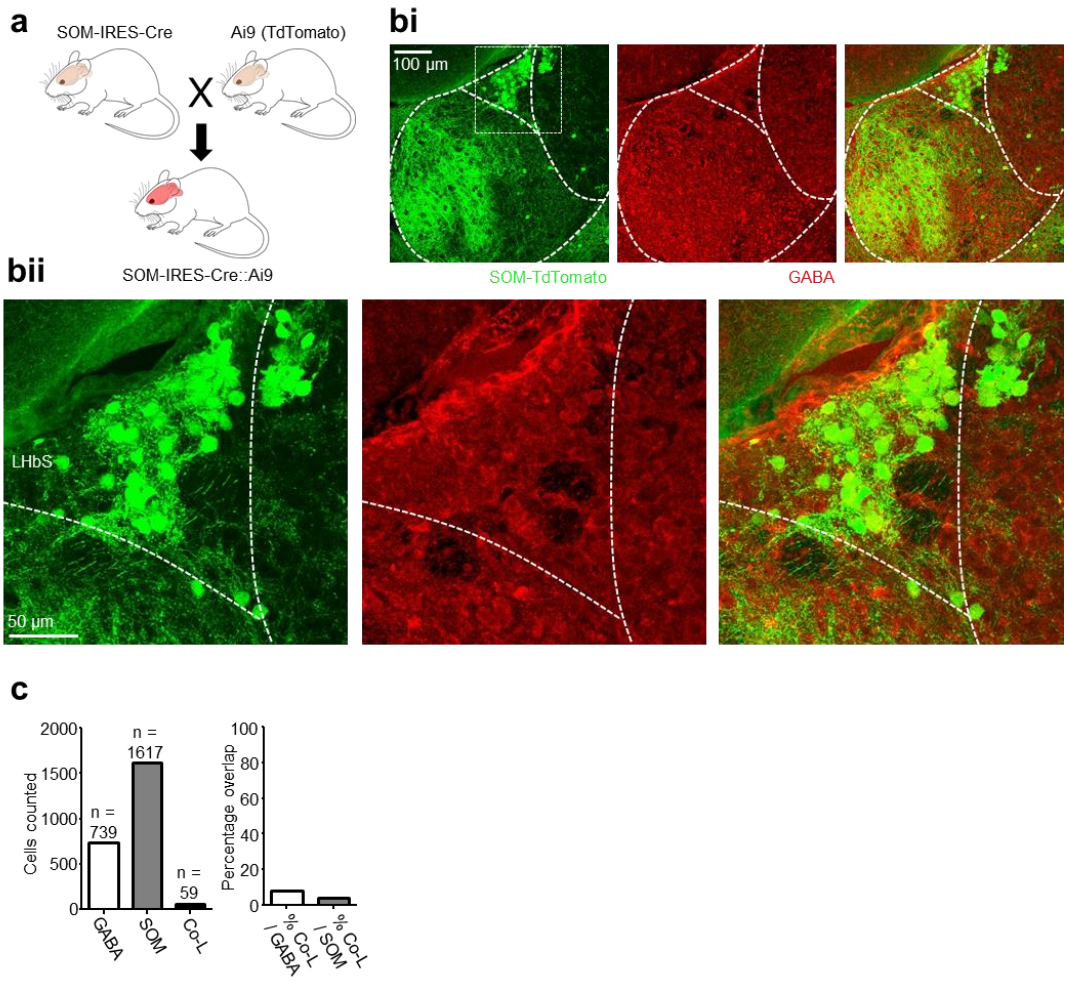

Figure 5.1: SOM-positive LHb neurons are a non-GABAergic population largely confined to the superior sub-nucleus of the LHb. (a) Schematic illustrating breeding scheme for generating SOM-IRES-Cre::Ai9 mice. **(bi)** Confocal micrograph from SOM-IRES-Cre::Ai9 slices depicting TdTomato-positive neurons in the LHb. **(bii)** Zoom of boxed region in (bi) depicting TdTomato-positive LHb neurons localized within the superior sub-nucleus (LHbS) of the LHb. **(c)** Left: bar chart quantifying total number of GABA-immunoreactive, and TdTomato-positive neurons counted and the number which co-expressed both (N = 2 mice). Right: fraction of neurons expressing

both markers as a percentage of GABA-immunoreactive neurons, and as a percentage of TdTomato-positive neurons.

We therefore sought to characterise the physiological properties of these neurons. Utilizing the same SOM-IRES-Cre::Ai9 transgenic mouse line (Fig. 5.2a; N = 3 mice), we created acute slices and recorded from TdTomato-positive LHb neurons (n = 24). The majority of these neurons (16 of 24) were located in the superior sub-nucleus (Fig. 5.2b). As with PV-positive LHb neurons (Fig. 4.2d), we observed the firing frequency of the first action potential induced in response to increasing depolarising current steps to be lower than that of the general population of LHb neurons (Fig. 5.2c; $p < 0.0001$; F = 44.6; df = 1; two-way ANOVA) as very few of these neurons (4 of 24) displayed any kind of bursting activity. When comparing passive properties (Fig. 5.2d), TdTomato-positive neurons had very similar resting membrane potentials to the general population of LHb neurons (-56.9 ± 1.7 mV vs -55.2 ± 1.4 mV for TdTomato-positive vs general population; $p = 0.42$; F = 1.2; df = 50; two-tailed unpaired t-test), but much greater input resistances (1364.0 ± 111.3 MΩ vs 544.0 ± 53.3 MΩ for TdTomato-positive vs general population; $p < 0.0001$; F = 4.2; df = 47; two-tailed unpaired t-test). Medial habenular neurons are known to have very large input resistances (Choi *et al.*, 2016), and as such this data lends support to our hypothesis that these SOM-positive LHb neurons are a population comprised of overlapping characteristics of both lateral and medial habenular neurons.

When recording active properties of these neurons, a striking pattern quickly emerged. Many of these neurons (15 of 24) displayed a prominent 'early spike' upon depolarising current injection (Fig. 5.2e; defined as spiking latency < 20 ms after current injection; current injection 20-150 pA, 1 s) that was not observed in the general population of LHb neurons. Furthermore, we observed that this spike became more pronounced upon hyperpolarisation (Fig. 5.2e and h; tested in 11 neurons). Upon hyperpolarisation as far as -70 mV, we could observe a greater interval between this spike and the next spike in the train (Fig. 5.2f; $p = 0.0014$; $F = 8.9$; $df = 2$; one-way ANOVA), and that this early spike had faster kinetics than when depolarized (Fig. 5.2h; rise time $p = 0.0011$; $F = 9.1$; $df = 2$; half-width $p < 0.0001$; $F = 24.6$; $df = 2$; one-way ANOVA). Additionally, we reconstructed a subset of these neurons (Fig. 5.2i; n = 10), and observed that of those in the superior sub-nucleus (n = 6), 5 of these displayed the short stubby dendrites associated with medial habenular neurons (Kim and Chang, 2005), while those outside of the superior sub-nucleus (n = 4) had the elongated dendrites known to be far more conventional of LHb neurons (Kim and Chang, 2005; Weiss and Veh, 2011). Membrane potential-mediated change in firing modality is a hallmark physiological characteristic of LHb neurons (Kim and Chang, 2005; Weiss and Veh, 2011; Yang *et al.*, 2018a). Yet these TdTomato-positive neurons discharge only one action potential as opposed to the bursting discharge commonly displayed by LHb neurons (Kim and Chang, 2005; Weiss and Veh, 2011; Yang *et al.*, 2018a), and then continue to discharge action potentials in a tonic train akin to that described in the medial habenula (Kim and Chang, 2005), and also

have morphological characteristics more similar to medial habenular neurons (Kim and Chang, 2005). Thus, while we conclude that SOM-positive neurons are not GABAergic (Fig. 5.1), we provide the first physiological evidence for a sub-class of habenular neurons in the superior sub-nucleus which possess intermediate characteristics of neurons from both the LHb and the MHb, adding support to transcriptomic data proposing the existence of the intermediary area 'HbX' (Wagner *et al.*, 2016b).

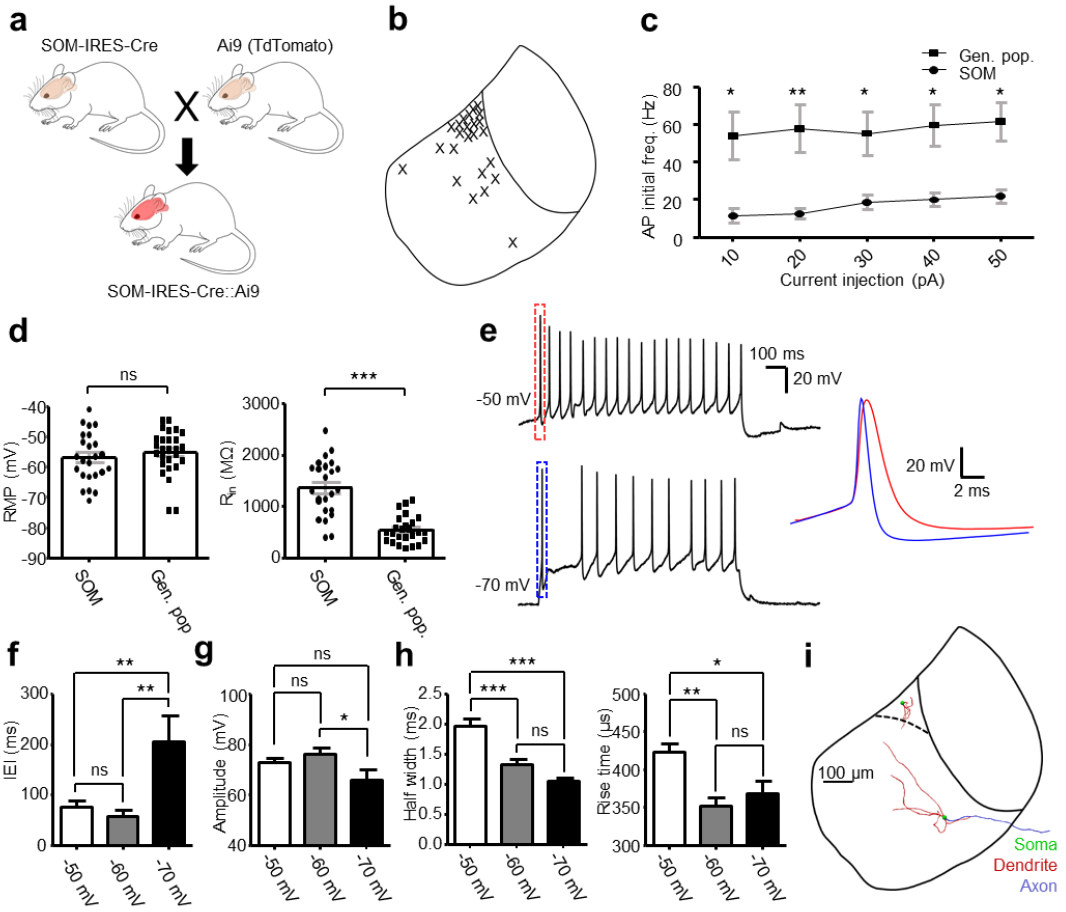

Figure 5.2: SOM-positive LHb neurons form a physiologically distinct sub-class. (a) Schematic illustrating breeding scheme for generating SOM-IRES-Cre::Ai9 mice. **(b)** Schematic illustrating location of patched neurons throughout the habenular complex. **(c)** Comparison of firing frequency of the first induced action potential versus current injection for both TdTomato-positive LHb neurons (n = 22; N = 3 mice) and the general population of LHb neurons (n = 28; N = 5 mice) recorded in C57 mice. An overall difference was observed in the response to current injection between TdTomato-positive neurons and the general population ($p < 0.0001$; $F = 4.2$; $df = 47$; two-way ANOVA), and for all individual current injections ($p < 0.05$; Bonferroni's multiple comparison test). Data are mean ± SEM. **(d)** Comparison of passive properties of TdTomato-positive LHb neurons (n = 24; N = 3 mice) and from the general population of LHb neurons recorded in C57 mice (n = 28; N = 5 mice). Data are mean ± SEM. **(e)** Example traces from one neuron when held at -50 mV and -70 mV in response to a 1 s injection of 50 pA current. Zoom: comparison of the first induced action potential at each holding potential. **(f)** Inter-event interval (IEI) between the first and second action potential induced in response to depolarising current injection (20-150 pA; 1 s) for neurons tested at different holding potentials (n = 11). **(g)** Comparison of amplitude of the first ('early spike') action potential induced in response to depolarising current injection (20-150 pA; 1 s) for neurons tested at different holding potentials (n = 11). **(h)** Comparison of kinetics (rise time and half-width) of the first action potential induced in response to depolarising current injection (20-150 pA; 1 s) for neurons tested at different holding potentials (n = 11). **(i)**

Example reconstructions from a TdTomato-positive neuron within the superior sub-nucleus (top; n = 6), and from another TdTomato-positive neuron out with the superior sub-nucleus (bottom; n = 4). Note that the neuron in the superior sub-nucleus displays short stubby dendrites, while the other neuron displays a more conventional LHb neuronal morphology.

SOM-positive neurons mediate primarily inhibitory transmission within the lateral habenula

Previous work has reported SOM-positive inhibitory projection neurons in the hippocampus (Jinno *et al.*, 2007), and LHb-targeting GABA / glutamate co-releasing SOM-positive neurons in the entopeduncular nucleus (Wallace *et al.*, 2017; Lazaridis *et al.*, 2019). Although we find that SOM-positive neurons within the LHb are not inhibitory (Fig. 5.1), we therefore sought to test if other long-distance SOM-positive projection neurons could be targeting and modulating the LHb.

As with the other molecular markers, we expressed ChR2 in SOM-positive neurons by crossing SOM-IRES-Cre mice with Ai32 mice (Fig. 5.3a; N = 5). We then created acute slices and recorded postsynaptic potentials upon photostimulation (Fig. 5.3b). We frequently observed postsynaptic potentials consisting of both an excitatory and inhibitory component (Fig. 5.3c and d; n = 5 of 21 neurons) that were largely confined to the caudal portion of the LHb (Fig. 5.3f); most likely arising from those previously described GABA /

glutamate co-releasing neurons in the entopeduncular nucleus (Wallace *et al.*, 2017; Lazaridis *et al.*, 2019). However, solely inhibitory responses were most frequent (Fig. 5.3c and e; n = 13 of 21 neurons) and recorded throughout the whole LHb (Fig. 5.3f), hence implying the presence of SOM-positive inhibitory projection neurons targeting the LHb.

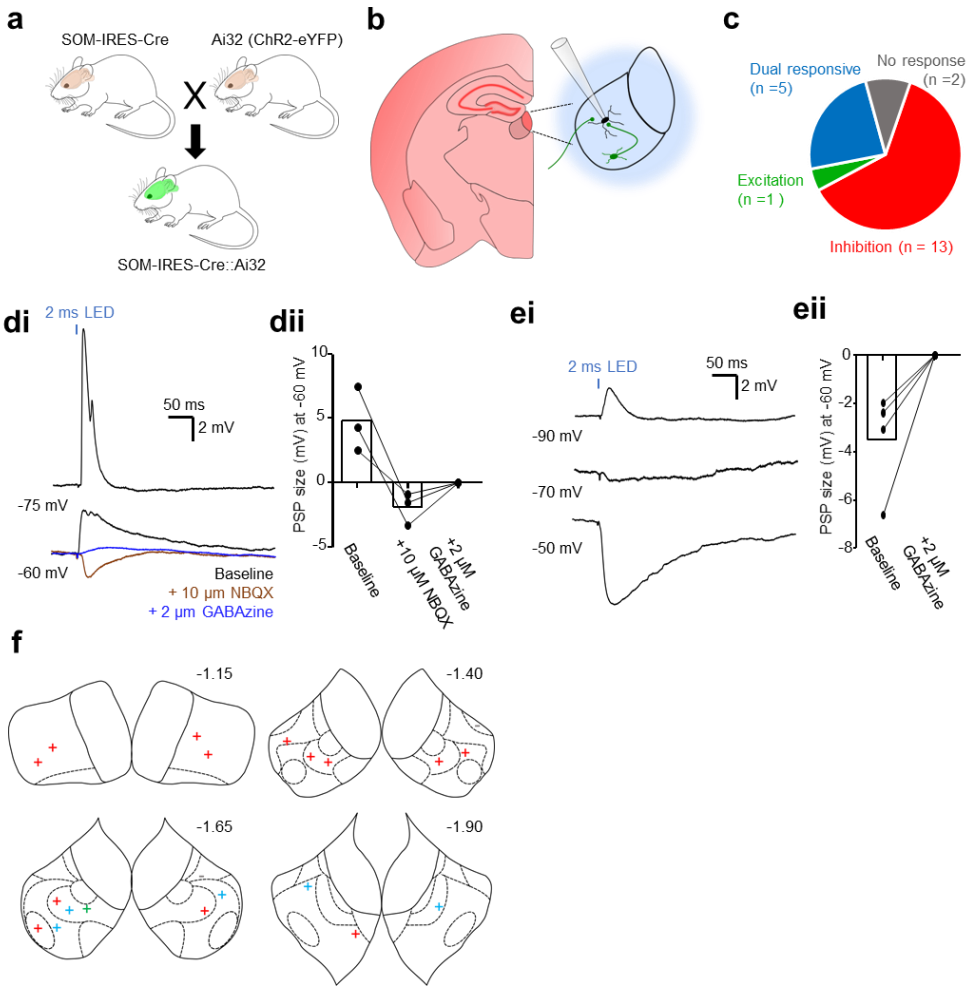

Figure 5.3: SOM-positive neurons mediate primarily inhibitory transmission within the LHb. (a) Schematic illustrating breeding scheme for

generating SOM-IRES-Cre::Ai32 mice. **(b)** Schematic of recording scheme. LHb neurons were patched and blue light was used to stimulate both local and long-distance ChR2-positive neurons. **(c)** Pie chart summarizing nature of neurons responsive to photostimulation. **(di)** Example traces from a neuron at two different holding potentials in which photostimulation elicited co-release of both GABA and glutamate. **(dii)** Before-after plot from neurons receiving GABA / glutamate co-releasing input in which both excitatory and inhibitory components of the postsynaptic potential were pharmacologically blocked (n = 3 neurons). **(ei)** Example traces from a neuron at three different holding potentials in which photostimulation elicited an inhibitory postsynaptic potential. **(eii)** Before-after plot from neurons receiving inhibitory input in which the IPSP was pharmacologically blocked (n = 4 neurons). **(f)** Schematic illustrating location of patched neurons within the habenular complex, projected rostrally (top left) through caudally (bottom right). Non-responsive neurons are indicated by – while responsive neurons are indicated by: + EPSP only; + IPSP only; + dual response consisting of both an excitatory and inhibitory component and; + ChR2-expressing neuron in which an action potential not sensitive to NBQX was triggered upon photostimulation. Sub-nuclear boundaries as defined by Andres et al., (1999) are indicated by dashed lines. Approximate rostral-caudal distances from Bregma (in mm) are indicated.

SOM-positive projection neurons in the ventral pallidum provide inhibitory input to the lateral habenula

We did identify a small sub-population of SOM-positive LHb neurons which appeared to co-localise with GABA (Fig. 5.1; 3.6 % of total SOM-positive neurons). It seemed unlikely that such a small population would be capable of mediating inhibition in more than half (Fig. 5.3c; 13 of 21) of the neurons tested. Nonetheless, to rule this out, we performed local injection of a Cre-dependent AAV encoding ChR2 and eYFP into the LHb (Fig. 5.4ai) in SOM-IRES-Cre mice (N = 4) and recorded from LHb neurons in acute slices while photostimulating (Fig. 5.4aii). As predicted, we did not observe photostimulation-induced postsynaptic potentials in any neurons (Fig. 5.4b and c; n = 0 of 25), although one recorded neuron expressed ChR2 and hence spiked upon photostimulation (Fig. 5.4b). Of note, we observed that eYFP expression in the superior sub-nucleus was rather limited (Fig. 5.4d), hence implying that most of these SOM-positive neurons had not been infected. Presumably, this infection resistance is as a result of a reduced viral tropism for these neurons in comparison to the majority of LHb neurons (Aschauer *et al.*, 2013; Murlidharan *et al.*, 2014); a plausible hypothesis on account of their clear differences in gene expression profile (Wagner *et al.*, 2016b). Nonetheless, as these neurons are not GABAergic (Fig. 5.1), this is highly unlikely to have affected this result.

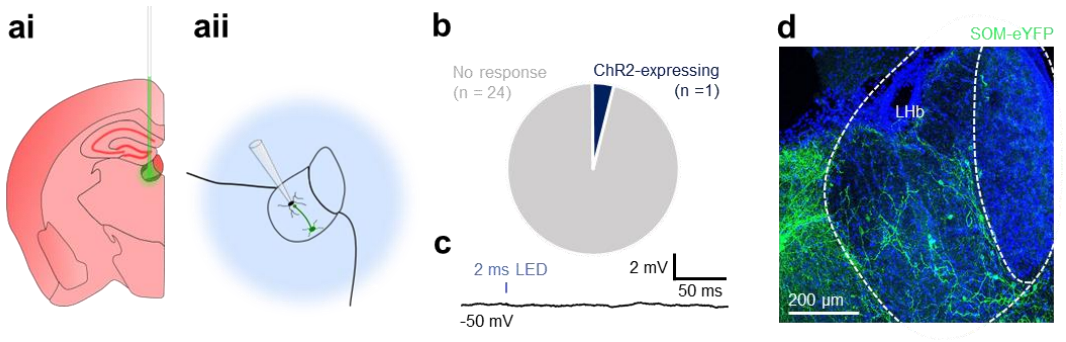

Figure 5.4 SOM-positive neurons do no mediate local inhibition within the LHb. (ai) Schematic illustrating stereotaxic injection protocol into the LHb. **(aii)** Schematic illustrating electrophysiology recording protocol for LHb neurons following stereotaxic viral injection. Transduced ChR2-positive neurons are photostimulated while recording from nearby LHb neurons. **(b)** Pie chart quantifying fraction of neurons responsive to photostimulation. **(c)** Representative example trace from a neuron which showed no response to photostimulation. Trace is an average of multiple individual sweeps. **(d)** Confocal micrograph depicting virally-transduced SOM-positive neurons within the LHb.

So if not local, where then could the observed inhibitory input (Fig. 5.3c and e) be arising from? To address this question, we again injected a Cre-dependent retrograde AAV encoding TdTomato (Tervo *et al.*, 2016) into the LHb of SOM-IRES-Cre mice (N = 3), to label all LHb input from SOM-positive neurons (Fig. 5.5). Brains were sectioned in both the coronal (N = 2) and sagittal (N = 1) planes (Fig. 5.5a and i). In both planes, we could observe

dense axonal terminals in the LHb (Fig. 5.5d, e, j and k) and labelling in three regions: the ventral pallidum (Fig. 5.5b, c j and l), the entopeduncular nucleus (Fig. 5.5d, f, j and l) and the thalamic reticular nucleus (Fig. 5.5g and h). In the sagittal plane, the stria medullaris, the primary afferent fibre tract to the LHb (Herkenham and Nauta, 1977) was clearly visible carrying fibres from neurons originating in the ventral pallidum and the entopeduncular nucleus (Fig. 5.5j). Additionally, we also observed labelling throughout the hippocampus directly dorsal to the LHb (Fig. 5.5d, g and j), however this was presumably as a result of viral spillage infecting locally-targeting hippocampal SOM-positive neurons (Stefanelli *et al.*, 2016) and hence was not pursued further.

As aforementioned, it is now accepted that SOM-positive GABA / glutamate co-releasing neurons in the entopeduncular nucleus project to the LHb (Wallace *et al.*, 2017; Lazaridis *et al.*, 2019), and thus the labelled neurons in this region are not the origin of the observed solely inhibitory input (Fig 5.3c and e). SOM-positive neurons in the thalamic reticular nucleus (TRN) are known to project to thalamic regions adjacent to the LHb (Clemente-Perez *et al.*, 2017). However, the TRN is not known to project to the LHb itself, and therefore the retrogradely labelled neurons here were most probably as a result of viral spillage into these regions.

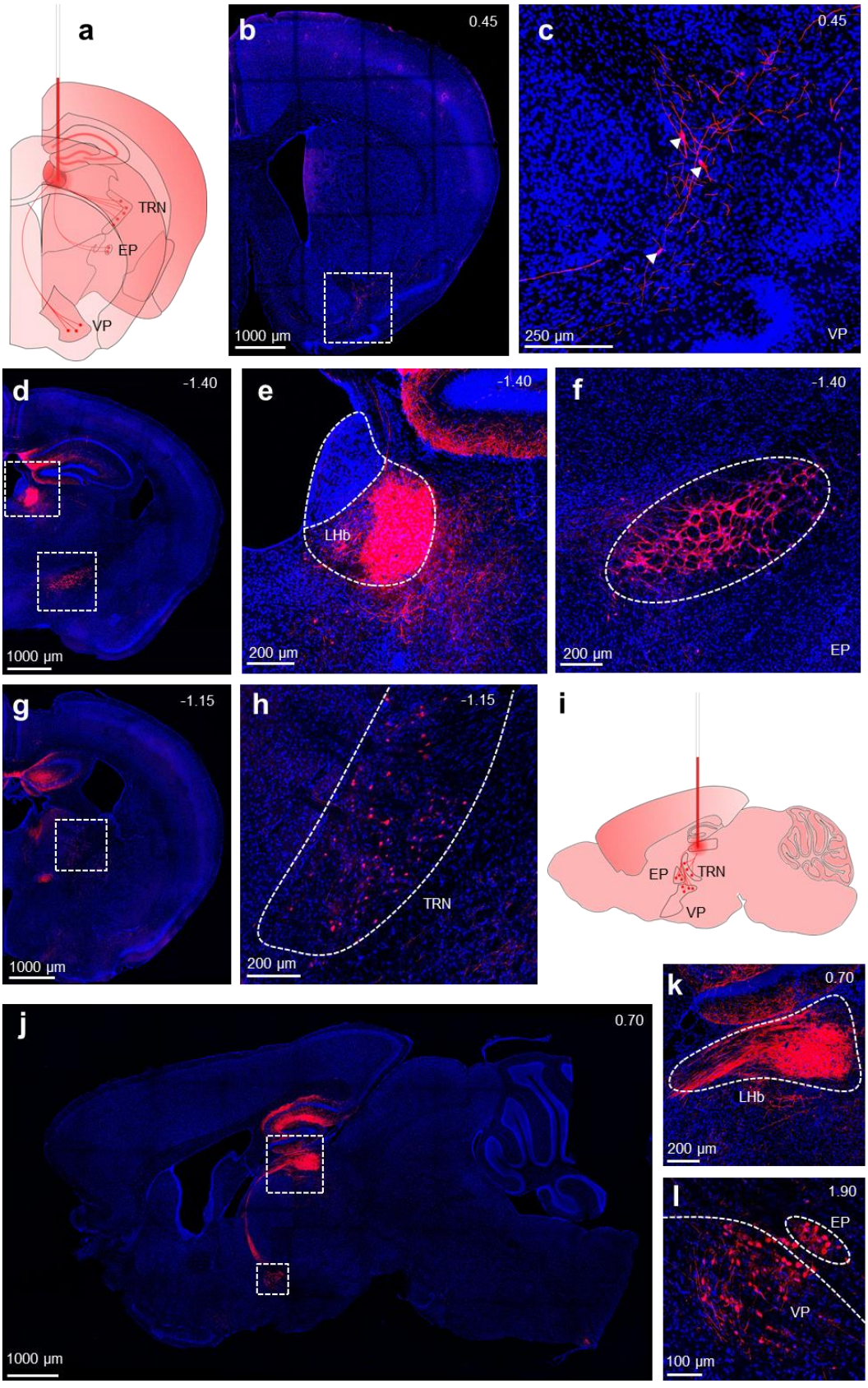
a
TRN
EP
VP
b
0.45
1000 µm
c
0.45
250 µm
VP
d
-1.40
1000 µm
e
-1.40
LHb
200 µm
f
-1.40
200 µm
EP
g
-1.15
1000 µm
h
-1.15
TRN
200 µm
i
EP
TRN
VP
j
0.70
1000 µm
k
0.70
LHb
200 µm
l
1.90
EP
VP
100 µm

Figure 5.5: Retrograde labelling of SOM-positive inputs to the LHb. (a) Schematic illustrating stereotaxic injection protocol into the LHb. Virus was injected, and brains were sectioned and imaged in the coronal plane (N = 2), allowing labelling of SOM-positive neurons which project to the LHb. VP = ventral pallidum. EP = entopeduncular nucleus. TRN = thalamic reticular nucleus. **(b)** Confocal micrograph of a whole coronal slice depicting labelled neurons in the VP. **(c)** Zoom of boxed area in (b). Labelled neurons are indicated by arrowheads. **(d)** Confocal micrograph depicting terminals of labelled neurons in the LHb, and labelled somata in the EP. **(e)** Zoom of top boxed area in (d). **(f)** Zoom of bottom boxed area in (d). **(g)** Confocal micrograph depicting labelled neurons in the TRN. **(h)** Zoom of boxed area in (g). **(i)** Schematic illustrating stereotaxic injection protocol into the LHb. Virus was injected, and brains were sectioned and imaged in the sagittal plane (N = 1), allowing labelling of SOM-positive neurons which project to the LHb. VP = ventral pallidum. EP = entopeduncular nucleus. TRN = thalamic reticular nucleus. **(j)** Confocal micrograph of a whole sagittal slice depicting labelled neurons in the EP and VP projecting to the LHb via the stria medullaris fibre tract. Note for this image the stria medullaris and EP / VP are separate confocal micrographs superimposed for illustration purposes, as these structures are not located in the same medio-lateral plane as the LHb. **(k)** Zoom of top boxed region in (j). **(l)** Zoom of bottom boxed region in (j). Numerical values in top right of images indicate approximate distance from Bregma (in mm) in the rostro-caudal axis (coronal images) or the medio-lateral axis (sagittal images).

However, to test this, we injected SOM-IRES-Cre mice (N = 2) with a Cre-dependent ChR2-eYFP encoding AAV into the TRN and recorded from neurons in both the LHb and adjacent thalamic regions while photostimulating (Fig. 5.6a and d). We could observe robust eYFP expression in the TRN at least 3 weeks post-injection (Fig. 5.6bi and ei), and consistent with previous reports (Clemente-Perez *et al.*, 2017), could observe terminals in the adjacent thalamic nuclei (primarily the lateral posterior and parafascicular thalamic nuclei), but not within the LHb itself (Fig. 5.6bii and eii). Furthermore, we observed IPSP's in 4 of 7 thalamic neurons (Fig. 5.6c), but in 0 of 6 LHb neurons (Fig. 5.6f), thus validating that the TRN projects to the thalamic regions adjacent to the LHb, but not the LHb itself. Hence, the observed retrograde labelling (Fig. 5.5) in the TRN was as a result of viral leakage into these nuclei.

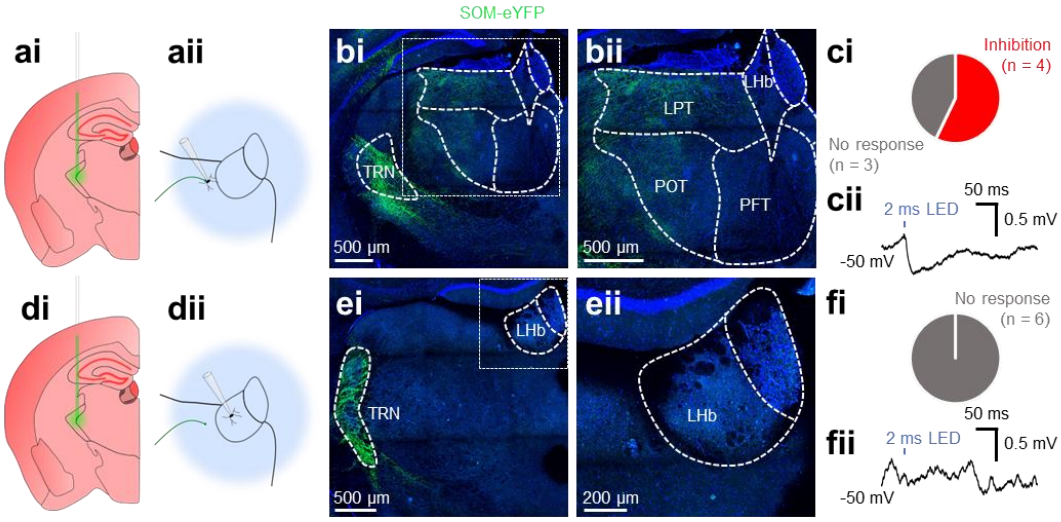

Figure 5.6: SOM-positive TRN neurons provide inhibitory input to thalamic nuclei adjacent to the LHb. (ai) Schematic illustrating stereotaxic injection protocol into the TRN. **(aii)** Schematic illustrating electrophysiology recording protocol for thalamic neurons following stereotaxic viral injection. Transduced SOM-positive neurons are photostimulated while recording from postsynaptic thalamic neurons. **(bi)** Confocal micrograph depicting the infected TRN, and thalamic nuclei adjacent to the LHb. LPT = lateral posterior thalamic nucleus. PFT = parafascicular thalamic nucleus. POT = posterior thalamic nucleus. **(bii)** Zoom of boxed region in (bi) depicting terminals from TRN neurons in thalamic nuclei adjacent to the LHb, but not within the LHb. **(ci)** Pie chart quantifying fraction of thalamic neurons responsive to photostimulation. **(cii)** Example traces from a thalamic neuron in which an IPSP was elicited upon photostimulation. Trace is an average of multiple sweeps. **(di)** and **(dii)** As for (ai) and (aii), recording from LHb. **(ei)** Confocal micrograph depicting the infected TRN, and the LHb. (eii) Zoom of boxed region in **(ei)**. Note that no axon terminals are present in the LHb. **(fi)** Pie chart quantifying fraction of LHb neurons responsive to photostimulation. **(fii)** Example traces from an LHb neuron in which no response was elicited upon photostimulation. Trace is an average of multiple sweeps.

Therefore, the ventral pallidum stood out as the most probable candidate as the source of the observed inhibitory input (Fig. 5.3c and e). We hence expressed ChR2 in SOM-positive ventral pallidal neurons by injection of Cre-

depedent AAV9 encoding ChR2 and eYFP (Fig. 5.7ai) in SOM-IRES-Cre mice (N = 3), to test if these neurons functionally projected to the LHb (Fig. 5.7aii). More than three weeks post-injection, we could clearly see virally-transduced eYFP-expressing neurons in the ventral pallidum (Fig. 5.7bi), which had dense terminals in the LHb (Fig. 5.7bii). Consistently, recording from LHb neurons in acute slices while photostimulating, we observed large (-8.8 ± 2.3 mV) GABAzine-senstive IPSPs in 6 of 13 recorded neurons (Fig. 5.7c and d) which were confined to the rostral portion of the LHb (Fig. 5.7e), consistent with the solely inhibitory responses observed in data from our SOM-IRES-Cre::Ai32 transgenic line (Fig. 5.3c and e). Hence, taking this data together with our retrograde labelling data, we therefore report a population of SOM-positive neurons in the ventral pallidum which project to and powerfully inhibit the LHb.

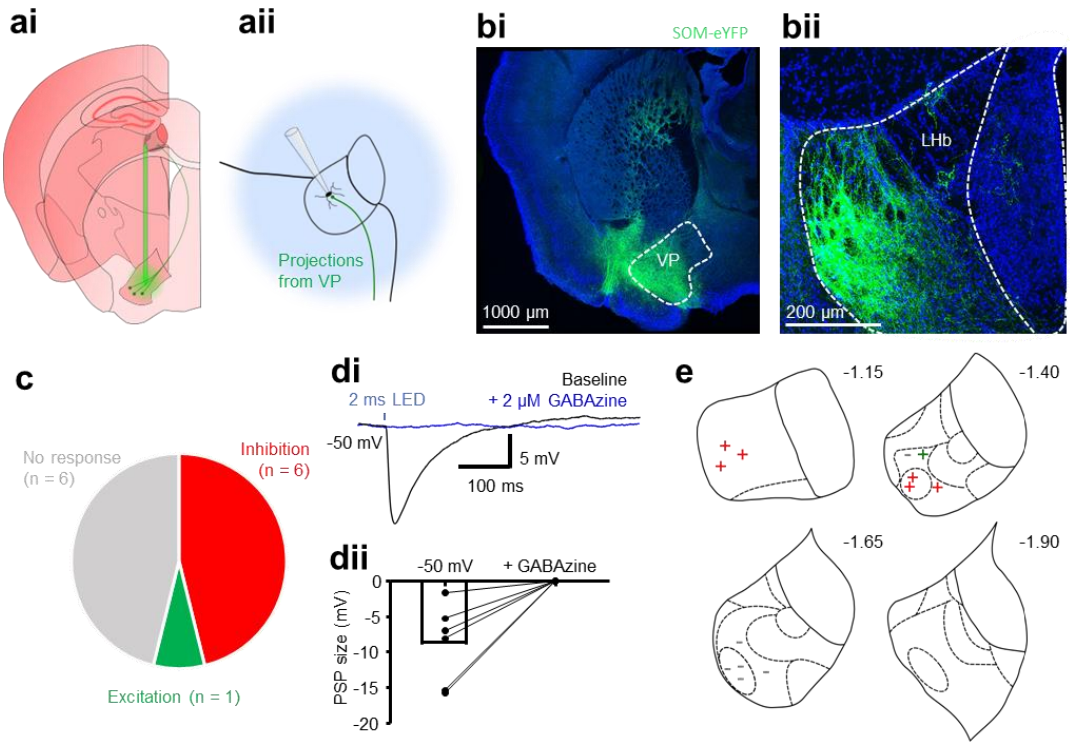

Figure 5.7: SOM-positive neurons in the ventral pallidum provide inhibitory input to the LHb. (ai) Schematic illustrating stereotaxic injection protocol into the VP. **(aii)** Schematic illustrating electrophysiology recording protocol for LHb neurons following stereotaxic viral injection. Transduced ChR2-positive neurons are photostimulated while recording from postsynaptic LHb neurons. **(bi)** Confocal micrograph depicting transduced neurons following injection into the VP. **(bii)** Confocal micrograph depicting terminals from transduced VP neurons in the LHb. **(c)** Pie chart quantifying fraction of neurons responsive to photostimulation. **(di)** Example traces from one neuron in which a GABAzine-sensitive IPSP could be elicited following photostimulation. Blue bar denotes 2 ms photostimulation. Traces are averages taken from multiple sweeps. **(dii)** Before-after plot showing amplitude of photostimulation-induced IPSPs before and after application of

GABAzine (n = 6 neurons). **(e)** Schematic illustrating location of patched neurons throughout the habenular complex. Sub-nuclear boundaries as defined by Andres et al., (1999) are indicated by dashed lines. Approximate rostral-caudal distances from Bregma (in mm) are indicated.

Discussion

From this work, we report two main findings: i) that SOM-positive neurons within the LHb are a novel sub-class distinct from the general population of LHb neurons, which have physiological characteristics comprised of traits of both LHb and MHb neurons, and ii) SOM-positive neurons in the ventral pallidum project to and powerfully inhibit the LHb.

SOM-positive lateral habenular neurons and the existence of the 'HbX' sub-nucleus

Wagner, French and Veh (2016) proposed that the superior region of the LHb should be termed 'HbX', as their thorough transcriptomic analysis revealed that neurons in this region contained genetic profiles associated with both the LHb and MHb. By assessing active and passive physiological properties (Fig. 5.2), we provide the first physiological evidence in support of this. We show that SOM-positive neurons in this region have the tonic firing activity and high input resistance of MHb neurons (Kim and Chang, 2005; Choi *et al.*, 2016),

and also the capacity to change firing modality in accordance with membrane potential classically associated with LHb neurons (Wilcox *et al.*, 1988; Kim and Chang, 2005; Yang *et al.*, 2018a).

What could be the functional importance of these neurons then? As previously discussed (introductory chapter), we now know that calcium-channel mediated bursting acts as a synchronization mechanism (Wilcox *et al.*, 1988; Gutnick and Yarom, 1989), which in the case of the LHb acts to increase overall output to downstream structures and is thus critical in the pathogenesis of depression (Cui *et al.*, 2018; Yang *et al.*, 2018b, 2018a). Assuming that the hyperpolarisation-induced change in firing modality in these neurons is at least in part mediated by similar low-threshold channels, one could then speculate that this may also be some form of synchronization mechanism specific for these SOM-positive 'HbX' neurons. It has also been proposed that this HbX area may act as an area of interaction between the LHb and MHb (Wagner *et al.*, 2016b). Assuming this to be true, perhaps then these neurons may act to synchronize activity between these two regions and increase overall habenular output, or perhaps they may have different downstream targets altogether from both the LHb and MHb. While further studies are still required to fully elucidate this function, we report here that SOM should at least act as a suitable molecular marker to investigate this.

Possible implications for inhibitory SOM-positive ventral pallidal neurons

We also report SOM-positive inhibitory projection neurons in the ventral pallidum which target the LHb (Fig. 5.7). Although inhibitory LHb-targeting ventral pallidal neurons have very recently been described (Faget *et al.*, 2018; Stephenson-Jones *et al.*, 2019), their function has remained largely elusive. Recent work suggests that LHb-projecting inhibitory and excitatory ventral pallidal neurons act oppositely to encode positive and negative motivational valence (Stephenson-Jones *et al.*, 2019). By identifying that SOM acts as a specific for these inhibitory neurons, we can thus facilitate further study of this pathway and more thoroughly investigate the role of the ventral pallidum > LHb pathway in controlling motivation.

Methodological considerations

As with the data from the PV-IRES-Cre transgenic line (chapter 4), the main methodological limitations from this body of work relate to the stereotaxic viral injections. In the case of the retrograde injections we saw infection in the hippocampus (Fig. 5.5). However, as the hippocampus does not project to the LHb, this is highly unlikely to have affected the results.

Another notable discrepancy was that comparably few of the SOM-positive neurons in the superior 'HbX' region were infected following injection (Fig. 5.4).

As discussed, this could be as a result of reduced viral tropism for these neurons (Aschauer *et al.*, 2013; Murlidharan *et al.*, 2014). Interestingly, we also never observed infection in the adjacent MHb, which should be expected as some MHb neurons are SOM-positive (Allen Brain Atlas ISH data). Perhaps then the MHb neurons and the SOM-positive 'HbX' neurons which have similar transcriptomic (Wagner *et al.*, 2016b) and physiological features (Fig. 5.2), have some intrinsic resistance to viral infection. This again is largely speculation, however certainly identifies a need for further studies investigating the specific tropisms of AAV and other viral vectors, and why the favourably infect some classes of neuron over others.

Chapter 6: General discussion

Within this study, the primary focus has been to study inhibitory input to the LHb; an important area of the research due to potentials implications for the treatment of major depressive disorder (MDD) (Geisler and Trimble, 2008; Hikosaka, 2010; Yang *et al.*, 2018b). To do so, we have implemented the use of multiple molecular markers generally considered to be associated with inhibitory identity in other brain regions (Klausberger and Somogyi, 2008; Tepper *et al.*, 2011; Overstreet-Wadiche and McBain, 2015; Tasic *et al.*, 2016; Tremblay *et al.*, 2016).

The key findings from this project are that we identify inhibitory input to the LHb arising from three distinct sources: from both local PV-positive neurons, and from PV-positive neurons in the medial dorsal thalamus (MDT); and from SOM-positive neurons in the ventral pallidum, and therefore it is not unlikely that further sources of inhibitory input remain to be defined. However, we also find that within the LHb, these molecular markers are not associated with exclusively inhibitory populations, hence challenging the classical association of these markers with inhibitory identity. Indeed, while we find Ndnf to be expressed seemingly without restriction within the LHb, we find both PV and SOM to be confined to neuronal sub-populations with physiological characteristics previously not reported in the LHb, which are likely projection neurons. Thus, we also provide evidence that the LHb is more neuronally diverse than previously thought (Christoph *et al.*, 1986; Chang and Kim, 2004; Kim and Chang, 2005; Weiss and Veh, 2011).

Readdressing the use of molecular markers as a means for sub-classifying inhibitory neurons

Testing for expression of a known molecular marker (eg. PV or SOM) is a well-accepted method of associating neurons with inhibitory identity (Ascoli *et al.*, 2008). Classically, this has been seen as a sufficient approach to further sub-classify inhibitory neurons into functionally distinct sub-populations (Klausberger and Somogyi, 2008; Tepper *et al.*, 2011; Tremblay *et al.*, 2016). Yet recent advances in single-cell sequencing approaches have revealed that sub-classifying inhibitory neurons is more complex than previously believed (Tasic *et al.*, 2016, 2018). Within the neocortex, these studies have revealed that PV-positive neurons and SOM-positive neurons alone can be further divided into at least 10 and 21 sub-populations respectively, based on gene expression profiles (Tasic *et al.*, 2016, 2018). Perhaps then each of these sub-classes may serve a different function, or perhaps have differing downstream targets. Further studies built on this novel data and taking advantage of, for example, novel techniques such as intersectional labelling approaches (Madisen *et al.*, 2015), will surely allow dissection of neuronal circuitry with an entirely new level of scrutiny.

Nonetheless, the debate as to what truly constitutes a ‘sub-class’ of inhibitory neuron is still ongoing and likely will be for the foreseeable future. While there is no entirely general consensus as to how to define a particular sub-population, most are in agreement that the main defining criteria are molecular marker expression, in combination with physiology and morphology

(Ascoli *et al.*, 2008). However, works that combine these factors are few, and have shown that substantial diversity exists even between neurons of the same proposed sub-population as defined by molecular marker (Schuman *et al.*, 2019). As an additional note, it is often overlooked that the molecular marker itself can influence neuronal function (eg. parvalbumin has been implicated in synaptic plasticity (Caillard *et al.*, 2000)), and perhaps therefore some implications regarding function of a particular sub-class could be associated with expression of a particular marker.

From our study, and from many other studies implementing the use of the 'classical' inhibitory markers PV and SOM, it is becoming more and more apparent that these markers are not sufficient tools to sub-classify and study inhibitory neurons in deeper brain structures (Shang *et al.*, 2015; Knowland *et al.*, 2017; Wallace *et al.*, 2017; Lazaridis *et al.*, 2019). Yet the use of these markers has still resulted in the generation of much novel and important data. So while recent advances are indeed progressively calling into question how best to identify and study particular populations of inhibitory neurons throughout the whole brain, the current molecular markers still clearly remain important tools for studying neuronal circuitry and function in general.

The role of inhibitory signalling within the lateral habenula

The primary goal of this project was to better understand neuronal populations that mediate inhibitory signalling within the LHb. But what is the physiological

importance of this? It is well established that the LHb is hyperactive in MDD (Sartorius *et al.*, 2010; Li *et al.*, 2011; Shabel *et al.*, 2014; Lecca *et al.*, 2016; Tchenio *et al.*, 2017; Cui *et al.*, 2018; Yang *et al.*, 2018a), and that reducing LHb hyperexcitability by altering the balance of excitatory and inhibitory signalling has an antidepressant effect (Li *et al.*, 2011; Shabel *et al.*, 2014; Lecca *et al.*, 2016; Meye *et al.*, 2016; Wallace *et al.*, 2017). A striking feature of many neurons innervating the LHb is that they co-release GABA and glutamate and hence much work has focussed on the role that these neurons play in modulating LHb excitability (Root *et al.*, 2014; Shabel *et al.*, 2014; Meye *et al.*, 2016; Wallace *et al.*, 2017; Lazaridis *et al.*, 2019). Yet, both local (Zhang *et al.*, 2018) and projection (Faget *et al.*, 2018; Huang *et al.*, 2019) GABAergic neurons are also known to innervate the LHb.

How these GABAergic neurons modulate the LHb in MDD remains to be fully established. Indeed, one could speculate that if excitatory inputs to the LHb are potentiated in MDD (Li *et al.*, 2011), then GABAergic tone may be reduced. If this were to be the case, then one may also speculate that increasing GABAergic tone should also have an antidepressant effect. For this reason, we believe GABAergic innervation of the LHb to be an important topic of study, and further clarification on the mechanisms of inhibitory control within the LHb should have the potential to lead to novel antidepressant therapies. Interestingly, our results seem to point to a target selectivity of inhibitory PV-positive neurons at the sub-regional, possibly even single cellular level (Chapter 4). We also show that these inhibitory neurons are capable of

silencing the spontaneous activity of LHb neurons. Therefore, it is reasonable to assume that the role played by these inhibitory neurons in modulating LHb neuronal excitability is not negligible, and hence a greater understanding of this inhibitory control is an exciting concept. Further work aiming to investigate the role of these pathways in an *in vivo* context, such as in animal models of depression (Henn and Vollmayr, 2005), should serve to elucidate the physiological purpose of such a selective inhibitory connection.

The organisation of the neuronal populations comprising lateral habenula at the sub-regional level

In this work we identify populations of both PV and SOM-positive neurons within the LHb with apparently novel physiological phenotypes, which also are confined to specific sub-regions within the LHb (chapters 4 and 5). Most previous work concerning the neuronal populations that constitute the LHb has traditionally looked at the LHb as a whole (Chang and Kim, 2004; Weiss and Veh, 2011; Yang *et al.*, 2018a), and indeed very little data exists regarding classification of neuronal populations at the sub-regional level (Andres *et al.*, 1999; Aizawa *et al.*, 2012; Wagner *et al.*, 2016b). To our knowledge, the evidence we provide is the first to identify physiologically distinct sub-populations of LHb neurons confined to a specific sub-region. This is indeed an interesting concept; as substantial evidence now exists implicating the LHb as a whole as a pathogenic node in depression (Sartorius *et al.*, 2010; Li *et*

al., 2011; Winter *et al.*, 2011; Shabel *et al.*, 2014; Lecca *et al.*, 2016; Tchenio *et al.*, 2017; Cui *et al.*, 2018; Yang *et al.*, 2018a), further revelations regarding the underlying circuitry implicated in this may arise from studying the contributions from individual sub-regions within the LHb.

In the case of our data, we report physiologically distinct populations of PV-positive neurons in the medial and lateral LHb (chapter 4), and SOM-positive neurons confined to the superior sub-region which appear to have hybrid physiological properties of LHb and MHb neurons (chapter 5). Do these neurons therefore have differing roles, or projection targets? Indeed, previous work has highlighted that neurons in the medial and lateral LHb have differing downstream targets (Quina *et al.*, 2015), while other work has highlighted that it is specifically bursting LHb neurons that contribute to the pathogenesis of depression (Yang *et al.*, 2018a). While these questions currently remain unanswered, further studies aiming to address the correlation between neuronal physiological properties and sub-regional localisation shall surely yield further insight into the regional connectivity of the LHb.

A possible role for local inhibitory neurons in controlling lateral habenular output

Following on from this; if it is the bursting LHb neurons that are believed to be the primary driving force in depression (Yang *et al.*, 2018a), then one must also ask whether neurons with different physiological properties play a

different role in in the pathogenesis of this disease. Recent work has proposed that the LHb acts as the primary pacemaker region in depression, in that the pathological changes in neuronal activity originate here and then propagate to downstream regions, resulting in enhanced suppression of these regions (Andalman *et al.*, 2019).

So how then does the LHb increase its overall output to elicit this effect? It is known that bursting activity is a general neuronal activity synchronizing mechanism (Gutnick and Yarom, 1989). Perhaps then most neurons within the LHb are well-connected to one another, and as these become hyperactive in depression they drive the activity of other LHb neurons, which results in an overall greater output to target regions. However, an alternative model could be that of a single (or perhaps multiple) 'control neuron' type (Fig. 6.1). In this model, another physiologically distinct class of neuron such as an inhibitory neuron may be well connected to all other LHb neurons, and this may act as the synchronising mechanism, hence resulting in the greater overall LHb output observed in depression. As of yet, little data exists regarding the local connectivity of LHb neurons, and whether or not this is different between sub-populations. However, further studies utilising, for example calcium or voltage indicators *in vitro* in combination with electrophysiology could serve as useful tools to study this, and hence shed greater light on the local connectivity of the LHb.

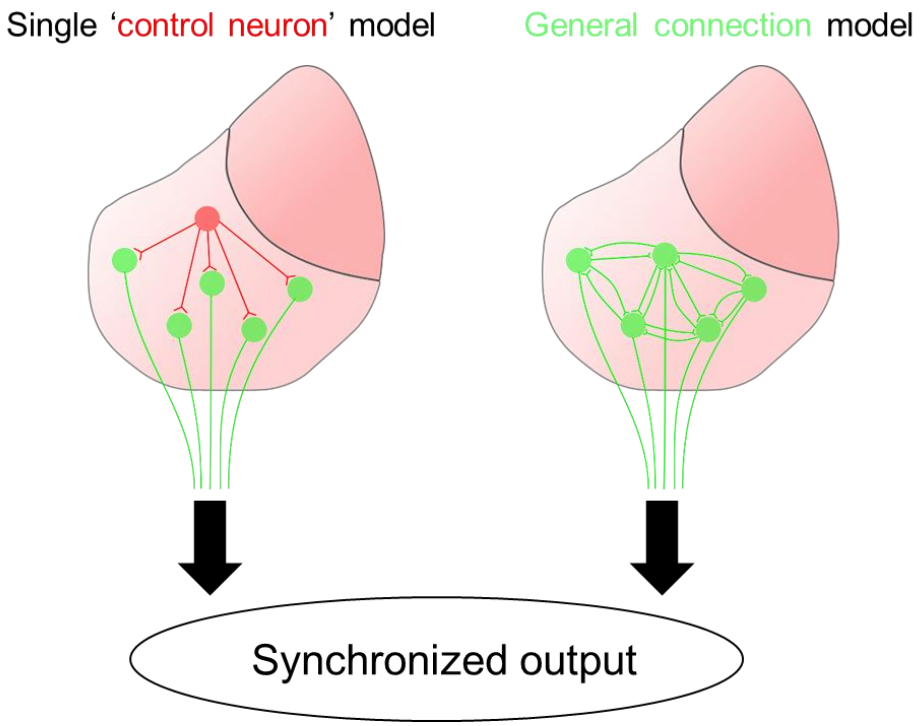

Figure 6.1: A schematic of how neurons within the LHb could be connected to synchronize activity. Left: one class of 'control neuron' acts as a central pacemaker by controlling and synchronizing the firing activity of many individual postsynaptic output neurons. Right: output neurons are generally connected to one another, and hence all act together to control the activity of other output neurons.

Future directions

In this work we have focused on studying inhibitory inputs to the LHb *in vitro*. The first question that arises from these results then is what is the physiological relevance of these circuits? Indeed, it is now well-accepted that

potentiating inhibitory input to the LHb has an antidepressant effect (Winter *et al.*, 2011; Lecca *et al.*, 2016; Huang *et al.*, 2019). Therefore, the next step for this work would be translate these findings to an *in vivo* context.

This could be approached by implementing the use of optogenetic and chemogenetic neuronal manipulations in rodent models of depression (Henn and Vollmayr, 2005). By selectively expressing an opsin or a DREADD in eg. our PV-positive MDT neurons (chapter 4), and activating these neurons while performing behaviourally-relevant tests for depression, we could therefore assess whether these circuits have implications in the treatment of this disease.

Another interesting question relates to the topological organisation of the circuitry within the LHb; indeed as it is now accepted that the LHb can be further divided into the medial and lateral portions of the LHb, each with its own projection targets (Quina et al., 2015), it may be the case that the LHb is organised in a manner consisting of multiple distinct neuronal circuits targeting different downstream regions. As such, it would also be interesting to look at the topological organisation of the LHb in the rostral-caudal axis; to date there is apparently very little data on this. Yet, our data suggests that the SOM-positive inhibitory neurons in the ventral pallidum target the rostral portion of the LHb (Fig. 5.7), and other data may imply that the SOM-positive neurons in the entopeduncular nucleus target the caudal portion of the LHb (Wallace et al., 2017; Lazaridis et al., 2019). Perhaps then if these two input regions do indeed target different portions of the LHb rostral-caudally, then the targets

downstream of the LHb may also be different, hence resulting in two discreet circuits in the rostral-caudal axis. Hence, it may be the case that the LHb is organised in a more complex manner than just two channels in the medial-lateral axis as it has been previously proposed (Kim and Chang, 2005).

Further to this, the question of defining all inhibitory inputs to the LHb is still most likely incompletely answered. As discussed in the introductory chapter, recent optogenetic studies have revealed that the inputs to the LHb are far more complex than were originally thought (Herkenham and Nauta, 1977). Indeed, by utilizing molecular markers and optogenetics, we have identified two sub-populations of inhibitory neurons in upstream regions which target the LHb (chapters 4 and 5), and thus it is highly likely that more remain to be identified. Further work utilizing other well-characterised molecular markers (Tremblay, Lee and Rudy, 2016) in combination with optogenetic circuitry interrogation techniques and viral tracing strategies should serve to identify novel sources of inhibition to the LHb. Assuming this to be true and that further inhibitory input is indeed identified, an interesting investigative route would be to test the exact mechanisms by which this inhibition is controlled. Eg. we identify a population of LHb neurons which mediate local inhibitory signalling (chapter 4). However whether these neurons are intrinsically activated, or activated by synaptic input is still unknown. One could test this by injecting a non Cre-dependent channelrhodopsin-encoding virus into a primarily excitatory region upstream to the LHb (eg. the lateral hypothalamus). If inhibition was still observed upon photostimulation, and was sensitive to a

sodium channel blocker such as tetrodotoxin, then one could assume that these local inhibitory neurons mediate local inhibition via feed-forward signalling from the tested upstream region. Such experiments would provide much novel information relating to inhibitory signalling within the LHb in the context of entire neural systems as opposed to local circuits, and hence would also serve as a suitable basis for investigating LHb inhibition in *in vivo* models of disease.

Finally, as briefly described above, the intrinsic connectivity of LHb neurons with one another is still very poorly understood. A greater understanding of this should have implications for understanding how LHb neurons act to synchronize activity (Yang *et al.*, 2018a; Andalman *et al.*, 2019). We have attempted to characterise this using dual electrophysiological recordings of PV-positive LHb neurons and other neurons (Fig. 4.2), with little success likely due to the fact that PV expression is not confined to GABAergic neurons within the LHb (Fig. 4.1). This question could be more successfully approached by identification of molecular markers more specific for inhibitory neurons within the LHb, or perhaps by use of intersectional labelling approaches where fluorescent proteins could be confined to eg. specifically inhibitory PV-positive neurons, by use of transgenic mouse lines such as PV-Flp (Madisen et al., 2015). Perhaps this question could also be approached by use of cell sequencing methods which aimed to identify gene transcripts for proteins known to be associated with local connectivity, such as connexins for example

(Bennett et al., 1991; C. Wozny, personal communication). All of these questions would be intriguing routes of further investigation to follow.

Implications in the wider context

Assuming that the above was true and activation of the identified inhibitory circuitry did indeed have some antidepressant roles in animal models, then further questions arising from this should aim to set these findings in a clinically-relevant context. While it is of course important to have a greater understanding of how the LHb is dysregulated in depression (Yang *et al.*, 2018b) in order to understand the disease, we must eventually ask how we can translate these findings to a potential treatment.

As discussed, direct inhibition of the LHb is known to have an antidepressant effect (Winter *et al.*, 2011), but how relevant is this in humans, and how could we utilise this information to develop novel treatments? At the present time, the concept of utilising optogenetic manipulations in humans to stimulate such groups of neurons is unethical. Nonetheless, clinical trials have already begun testing the potential of opsins for restoring vision loss (Baker and Flannery, 2018), and surgical interventions such as deep brain stimulation of the LHb have already shown efficacy in treatment-resistant depression (Sartorius *et al.*, 2010). For the time being, far more data regarding the potential benefits and risks of utilising such surgical and viral gene therapy approaches in humans are required, but perhaps these revolutionary

techniques may pave the way to novel treatments for depression, and many other neurological diseases, in the not-too-distant future.

Conclusions

In this work we have used an approach of electrophysiology, optogenetics and immunohistochemistry to specifically manipulate populations of neurons expressing Ndnf, PV and SOM (Tasic *et al.*, 2016, 2018; Tremblay *et al.*, 2016; Abs *et al.*, 2018) *in vitro* and assess the circuitry they constitute within and projecting to the LHb. Our work identifies three inhibitory inputs to the LHb, and also provides evidence that the LHb is more neuronally diverse than previously thought. This work hence helps elucidate the circuitry by which inhibitory signalling is processed within the LHb, which will help facilitate the study of the neural circuitry implicated in depression. Furthermore, with our identification of three distinct sources of inhibitory input to the LHb, it remains likely that other sources remain to be defined, and further works should seek to describe these in order to heighten our understanding of the LHb, and how it becomes maladaptive in depression.

Bibliography

Abs, E., Poorthuis, R. B., Apelblat, D., Muhammad, K., Pardi, M. B., Enke, L., Kushinsky, D., Pu, D. L., Eizinger, M. F., Conzelmann, K. K., Spiegel, I. and Letzkus, J. J. (2018) 'Learning-Related Plasticity in Dendrite-Targeting Layer 1 Interneurons', *Neuron*, 100(3), pp. 684–699.

Aizawa, H., Kobayashi, M., Tanaka, S., Fukai, T. and Okamoto, H. (2012) 'Molecular characterization of the subnuclei in rat habenula', *Journal of Comparative Neurology*, 520(18), pp. 4051–4066.

Andalman, A. S., Burns, V. M., Lovett-Barron, M., Broxton, M., Poole, B., Yang, S. J., Grosenick, L., Lerner, T. N., Chen, R., Benster, T., Mourrain, P., Levoy, M., Rajan, K. and Deisseroth, K. (2019) 'Neuronal Dynamics Regulating Brain and Behavioral State Transitions', *Cell*, 177(4), pp. 970–985.

Andres, K. H., Von Düring, M. and Veh, R. W. (1999) 'Subnuclear organization of the rat habenular complexes', *Journal of Comparative Neurology*, 407(1), pp. 130–150.

Armstrong, C., Szabadics, J., Tamas, G. and Soltesz, I. (2011) 'Neurogliaform cells in the molecular layer of the dentate gyrus as feed-forward GABAergic modulators of entorhino-hippocampal interplay', *The Journal of Comparative Neurology*, 519(8), pp. 1476–91.

Aschauer, D. F., Kreuz, S. and Rumpel, S. (2013) 'Analysis of Transduction Efficiency, Tropism and Axonal Transport of AAV Serotypes 1, 2, 5, 6, 8

and 9 in the Mouse Brain', *PLoS ONE*, 8(9).

Ascoli, G. a, Alonso-Nanclares, L., Anderson, S. a, Barrionuevo, G., Benavides-Piccione, R., Burkhalter, A., Buzsáki, G., Cauli, B., Defelipe, J., Fairén, A., Feldmeyer, D., Fishell, G., Fregnac, Y., Freund, T. F., Gardner, D., Gardner, E. P., Goldberg, J. H., Helmstaedter, M., Hestrin, S., Karube, F., Kisvárday, Z. F., Lambolez, B., Lewis, D. a, Marin, O., Markram, H., Muñoz, A., Packer, A., Petersen, C. C. H., Rockland, K. S., Rossier, J., Rudy, B., Somogyi, P., Staiger, J. F., Tamas, G., Thomson, A. M., Toledo-Rodriguez, M., Wang, Y., West, D. C. and Yuste, R. (2008) 'Petilla terminology: nomenclature of features of GABAergic interneurons of the cerebral cortex.', *Nature reviews. Neuroscience*, 9(7), pp. 557–568.

Atallah, B. V., Bruns, W., Carandini, M. and Scanziani, M. (2012) 'Parvalbumin-Expressing Interneurons Linearly Transform Cortical Responses to Visual Stimuli', *Neuron*, 73(1), pp. 159–170.

Baker, C. K. and Flannery, J. G. (2018) 'Innovative Optogenetic Strategies for Vision Restoration', *Frontiers in Cellular Neuroscience*, 12(316).

Baker, P. M., Oh, S. E., Kidder, K. S. and Mizumori, S. J. Y. (2015) 'Ongoing behavioral state information signaled in the lateral habenula guides choice flexibility in freely moving rats', *Frontiers in Behavioral Neuroscience*, 9(295), pp. 1–22.

Baker, P. M., Rao, Y., Rivera, Z. M. G., Garcia, E. M. and Mizumori, S. J. Y.

(2019) ‘Selective Functional Interaction Between the Lateral Habenula and Hippocampus During Different Tests of Response Flexibility’, *Frontiers in Molecular Neuroscience*, 12(245).

Barker, D. J., Miranda-Barrientos, J., Zhang, S., Root, D. H., Wang, H.-L., Liu, B., Calipari, E. S. and Morales, M. (2017) ‘Lateral Preoptic Control of the Lateral Habenula through Convergent Glutamate and GABA Transmission’, *Cell Reports*, 21(7), pp. 1757–1769.

Bennett, B. D. and Bolam, J. P. (1994) ‘Synaptic input and output of parvalbumin-immunoreactive neurons in the neostriatum of the rat’, *Neuroscience*, 62(3), pp. 707–719.

Bernstein, J. G. and Boyden, E. S. (2011) ‘Optogenetic tools for analyzing the neural circuits of behavior’, *Trends in Cognitive Sciences*, pp. 592–600.

Bouabe, H. and Okkenhaug, K. (2013) ‘Gene targeting in mice: A review’, *Methods in Molecular Biology*, 1064, pp. 315–336.

Boyden, E. S., Zhang, F., Bamberg, E., Nagel, G. and Deisseroth, K. (2005) ‘Millisecond-timescale, genetically targeted optical control of neural activity’, *Nature Neuroscience*, 8(9), pp. 1263–1268.

Brinschwitz, K., Dittgen, A., Madai, V. I., Lommel, R., Geisler, S. and Veh, R. W. (2010) ‘Glutamatergic axons from the lateral habenula mainly terminate on GABAergic neurons of the ventral midbrain’, *Neuroscience*, 168(2), pp. 463–476.

Caillard, O., Moreno, H., Schwaller, B., Llano, I., Celio, M. R. and Marty, A. (2000) ‘Role of the calcium-binding protein parvalbumin in short-term synaptic plasticity’, *Proceedings of the National Academy of Sciences of the United States of America*, 97(24), pp. 13372–13377.

Celio, M. R. (1986) ‘Parvalbumin in most gamma-aminobutyric acid-containing neurons of the rat cerebral cortex.’, *Science*, 231, pp. 995–997.

Chang, S. and Kim, U. (2004) ‘Ionic Mechanism of Long-Lasting Discharges of Action Potentials Triggered by Membrane Hyperpolarization in the Medial Lateral Habenula’, *Journal of Neuroscience*, 24(9), pp. 2172–2181.

Choi, K., Lee, Y., Lee, C., Hong, S., Lee, S., Kang, S. J. and Shin, K. S. (2016) ‘Optogenetic activation of septal GABAergic afferents entrains neuronal firing in the medial habenula’, *Scientific Reports*, 6(34800).

Christoph, G. R., Leonzio, R. J. and Wilcox, K. S. (1986) ‘Stimulation of the lateral habenula inhibits dopamine-containing neurons in the substantia nigra and ventral tegmental area of the rat.’, *The Journal of Neuroscience*, 6(3), pp. 613–619.

Clemente-Perez, A., Makinson, S. R., Higashikubo, B., Brovarney, S., Cho, F. S., Urry, A., Holden, S. S., Wimer, M., Dávid, C., Fenno, L. E., Acsády, L., Deisseroth, K. and Paz, J. T. (2017) ‘Distinct Thalamic Reticular Cell Types Differentially Modulate Normal and Pathological

Cortical Rhythms', *Cell Reports*, 19(10), pp. 2130–2142.

Cui, Y., Yang, Y., Ni, Z., Dong, Y., Cai, G., Foncelle, A., Ma, S., Sang, K., Tang, S., Li, Y., Shen, Y., Berry, H., Wu, S. and Hu, H. (2018) 'Astroglial Kir4.1 in the lateral habenula drives neuronal bursts in depression', *Nature*, 554(7692), pp. 323–327.

Delgado, P. L. (2000) 'Depression: The case for a monoamine deficiency', *Journal of Clinical Psychiatry*, 61, pp. 7–11.

Faget, L., Zell, V., Souter, E., McPherson, A., Ressler, R., Gutierrez-reed, N., Yoo, J. H., Dulcis, D. and Hnasko, T. S. (2018) 'Opponent control of behavioral reinforcement by inhibitory and excitatory projections from the ventral pallidum', *Nature Communications*, 9(1), pp. 1–14.

Fakhoury, M. (2018) 'The dorsal diencephalic conduction system in reward processing: Spotlight on the anatomy and functions of the habenular complex', *Behavioural Brain Research*, 348, pp. 115–126.

Feng, L., Zhao, T. and Kim, J. (2015) 'neuTube 1.0: A New Design for Efficient Neuron Reconstruction Software Based on the SWC Format', *eNeuro*, 2(1).

Ferguson, B. R. and Gao, W.-J. (2018) 'PV Interneurons: Critical Regulators of E/I Balance for Prefrontal Cortex-Dependent Behavior and Psychiatric Disorders', *Frontiers in Neural Circuits*, 12(37).

Ferraro, G., Montalbano, M. E., Sardo, P. and La Grutta, V. (1996) 'Lateral habenular influence on dorsal raphe neurons', *Brain Research Bulletin*,

41(1), pp. 47–52.

Geisler, S. and Trimble, M. (2008) ‘The lateral habenula: No longer neglected’, *CNS Spectrums*, 13(6), pp. 484–489.

Gutnick, M. J. and Yarom, Y. (1989) ‘Low threshold calcium spikes, intrinsic neuronal oscillation and rhythm generation in the CNS’, *Journal of Neuroscience Methods*, 28(1–2), pp. 93–99.

Heffner, C. S., Herbert Pratt, C., Babiuk, R. P., Sharma, Y., Rockwood, S. F., Donahue, L. R., Eppig, J. T. and Murray, S. A. (2012) ‘Supporting conditional mouse mutagenesis with a comprehensive cre characterization resource’, *Nature Communications*, 3.

Henn, F. A. and Vollmayr, B. (2005) ‘Stress models of depression: Forming genetically vulnerable strains’, *Neuroscience and Biobehavioral Reviews*, 29(4–5), pp. 799–804.

Herkenham, M. and Nauta, W. J. (1977) ‘Afferent connections of the habenular nuclei in the rat. A horseradish peroxidase study, with a note on the fiber-of-passage problem.’, *The Journal of Comparative Neurology*, 173(1), pp. 123–146.

Herkenham, M. and Nauta, W. J. H. (1979) ‘Efferent connections of the habenular nuclei in the rat’, *The Journal of Comparative Neurology*, 187(1), pp. 19–47.

Hikosaka, O. (2010) ‘The habenula: from stress evasion to value-based decision-making’, *Nat Rev Neuroscience*, 11(7), pp. 503–513.

Hippenmeyer, S., Vrieseling, E., Sigrist, M., Portmann, T., Laengle, C., Ladle, D. R. and Arber, S. (2005) ‘A developmental switch in the response of DRG neurons to ETS transcription factor signaling’, *PLoS Biology*, 3(5), pp. 0878–0890.

Hirschfeld, R. M. A. (2000) ‘History and evolution of the monoamine hypothesis of depression’, *Journal of Clinical Psychiatry*, 61, pp. 4–6.

Huang, L., Xi, Y., Peng, Y., Yang, Y., Huang, X., Fu, Y., Tao, Q., Xiao, J., Yuan, T., An, K., Zhao, H., Pu, M., Xu, F., Xue, T., Luo, M., So, K. and Ren, C. (2019) ‘A Visual Circuit Related to Habenula Underlies the Antidepressive Effects of Light Therapy’, *Neuron*, 102(1), pp. 128–142.

Ibanez-Sandoval, O., Tecuapetla, F., Unal, B., Shah, F., Koos, T. and Tepper, J. M. (2011) ‘A Novel Functionally Distinct Subtype of Striatal Neuropeptide Y Interneuron’, *Journal of Neuroscience*, 31(46), pp. 16757–16769.

Ikemoto, S. (2010) ‘Brain reward circuitry beyond the mesolimbic dopamine system: A neurobiological theory’, *Neuroscience and Biobehavioral Reviews*, pp. 129–150.

Jhou, T. C., Fields, H. L., Baxter, M. G., Saper, C. B. and Holland, P. C. (2009a) ‘The Rostromedial Tegmental Nucleus (RMTg), a major GABAergic afferent to midbrain dopamine neurons, encodes aversive stimuli and inhibits motor responses’, *Neuron*, 61(5), pp. 786–800.

Jhou, T. C., Geisler, S., Marinelli, M., Degarmo, B. A. and Zahm, D. S.

(2009b) ‘The mesopontine rostromedial tegmental nucleus: A structure targeted by the lateral habenula that projects to the ventral tegmental area of Tsai and substantia nigra compacta’, *Journal of Comparative Neurology*, 513(6), pp. 566–596.

Ji, H. and Shepard, P. D. (2007) ‘Lateral habenula stimulation inhibits rat midbrain dopamine neurons through a GABA(A) receptor-mediated mechanism.’, *The Journal of neuroscience : the official journal of the Society for Neuroscience*, 27(26), pp. 6923–6930.

Jinno, S., Klausberger, T., Marton, L. F., Dalezios, Y., Roberts, J. D. B., Fuentealba, P., Bushong, E. A., Henze, D., Buzsaki, G. and Somogyi, P. (2007) ‘Neuronal Diversity in GABAergic Long-Range Projections from the Hippocampus’, *Journal of Neuroscience*, 27(33), pp. 8790–8804.

Jinno, S. and Kosaka, T. (2004) ‘Parvalbumin is expressed in glutamatergic and GABAergic corticostriatal pathway in mice’, *Journal of Comparative Neurology*, 477(2), pp. 188–201.

Karagiannis, A., Gallopin, T., David, C., Battaglia, D., Geoffroy, H., Rossier, J., Hillman, E. M. C., Staiger, J. F. and Cauli, B. (2009) ‘Classification of NPY-Expressing Neocortical Interneurons’, *Journal of Neuroscience*, 29(11), pp. 3642–3659.

Karayannis, T., Elfant, D., Huerta-Ocampo, I., Teki, S., Scott, R. S., Rusakov, D. A., Jones, M. V and Capogna, M. (2010) ‘Slow GABA transient and receptor desensitization shape synaptic responses evoked

by hippocampal neurogliaform cells.', *The Journal of neuroscience : the official journal of the Society for Neuroscience*, 30(29), pp. 9898–909.

Kawaguchi, Y., Katsumaru, H., Kosaka, T., Heizmann, C. W. and Hama, K. (1987) 'Fast spiking cells in rat hippocampus (CA1 region) contain the calcium-binding protein parvalbumin', *Brain Research*, 416(2), pp. 369–374.

Kawaguchi, Y. and Kubota, Y. (1997) 'GABAergic cell subtypes and their synaptic connections in rat frontal cortex', *Cerebral Cortex*, 7(6), pp. 476–486.

Kiening, K. and Sartorius, A. (2013) 'A new translational target for deep brain stimulation to treat depression', *EMBO Molecular Medicine*, 5(8), pp. 1151–1153.

Kim, U. and Chang, S. Y. (2005) 'Dendritic morphology, local circuitry, and intrinsic electrophysiology of neurons in the rat medial and lateral habenular nuclei of the epithalamus', *Journal of Comparative Neurology*, 483(2), pp. 236–250.

Klausberger, T. and Somogyi, P. (2008) 'Neuronal diversity and temporal dynamics: the unity of hippocampal circuit operations.', *Science*, 321(5885), pp. 53–7.

Knowland, D., Lilascharoen, V., Pham Pacia, C., Shin, S., Hou-Jen Wang, E., Kook Lim, B. and Knowland, D. (2017) 'Distinct Ventral Pallidal Neural Populations Mediate Separate Symptoms of Depression', *Cell*,

170(2), pp. 284–297.

Lammel, S., Steinberg, E. E., Földy, C., Wall, N. R., Beier, K., Luo, L. and Malenka, R. C. (2015) ‘Diversity of transgenic mouse models for selective targeting of midbrain dopamine neurons’, *Neuron*, 85(2), pp. 429–438.

Lazaridis, I., Tzortzi, O., Weglage, M., Märtin, A., Xuan, Y., Parent, M., Johansson, Y., Fuzik, J., Fürth, D., Fenno, L. E., Ramakrishnan, C., Silberberg, G., Deisseroth, K., Carlén, M. and Meletis, K. (2019) ‘A hypothalamus-habenula circuit controls aversion’, *Molecular Psychiatry*, 24(9), pp. 1351–1368.

Lecca, S., Meye, F. J., Trusel, M., Tchenio, A., Harris, J., Schwarz, M. K., Burdakov, D., Georges, F. and Mameli, M. (2017) ‘Aversive stimuli drive hypothalamus-to-habenula excitation to promote escape behavior’, *eLife*, 6, pp. 1–16.

Lecca, S., Pelosi, A., Tchenio, A., Moutkine, I., Lujan, R., Hervé, D. and Mameli, M. (2016) ‘Rescue of GABAB and GIRK function in the lateral habenula by protein phosphatase 2A inhibition ameliorates depression-like phenotypes in mice.’, *Nature medicine*, 22(3), pp. 254–61.

Lecea, L. de, del Río, J. A. and Soriano, E. (1995) ‘Developmental expression of parvalbumin mRNA in the cerebral cortex and hippocampus of the rat’, *Molecular Brain Research*, 32(1), pp. 1–13.

Li, B., Piriz, J., Mirrione, M., Chung, C., Proulx, C. D., Schulz, D., Henn, F.

and Malinow, R. (2011) ‘Synaptic potentiation onto habenula neurons in the learned helplessness model of depression.’, *Nature*, 470(7335), pp. 535–539.

Li, L. Y., Xiong, X. R., Ibrahim, L. A., Yuan, W., Tao, H. W. and Zhang, L. I. (2015) ‘Differential Receptive Field Properties of Parvalbumin and Somatostatin Inhibitory Neurons in Mouse Auditory Cortex’, *Cerebral Cortex*, 25(7), pp. 1782–1791.

Madisen, L., Garner, A. R., Shimaoka, D., Chuong, A. S., Klapoetke, N. C., Li, L., van der Bourg, A., Niino, Y., Egolf, L., Monetti, C., Gu, H., Mills, M., Cheng, A., Tasic, B., Nguyen, T. N., Sunkin, S. M., Benucci, A., Nagy, A., Miyawaki, A., Helmchen, F., Empson, R. M., Knöpfel, T., Boyden, E. S., Reid, R. C., Carandini, M. and Zeng, H. (2015) ‘Transgenic mice for intersectional targeting of neural sensors and effectors with high specificity and performance’, *Neuron*, 85(5), pp. 942–58.

Madisen, L., Mao, T., Koch, H., Zhuo, J. M., Berenyi, A., Fujisawa, S., Hsu, Y. W. A., Garcia, A. J., Gu, X., Zanella, S., Kidney, J., Gu, H., Mao, Y., Hooks, B. M., Boyden, E. S., Buzsáki, G., Ramirez, J. M., Jones, A. R., Svoboda, K., Han, X., Turner, E. E. and Zeng, H. (2012) ‘A toolbox of Cre-dependent optogenetic transgenic mice for light-induced activation and silencing’, *Nature Neuroscience*, 15(5), pp. 793–802.

Madisen, L., Zwingman, T. A., Sunkin, S. M., Oh, S. W., Zariwala, H. A., Gu, H., Ng, L. L., Palmiter, R. D., Hawrylycz, M. J., Jones, A. R., Lein, E. S.

and Zeng, H. (2010) ‘A robust and high-throughput Cre reporting and characterization system for the whole mouse brain’, *Nature Neuroscience*, 13(1), pp. 133–140.

Marín, O. (2012) ‘Interneuron dysfunction in psychiatric disorders.’, *Nature reviews. Neuroscience*, 13(2), pp. 107–20.

Mathis, V., Barbelivien, A., Majchrzak, M., Mathis, C., Cassel, J. C. and Lecourtier, L. (2017) ‘The Lateral Habenula as a Relay of Cortical Information to Process Working Memory’, *Cerebral cortex*, 27(12), pp. 5485–5495.

Mathis, V., Cosquer, B., Avallone, M., Cassel, J. C. and Lecourtier, L. (2015) ‘Excitatory transmission to the lateral habenula is critical for encoding and retrieval of spatial memory’, *Neuropsychopharmacology*, 40(12), pp. 2843–2851.

Mathis, V. and Lecourtier, L. (2017) ‘Role of the lateral habenula in memory through online processing of information’, *Pharmacology Biochemistry and Behavior*. Elsevier, 162, pp. 69–78.

Matsumoto, M. and Hikosaka, O. (2007) ‘Lateral habenula as a source of negative reward signals in dopamine neurons.’, *Nature*, 447(7148), pp. 1111–1115.

Meye, F. J., Soiza-Reilly, M., Smit, T., Diana, M. A., Schwarz, M. K. and Mameli, M. (2016) ‘Shifted pallidal co-release of GABA and glutamate in habenula drives cocaine withdrawal and relapse’, *Nature Neuroscience*,

19(8), pp. 1019–1024.

Mizumori, S. J. Y. and Baker, P. M. (2017) ‘The Lateral Habenula and Adaptive Behaviors’, *Trends in Neurosciences*, 40(8), pp. 481–493.

Murlidharan, G., Samulski, R. J. and Asokan, A. (2014) ‘Biology of adeno-associated viral vectors in the central nervous system’, *Frontiers in Molecular Neuroscience*, 7(76).

Ognjanovski, N., Schaeffer, S., Wu, J., Mofakham, S., Maruyama, D., Zochowski, M. and Aton, S. J. (2017) ‘Parvalbumin-expressing interneurons coordinate hippocampal network dynamics required for memory consolidation’, *Nature communications*, p. 150329.

Oláh, S., Füle, M., Komlósi, G., Varga, C., Báldi, R., Barzó, P. and Tamás, G. (2009) ‘Regulation of cortical microcircuits by unitary GABA-mediated volume transmission.’, *Nature*, 461(7268), pp. 1278–81.

Olah, S., Komlosi, G., Szabadics, J., Varga, C., Toth, E., Barzo, P. and Tamas, G. (2007) ‘Output of neurogliaform cells to various neuron types in the human and rat cerebral cortex’, *Front Neural Circuits.*, 1(4).

Omelchenko, N., Bell, R. and Sesack, S. R. (2009) ‘Lateral Habenula Projections to the Rat Ventral Tegmental Area: Sparse Synapses Observed Onto Dopamine and GABA Neurons’, *European Journal of Neuroscience*, 30(7), pp. 1239–1250.

Organization, W. H. (2017) *Depression and Other Common Mental Disorders*, *Global Health Estimates.* doi: CC BY-NC-SA 3.0 IGO.

Otte, C., Gold, S. M., Penninx, B. W., Pariante, C. R., Etkin, A., Fava, M., Mohr, D. C. and Schatzberg, A. F. (2016) 'Major depressive disorder', *Nature Reviews Disease Primers*, 2(16065).

Overstreet-Wadiche, L. and McBain, C. J. (2015) 'Neurogliaform cells in cortical circuits', *Nature Reviews Neuroscience*, 16(8), pp. 458–468.

Paxinos, G. and Franklin, K. (2012) *Paxinos and Franklin's the Mouse Brain in Stereotaxic Coordinates*, *São Paulo, Academic Press*.

Phillipson, O. T. T. and Pycock, C. J. J. (1982) 'Dopamine Neurones of the Ventral Tegmentum Project to Both Medial and Lateral Habenula', *Experimental Brain Research*, 45(1–2), pp. 89–94.

van den Pol, A. N., Yao, Y., Fu, L.-Y., Foo, K., Huang, H., Coppari, R., Lowell, B. B. and Broberger, C. (2009) 'Neuromedin B and Gastrin-Releasing Peptide Excite Arcuate Nucleus Neuropeptide Y Neurons in a Novel Transgenic Mouse Expressing Strong Renilla Green Fluorescent Protein in NPY Neurons', *Journal of Neuroscience*, 29(14), pp. 4622–4639.

Price, C. J., Cauli, B., Kovacs, E. R., Kulik, A., Lambolez, B., Shigemoto, R. and Capogna, M. (2005) 'Neurogliaform Neurons Form a Novel Inhibitory Network in the Hippocampal CA1 Area', *Journal of Neuroscience*, 25(29), pp. 6775–6786. Available at: http://www.jneurosci.org/cgi/doi/10.1523/JNEUROSCI.1135-05.2005.

Price, C. J., Scott, R., Rusakov, D. A. and Capogna, M. (2008) 'GABA(B)

receptor modulation of feedforward inhibition through hippocampal neurogliaform cells', *Journal of Neuroscience*, 28(27), pp. 6974–6982.

Quina, L. A., Tempest, L., Ng, L., Harris, J. A., Ferguson, S., Jhou, T. C. and Turner, E. E. (2015) 'Efferent pathways of the mouse lateral habenula', *Journal of Comparative Neurology*, 523(1), pp. 32–60.

Root, D. H., Mejias-Aponte, C. A., Zhang, S., Wang, H. L., Hoffman, A. F., Lupica, C. R. and Morales, M. (2014) 'Single rodent mesohabenular axons release glutamate and GABA', *Nature Neuroscience*, 17(11), pp. 1543–1551.

Sartorius, A. and Henn, F. A. (2007) 'Deep brain stimulation of the lateral habenula in treatment resistant major depression', *Medical Hypotheses*, 69(6), pp. 1305–1308.

Sartorius, A., Kiening, K. L., Kirsch, P., von Gall, C. C., Haberkorn, U., Unterberg, A. W., Henn, F. A. and Meyer-Lindenberg, A. (2010) 'Remission of Major Depression Under Deep Brain Stimulation of the Lateral Habenula in a Therapy-Refractory Patient', *Biological Psychiatry*, 67(2), pp. 9–11.

Schuman, B., Machold, R. P., Hashikawa, Y., Fuzik, J., Fishell, G. J. and Rudy, B. (2019) 'Four Unique Interneuron Populations Reside in Neocortical Layer 1', *The Journal of Neuroscience*, 39(1), pp. 125–139.

Shabel, S. J., Proulx, C. D., Piriz, J. and Manilow, R. (2014) 'Mood regulation. GABA/glutamate co-release controls habenula output and is

modified by antidepressant treatment.', *Science*, 345(6203), pp. 1494–1498.

Shang, C., Liu, Z., Chen, Z., Shi, Y., Wang, Q., Liu, S., Li, D. and Cao, P. (2015) 'A parvalbumin-positive excitatory visual pathway to trigger fear responses in mice', *Science*, 348(6242), pp. 1472–1477.

Stamatakis, A. M., Jennings, J. H., Ung, R. L., Blair, G. A., Weinberg, R. J., Neve, R. L., Boyce, F., Mattis, J., Ramakrishnan, C., Deisseroth, K. and Stuber, G. D. (2013) 'A Unique Population of Ventral Tegmental Area Neurons Inhibits the Lateral Habenula to Promote Reward', *Neuron*, 80(4), pp. 1039–1053.

Stefanelli, T., Bertollini, C., Lüscher, C., Muller, D. and Mendez, P. (2016) 'Hippocampal Somatostatin Interneurons Control the Size of Neuronal Memory Ensembles', *Neuron*, 89(5), pp. 1074–1085.

Stephenson-Jones, M., Bravo-Rivera, C., Ahrens, S., Furlan, A., Fernandes-Henriques, C. and Li, B. (2019) 'Opposing Contributions of GABAergic and Glutamatergic Ventral Pallidal Neurons to Motivational Behaviours', *SSRN Electronic Journal*. doi: 10.2139/ssrn.3367001.

Szabadics, J., Tamás, G. and Soltesz, I. (2007) 'Different transmitter transients underlie presynaptic cell type specificity of GABAA,slow and GABAA,fast.', *Proceedings of the National Academy of Sciences*, 104(37), pp. 14831–14836.

Takesian, A. E., Bogart, L. J., Lichtman, J. W. and Hensch, T. K. (2018)

‘Inhibitory circuit gating of auditory critical-period plasticity’, *Nature Neuroscience*, 21(2), pp. 218–227.

Tamás, G., Lorincz, A., Simon, A. and Szabadics, J. (2003) ‘Identified sources and targets of slow inhibition in the neocortex.’, *Science*, 299(5614), pp. 1902–5.

Taniguchi, H., He, M., Wu, P., Kim, S., Paik, R., Sugino, K., Kvitsani, D., Fu, Y., Lu, J., Lin, Y., Miyoshi, G., Shima, Y., Fishell, G., Nelson, S. B. and Huang, Z. J. (2011) ‘A Resource of Cre Driver Lines for Genetic Targeting of GABAergic Neurons in Cerebral Cortex’, *Neuron*, 71(6), pp. 995–1013.

Tasic, B., Menon, V., Nguyen, T. N. T., Kim, T. T. K., Jarsky, T., Yao, Z., Levi, B. B., Gray, L. T., Sorensen, S. A., Dolbeare, T., Bertagnolli, D., Goldy, J., Shapovalova, N., Parry, S., Lee, C. C., Smith, K., Bernard, A., Madisen, L., Sunkin, S. M., Hawrylycz, M., Koch, C., Zeng, H., Yao, Z., Lee, C. C., Shapovalova, N., Parry, S., Madisen, L., Sunkin, S. M., Hawrylycz, M., Koch, C. and Zeng, H. (2016) ‘Adult mouse cortical cell taxonomy revealed by single cell transcriptomics’, *Nature Neuroscience*, 19(2), pp. 335–46.

Tasic, B., Yao, Z., Graybuck, L. T., Smith, K. A., Nguyen, T. N., Bertagnolli, D., Goldy, J., Garren, E., Economo, M. N., Viswanathan, S., Penn, O., Bakken, T., Menon, V., Miller, J., Fong, O., Hirokawa, K. E., Lathia, K., Rimorin, C., Tieu, M., Larsen, R., Casper, T., Barkan, E., Kroll, M., Parry, S., Shapovalova, N. V., Hirschstein, D., Pendergraft, J., Sullivan,

H. A., Kim, T. K., Szafer, A., Dee, N., Groblewski, P., Wickersham, I., Cetin, A., Harris, J. A., Levi, B. P., Sunkin, S. M., Madisen, L., Daigle, T. L., Looger, L., Bernard, A., Phillips, J., Lein, E., Hawrylycz, M., Svoboda, K., Jones, A. R., Koch, C. and Zeng, H. (2018) 'Shared and distinct transcriptomic cell types across neocortical areas', *Nature*, 563(7729), pp. 72–78.

Tchenio, A., Lecca, S., Valentinova, K. and Mameli, M. (2017) 'Limiting habenular hyperactivity ameliorates maternal separation-driven depressive-like symptoms', *Nature Communications*, 8(1), p. 1135.

Tepper, J. M., Tecuapetla, F., Koós, T. and Ibáñez-Sandoval, O. (2011) 'Heterogeneity and Diversity of Striatal GABAergic Interneurons', *Frontiers in Neuroanatomy*, 4(150).

Tervo, D. G., Hwang, B. Y., Viswanathan, S., Gaj, T., Lavzin, M., Ritola, K. D., Lindo, S., Michael, S., Kuleshova, E., Ojala, D., Huang, C. C., Gerfen, C. R., Schiller, J., Dudman, J. T., Hantman, A. W., Looger, L. L., Scahffer, D. V. and Karpova, A. Y. (2016) 'A Designer AAV Variant Permits Efficient Retrograde Access to Projection Neurons.', *Neuron*, 92(2), pp. 372–382.

Tremblay, R., Lee, S. and Rudy, B. (2016) 'GABAergic Interneurons in the Neocortex: From Cellular Properties to Circuits', *Neuron*, 91(2), pp. 260–292.

Tricoire, L., Pelkey, K. A., Daw, M. I., Sousa, V. H., Miyoshi, G., Jeffries, B.,

Cauli, B., Fishell, G. and McBain, C. J. (2010) ‘Common origins of hippocampal Ivy and nitric oxide synthase expressing neurogliaform cells.’, *The Journal of Neuroscience*, 30(6), pp. 2165–76.

Trusel, M., Nuno-perez, A., Lecca, S., Harada, H., Lalive, A., Congui, M., Takemoto, K., Takahashi, T., Ferraguti, F. and Mameli, M. (2019) ‘Punishment-Predictive Cues Guide Avoidance through Potentiation of Hypothalamus-to-Habenula Report Punishment-Predictive Cues Guide Avoidance through Potentiation of Hypothalamus-to-Habenula Synapses’, *Neuron*, 102, pp. 1–8.

Vale-Martinez, A., Marti-Nicolovius, G., Guilazzo-Blanch, M., Coll-Andreu, M. and Mergado-Bernal, I. (1997) ‘Effects of Habenular Lesions upon Two-Way Active Avoidance Conditioning in Rats’, *Neurobiology of learning and memory*, 68(1), pp. 68–74.

Vida, I., Halasy, K., Szinyei, C., Somogyi, P. and Buhl, E. H. (1998) ‘Unitary IPSPs evoked by interneurons at the stratum radiatum-stratum lacunosum-moleculare border in the CA1 area of the rat hippocampus in vitro’, *Journal of Physiology*, 506(3), pp. 755–773.

Villalobos, C. A., Wu, Q., Lee, P. H., May, P. J. and Basso, M. A. (2018) ‘Parvalbumin and GABA Microcircuits in the Mouse Superior Colliculus’, *Frontiers in Neural Circuits*, 12, pp. 1–16.

Wagner, F., Bernard, R., Derst, C., French, L. and Veh, R. W. (2016a) ‘Microarray analysis of transcripts with elevated expressions in the rat

medial or lateral habenula suggest fast GABAergic excitation in the medial habenula and habenular involvement in the regulation of feeding and energy balance', *Brain Structure and Function*, 221(9), pp. 4463–89.

Wagner, F., French, L. and Veh, R. W. (2016b) 'Transcriptomic-anatomic analysis of the mouse habenula uncovers a high molecular heterogeneity among neurons in the lateral complex, while gene expression in the medial complex largely obeys subnuclear boundaries', *Brain Structure and Function*, 221(1), pp. 39–58.

Wallace, M. L., Saunders, A., Huang, K. W., Philson, A. C., Goldman, M., Macosko, E. Z., McCarroll, S. A. and Sabatini, B. L. (2017) 'Genetically Distinct Parallel Pathways in the Entopeduncular Nucleus for Limbic and Sensorimotor Output of the Basal Ganglia', *Neuron*, 94(1), pp. 138–152.

Wang, R. Y. and Aghajanian, G. K. (1977) 'Physiological evidence for habenula as major link between forebrain and midbrain raphe', *Science*, 197(4298), pp. 89–91.

Wang, Y., Toledo-Rodriguez, M., Gupta, A., Wu, C., Silberberg, G., Luo, J. and Markram, H. (2004) 'Anatomical, physiological and molecular properties of Martinotti cells in the somatosensory cortex of the juvenile rat', *Journal of Physiology*, 561(1), pp. 65–90.

Webster, J. F., Vroman, R., Balueva, K., Wulff, P., Sakata, S. and Wozny, C. (2019) 'Disentangling neuronal inhibition and inhibitory pathways in the lateral habenula', *bioRxiv*. doi: 10.1101/633271.

Weiss, T. and Veh, R. W. (2011) ‘Morphological and electrophysiological characteristics of neurons within identified subnuclei of the lateral habenula in rat brain slices’, *Neuroscience*, 172, pp. 74–93.

Wilcox, K. S., Christoph, G. R., Double, B. A. and Leonzio, R. J. (1986) ‘Kainate and electrolytic lesions of the lateral habenula: Effect on avoidance responses’, *Physiology and Behavior*, 36(3), pp. 413–417.

Wilcox, K. S., Gutnick, M. J. and Christoph, G. R. (1988) ‘Electrophysiological properties of neurons in the lateral habenula nucleus: An in vitro study’, *Journal of Neurophysiology*, 59(1).

Wilson, J. R., Mitchell, J. C. and Van Hoesen, G. W. (1972) ‘Epithalamic and ventral tegmental contributions to avoidance behavior in rats’, *Journal of Comparative and Physiological Psychology*, 78(3), pp. 442–449.

Wilson, N. R., Runyan, C. a, Wang, F. L. and Sur, M. (2012) ‘Division and subtraction by distinct cortical inhibitory networks in vivo.’, *Nature*, 488(7411), pp. 343–8.

Winter, C., Vollmayr, B., Djodari-Irani, A., Klein, J. and Sartorius, A. (2011) ‘Pharmacological inhibition of the lateral habenula improves depressive-like behavior in an animal model of treatment resistant depression’, *Behav Brain Res*, 216(1), pp. 463–465.

Wise, R. A. (2004) ‘Dopamine, learning and motivation’, *Nature Reviews Neuroscience*, 5, pp. 483–494.

Wolpert, L. (2001) ‘Stigma of depression - A personal view’, *British Medical*

Bulletin, pp. 221–224.

Wozny, C., Beed, P., Nitzan, N., Pössnecker, Y., Rost, B. R. and Schmitz, D. (2018) 'VGLUT2 functions as a differential marker for hippocampal output neurons', *Frontiers in Cellular Neuroscience*, 12(337).

Wozny, C. and Williams, S. R. (2011) 'Specificity of synaptic connectivity between layer 1 inhibitory interneurons and layer 2/3 pyramidal neurons in the rat neocortex', *Cerebral Cortex*, 21(8), pp. 1818–1826.

Yang, Y., Cui, Y., Sang, K., Dong, Y., Ni, Z., Ma, S. and Hu, H. (2018a) 'Ketamine blocks bursting in the lateral habenula to rapidly relieve depression', *Nature*, 554(7692), pp. 317–322.

Yang, Y., Wang, H., Hu, J. and Hu, H. (2018b) 'Lateral habenula in the pathophysiology of depression', *Current Opinion in Neurobiology*, pp. 90–96.

Yavorska, I. and Wehr, M. (2016) 'Somatostatin-Expressing Inhibitory Interneurons in Cortical Circuits', *Frontiers in Neural Circuits*, 10.

Zanos, P. and Gould, T. D. (2018) 'Mechanisms of ketamine action as an antidepressant', *Molecular Psychiatry*, 23(4), pp. 801–811.

Zhang, L., Hernández, V. S., Swinny, J. D., Verma, A. K., Giesecke, T., Emery, A. C., Mutig, K., Garcia-Segura, L. M. and Eiden, L. E. (2018) 'A GABAergic cell type in the lateral habenula links hypothalamic homeostatic and midbrain motivation circuits with sex steroid signaling', *Translational Psychiatry*, 8(1), p. 50.

Zhao, H., Zhang, B. L., Yang, S. J. and Rusak, B. (2015) ‘The role of lateral habenula-dorsal raphe nucleus circuits in higher brain functions and psychiatric illness’, *Behavioural Brain Research*, pp. 89–98.